



INSTYTUT INFORMATYKI TEORETYCZNEJ I STOSOWANEJ  
POLSKIEJ AKADEMII NAUK

---

WYKORZYSTANIE TEORII GRAFÓW W  
INFORMATYCE KWANTOWEJ

---

ROZPRAWA DOKTORSKA

mgr Adam GŁOS  
Promotor: dr hab. Jarosław Adam MISZCZAK

Gliwice, Luty 2021





INSTITUTE OF THEORETICAL AND APPLIED INFORMATICS,  
POLISH ACADEMY OF SCIENCES

---

# APPLICATION OF GRAPH THEORY IN QUANTUM COMPUTER SCIENCE

---

DOCTORAL DISSERTATION

mgr Adam GLOS  
Supervisor: dr hab. Jarosław Adam MISZCZAK

Gliwice, February 2021



# Dedication

The arrogance of a young scientist who claims that everything he owes is only due to his hard work is truly remarkable. Looking back these few years, at the beginnings of my scientific work, I can see how much of hard work, trust of other people, but also random meetings have led me to the place where I am. Due to the multitude of people who helped me reach the first giant leap for me (small for mankind, though), I am fully aware that I will not be able to sufficiently thank everyone for their help.

However, there are people who deserve special thanks. My greatest thanks go to my family for supporting me in this path. Special thanks go to my wife, whose support without doubt strengthened me in following my scientific career.

I would also like to thank Prof. Jarosław Miszczak, not only for being my supervisor, but also (or perhaps particularly) for teaching me what science should look like and that it is something more than just optimizing quality measures required for various grant calls. I would like to thank Foundation for Polish Science for convincing me that my supervisor was right.

Special thanks go to all who helped me keeping open-minded. In particular, I would like to thank Piotr Gawron, Mateusz Ostaszewski, Łukasz Paweła, Przemysław Sadowski, Alexander Rivosh, Abuzer Yakaryilmaz and others for discussions on many (not necessarily quantum) topics.

I would like to thank the National Science Center, for granting me scholarship Etiuda, which enabled me to revisit Centre for Quantum Computer Science from the University of Latvia. This dissertation was also prepared under the scholarship Etiuda, no. 2019/32/T/ST6/00158.

Finally, I would like to thank Ryszard Kukulski for many discussions on the convergence of random variables in context of random graphs, and Bruno Coutinho for discussion on efficiency of the classical search. I would also like to Izabela Miszczak for reviewing dissertation and Aleksandra Krawiec for reviewing this dedication.



# Contents

List of publications	xi
Streszczenie w języku polskim	xiii
Abstract in English	xv
<b>1 Introduction</b>	<b>1</b>
<b>2 Preliminaries</b>	<b>5</b>
2.1 General preliminaries . . . . .	5
2.1.1 Set theory notation . . . . .	5
2.1.2 Complexity notation . . . . .	5
2.1.3 Linear algebra . . . . .	6
2.2 Graph theory . . . . .	8
2.2.1 General concepts . . . . .	8
2.2.2 Random graphs . . . . .	10
2.3 Stochastic and quantum dynamics . . . . .	12
2.3.1 Stochastic evolution . . . . .	12
2.3.2 Evolution in quantum systems . . . . .	13
2.4 Random and quantum walk theory . . . . .	15
2.4.1 Typical random and quantum walks . . . . .	15
2.4.2 Walk quality measures . . . . .	18
2.5 Numerical analysis and tools . . . . .	21
2.5.1 Exponent estimation . . . . .	21
2.5.2 Software used . . . . .	22
<b>3 Non-moralizing Quantum Stochastic Walk</b>	<b>23</b>
3.1 Ballistic propagation for GQSW . . . . .	25
3.2 Spontaneous moralization in GQSW . . . . .	27
3.2.1 Spontaneous moralization removal . . . . .	30
3.2.2 Premature localization . . . . .	32

3.2.3	Final model and correction cost . . . . .	36
3.3	Propagation of standard NGQSW . . . . .	38
3.3.1	Lack of symmetry on infinite path . . . . .	38
3.3.2	Propagation analysis . . . . .	39
<b>4</b>	<b>Convergence of quantum stochastic walks</b>	<b>43</b>
4.1	Convergence of LQSW . . . . .	44
4.2	Convergence of GQSW . . . . .	47
4.3	Convergence of standard NGQSW . . . . .	50
4.4	Digraph structure observance . . . . .	53
<b>5</b>	<b>Hiding vertices for quantum spatial search</b>	<b>57</b>
5.1	Adjacency matrix . . . . .	60
5.1.1	Issues found in the paper of Chakraborty et al. . . . .	60
5.1.2	Quantum search is almost always optimal . . . . .	62
5.1.3	No-hiding theorem . . . . .	64
5.1.4	Conclusions for adjacency matrix . . . . .	64
5.2	Laplacian matrix . . . . .	65
5.2.1	Case $p = \omega(\log n/n)$ . . . . .	65
5.2.2	Case $p = p_0 \ln n/n$ . . . . .	66
5.3	Conclusions . . . . .	69
<b>6</b>	<b>Quantum spatial search on heterogeneous graphs</b>	<b>71</b>
6.1	Choice of $H_G$ for heterogeneous graphs . . . . .	72
6.2	Special random graph models . . . . .	73
6.2.1	Chung-Lu graphs . . . . .	73
6.2.2	Barabási-Albert graphs . . . . .	75
6.3	Optimal measurement time . . . . .	78
6.4	Conclusions . . . . .	82
<b>7</b>	<b>Final remarks</b>	<b>83</b>
	<b>Bibliography</b>	<b>92</b>
<b>A</b>	<b>Proofs for Quantum Stochastic Walks</b>	<b>93</b>
A.1	Probability distributions of GQSW on finite and infinite paths	93
A.1.1	Probability distribution for finite path . . . . .	93
A.1.2	Probability distribution for infinite path . . . . .	94
A.2	Scaling exponent of interpolated standard GQSW on infinite path graph . . . . .	95
A.2.1	Case $\omega = 1$ . . . . .	95
A.2.2	Case $\omega < 1$ . . . . .	99



<b>B</b>	<b>Proofs for quantum search</b>	<b>103</b>
B.1	Proofs for Erdős-Rényi graphs . . . . .	103
B.1.1	Convergence of the principal eigenvector of adjacency matrix . . . . .	103
B.1.2	Convergence of the largest eigenvalue of Laplacian . . .	106
B.2	Proofs for Chung-Lu graphs . . . . .	107
B.2.1	Complexity of $p$ -norm of $\omega$ . . . . .	107
B.2.2	Number of edges for Chung-Lu graphs . . . . .	107
B.2.3	Degree convergence . . . . .	108
B.2.4	Convergence of $ \lambda_1\rangle$ for adjacency graphs . . . . .	109
B.3	Classical search . . . . .	111



# List of publications

Publications and preprints relevant to the dissertation are highlighted with **bold**.

## Published work

1. A. Glos, A. Krawiec, and Ł. Pawela, “Asymptotic entropy of the Gibbs state of complex networks,” *Scientific Reports*, vol. 11, p. 311, 2021.
2. A. Glos, N. Nahimovs, K. Balakirev, and K. Khadiev, “Upperbounds on the probability of finding marked connected components using quantum walks,” *Quantum Information Processing*, vol. 20, p. 6, 2021.
3. Z. Tabi, K. H. El-Safty, Z. Kallus, P. Haga, T. Kozsik, A. Glos, and Z. Zimboras, “Quantum optimization for the graph coloring problem with space-efficient embedding,” in *2020 IEEE International Conference on Quantum Computing and Engineering (QCE)*, pp. 56–62, 2020.
4. A. Glos, “Spectral similarity for Barabasi–Albert and Chung–Lu models,” *Physica A: Statistical Mechanics and its Applications*, vol. 516, pp. 571–578, 2019.
5. A. Glos and J. A. Miszczak, “The role of quantum correlations in Cop and Robber game,” *Quantum Studies: Mathematics and Foundations*, vol. 6, no. 1, pp. 15–26, 2019.
6. A. Glos and J. A. Miszczak, “Impact of the malicious input data modification on the efficiency of quantum spatial search,” *Quantum Information Processing*, vol. 18, p. 343, 2019.
7. A. Glos and T. Januszek, “Impact of global and local interaction on quantum spatial search on Chimera graph,” *International Journal of Quantum Information*, p. 1950040, 2019.
8. A. Glos, J. Miszczak, and M. Ostaszewski, “**QSWalk.jl: Julia package for quantum stochastic walks analysis**,” *Computer Physics Communications*, 2018.
9. K. Domino, A. Glos, M. Ostaszewski, P. Sadowski, and Ł. Pawela, “**Properties of Quantum Stochastic Walks from the asymptotic scaling**

- exponent,”** *Quantum Information and Computation*, vol. 18, no. 3&4, pp. 0181–0199, 2018.
10. A. Glos, A. Krawiec, R. Kukulski, and Z. Puchała, “**Vertices cannot be hidden from quantum spatial search for almost all random graphs,**” *Quantum Information Processing*, vol. 17, no. 4, p. 81, 2018.
  11. A. Glos and T. Wong, “**Optimal quantum-walk search on Kronecker graphs with dominant or fixed regular initiators,**” *Physical Review A*, vol. 98, no. 6, p. 062334, 2018.
  12. K. Domino, A. Glos, and M. Ostaszewski, “**Superdiffusive Quantum Stochastic Walk definable on arbitrary directed graph,**” *Quantum Information & Computation*, vol. 17, no. 11-12, pp. 973-986, 2017.
  13. A. Glos, J. A. Miszczak, and M. Ostaszewski, “**Limiting properties of stochastic quantum walks on directed graphs,**” *Journal of Physics A: Mathematical and Theoretical*, vol. 51, no. 3, p. 035304, 2017.
  14. A. Glos and P. Sadowski, “Constructive quantum scaling of unitary matrices,” *Quantum Information Processing*, vol. 15, no. 12, pp. 5145–5154, 2016.
  15. D. Kurzyk and A. Glos, “Quantum inferring acausal structures and the Monty Hall problem,” *Quantum Information Processing*, vol. 15, no. 12, pp. 4927–4937, 2016.

## Preprints

1. R. Kukulski and A. Glos, “**Comment to ‘Spatial search by quantum walk is optimal for almost all graphs’,**” *arXiv:2009.13309*, 2020.
2. A. Glos, A. Krawiec, and Z. Zimborás, “Space-efficient binary optimization for variational computing,” *arXiv:2009.07309*, 2020.
3. K. Domino and A. Glos, “Hiding higher order cross-correlations of multivariate data using Archimedean copulas,” *arXiv:1803.07813*, 2018.

# Streszczenie w języku polskim

W ramach rozprawy wykazałem, że ciągle w czasie błędzenie kwantowe pozostaje skuteczne dla ogólnych struktur grafowych. Przeanalizowałem dwa aspekty tego problemu.

Po pierwsze, wiadomym jest, że model *Continuous-Time Quantum Walk* (CTQW), zaproponowany przez Childsa i Goldstone'a, potrafi szybko propagować na grafie będącym nieskończoną ścieżką. Jednak równanie Schrödingera wymaga, aby Hamiltonian był symetryczny, przez co mogą być zaimplementowane jedynie nieskierowane grafy. W ramach tej rozprawy przeanalizowałem, czy możliwe jest zaprojektowanie ciągłego w czasie błędzenia kwantowego dla ogólnego grafu skierowanego, tak aby zachowywał on szybką propagację.

Po drugie, przeszukiwanie grafów zdefiniowane przez CTQW jest efektywne dla wielu różnych rodzajów grafów. Jednakże większość z tych grafów miała bardzo prostą strukturę. Najbardziej zaawansowanymi przypadkami były model grafów losowych Erdősa-Rényiego, który choć najpopularniejszy nie daje grafów opisujących rzeczywiste interakcje spotykane w przyrodzie, oraz model grafów Barabásiego-Alberta, dla których kwadratowe przyspieszenie nie było udowodnione. W ramach tego aspektu przeanalizowałem, czy przyspieszenie kwantowe jest możliwe także dla skomplikowanych struktur grafowych.

Rozprawa składa się z siedmiu rozdziałów. W rozdziale 1 umieszczony został wstęp oraz motywacja podjęcia tematu. W rozdziale 2 wprowadziłem notację oraz podstawowe koncepcje użyte w rozprawie.

W rozdziałach 3 oraz 4 przeanalizowałem pierwszy wprowadzony problem. W rozdziale 3 zaproponowałem błędzenie niemoralizujące kwantowo-stochastyczne o globalnych interakcjach, które jest dobrze zdefiniowane dla grafów skierowanych. Wykazałem, że dla tego modelu obserwujemy szybką propagację dla nieskończonej ścieżki. Aby uzyskać ten efekt, istotnie lepszy niż dla klasycznego błędzenia, wprowadziłem mały transfer amplitudy w kierunku niezgodnym z kierunkiem istniejących łuków grafu. W rozdziale 4 przeanalizowałem własności graniczne wprowadzonego modelu. Zbadałem również dwa inne błędzenia zwane odpowiednio lokalnymi i globalnymi kwantowo-stochastycznymi. Pokazałem, że każdy z wprowadzonych do tej pory modeli miał inne właściwości. W szczególności, w przypadku błędzeń lokalnego i niemoralizującego globalnego wskazałem najbardziej intuicyjne zachowanie dla grafów skierowanych. Badania pokazują, że możliwe jest zaproponowanie szybkiego, ciągłego w czasie błędzenia kwantowego, które jest dobrze zdefiniowane dla ogólnego grafu skierowanego.

W rozdziałach 5 oraz 6 przeanalizowałem drugi z postawionych proble-

mów badawczych. W rozdziale 5 poprawiłem i wzmocniłem obecnie wiodące wyniki dotyczące grafów Erdősa-Rényiego. Wykazałem, że przyspieszenie kwantowe jest poprawne dla wszystkich wierzchołków, nie tylko dla „prawie wszystkich”. W porównaniu z obecnie wiodącymi wynikami pokazałem, że Laplasjan jest o wiele prostszym operatorem w analizie niż macierz sąsiedztwa. W rozdziale 6 porównałem trzy różne operatory możliwe do wykorzystania w ramach kwantowego przeszukiwania przestrzennego. Pokazałem, że znormalizowany Laplasjan, przy pewnych założeniach, umożliwia osiągnięcie pełnego, kwadratowego przyspieszenia. Przeanalizowałem dwa modele grafów losowych, które zwracają grafy o skomplikowanej strukturze z wysokim prawdopodobieństwem. Analiza potwierdziła, że zaproponowana macierz jest lepsza niż te dotychczas używane. Ostatecznie, zaproponowałem procedurę, która powala rozwiązać problem znajdowania optymalnego czasu pomiaru dla kwantowego przeszukiwania.

W rozdziale 7 podsumowałem uzyskane wyniki. Rozprawa zawiera również dwa dodatki, gdzie umieszczone zostały dowody wyników użytych w rozprawie.

# Abstract in English

In this dissertation we demonstrate that the continuous-time quantum walk models remain powerful for nontrivial graph structures. We consider two aspects of this problem.

First, it is known that the standard Continuous-Time Quantum Walk (CTQW), proposed by Childs and Goldstone, can propagate quickly on the infinite path graph. However, the Schrödinger equation requires the Hamiltonian to be symmetric, and thus only undirected graphs can be implemented. In this thesis, we address the question, whether it is possible to construct a continuous-time quantum walk on general directed graphs, preserving its propagation properties.

Secondly, the quantum spatial search defined through CTQW has been proven to work well on various undirected graphs. However, most of these graphs have very simple structures. The most advanced results concerned the Erdős-Rényi model of random graphs, which is the most popular but not realistic random graph model, and Barabási-Albert random graphs, for which full quadratic speed-up was not confirmed. In the scope of this aspect we analyze, whether quantum speed-up is observed for complicated graph structures as well.

The dissertation consists of seven chapters. In Chapter 1 we provide an introduction and motivation. In Chapter 2 we present a notation and preliminary concepts used in the dissertation.

In Chapters 3 and 4 we approach the first aspect. In Chapter 3 we propose a nonmoralizing global interaction quantum stochastic walk, which is well-definable on an arbitrary directed graph. We show that this model propagates rapidly on an infinite path graph. In order to achieve the propagation speed better than the classical one, we introduce a small amplitude transfer in the direction opposite to the direction of the existing arcs. In Chapter 4 we analyze the convergence properties of the introduced model. We also analyze two other quantum stochastic walk models called local and global interaction quantum stochastic walks. We show that each of these models has very different properties. In particular, local and nonmoralizing global models present the most intuitive behavior on directed graphs. Our analysis shows that it is indeed possible to introduce a fast continuous-time quantum walk which is well-definable on general directed graphs.

In Chapters 5 and 6 we study the second of the posed questions. In Chapter 5 we correct and improve state-of-the-art results on Erdős-Rényi graphs. We also demonstrate that the quantum speed-up is correct for all vertices, instead of only ‘most of them’. Compared to the previous state-of-the-art results we show that Laplacian matrix is a much simpler operator to

be taken into consideration compared to the adjacency matrix. In Chapter 6 we compare three different operators plausible for the quantum spatial search. We show that the normalized Laplacian, under certain conditions, provides the full quadratic speed-up. We analyze two random graph models which output the graphs with complex structure with high probability. The analysis confirms that the proposed operator is indeed better than other commonly used operators. Finally, we propose the procedure which solves the problem of determining the optimal time for running the quantum search algorithm.

Finally, in Chapter 7 we review and conclude our results. The dissertation also consists of two Appendix sections, which provide the proofs for the results used in the dissertation.



# Chapter 1

## Introduction

Recently, quantum computers have attracted a huge attention. This is because such devices can solve vital computational problems faster than their classical counterparts. What is more interesting, the speed-up is observable even in the complexity of algorithms. The best example is the Shor's algorithm [1] which solves the integer factorization problem in polynomial time in the terms of number length. It is notable to recall that any known classical algorithm that solves the same problem requires exponential time in a number of bits. Furthermore, the algorithm may threaten the current cryptographic protocols, as it can easily break RSA encryption.

The Shor's algorithm and other quantum algorithms [2, 3] started an important and beautiful field called quantum computer science. The goal of this discipline is to construct the algorithms which are faster compared to the currently known algorithms for conventional computers. Despite numerous important theoretical algorithms [2, 4, 5], there are also the algorithms which have the potential practical application. One can point to the Grover's algorithm and its extensions [3, 6], quantum annealing algorithms [7, 8], variational optimization algorithms [9–12], and Quantum PageRank [13, 14].

Quantum algorithms can be divided into various classes according to the problem they solve or the computational model they are based on [15]. In this dissertation, we focus on a particularly important class called *quantum walks*, in which the amplitude transfer is done within some underlying graph structure [16–18]. It can be considered as an equivalent of random walk algorithms, where the probability mass transfer is not allowed when the states are not connected.

Quantum walks application comes in particular from its ballistic propagation. Let us consider a random walk on an infinite path with the probability localized at position 0. Then after time  $t$ , the probability distribution of finding the walker can be well approximated by Gauss distribution

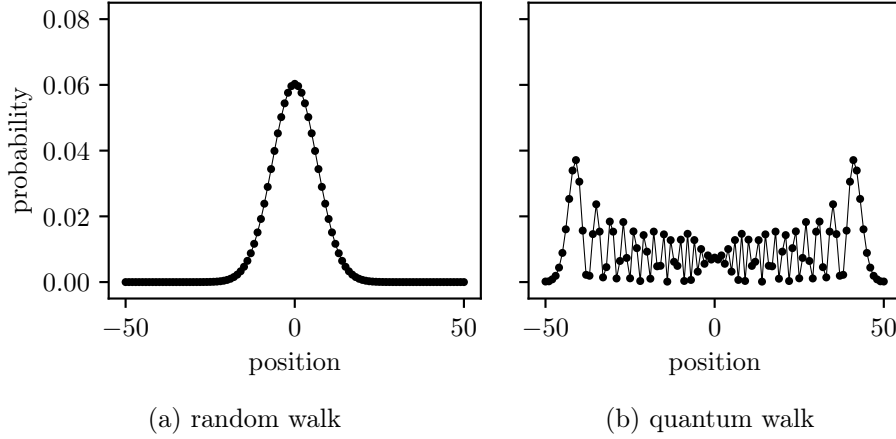


Figure 1.1: Distribution of continuous-time random walk (left) vs continuous-time quantum walk (right) on a path graph with 101 nodes and after evolution time 22. The evolution starts in the middle of the graph.

$N(0, \Theta(t))$  [19]. Since the standard deviation grows proportionally to the square root of time, we say that the stochastic process obeys a normal diffusion. This is contrary to a quantum walk, where the variance grows like  $\Theta(t^2)$  [20], i.e. we can observe the ballistic diffusion. Thus the propagation in a quantum walk may be much faster which may explain the speed-up appearing in quantum walk algorithms. The resulting distributions for both classical and quantum walks are presented in Fig. 1.1.

Despite the fact that the very first quantum walk is almost 20 years old, there are two important questions regarding the generality of the results in the terms of graph structure. Many quantum closed-system walk models, proposed so far, were definable on relatively general graph structures [18, 21, 22]. However, it was shown under general and reasonable assumptions that by using the closed-system quantum evolution one cannot define a quantum walk on a general directed graph [23]. This results from the quasi-periodicity of the closed-system evolution, i.e. there exists an arbitrarily large time evolution  $t$  after which the system evolves to the state close to the initial state. This in turn implies that a closed-system quantum walk can only be well-defined for graphs, where, for arbitrary two nodes, there is a path connecting them.

Since close-system quantum walks are not sufficient to model the evolution on general directed graphs, interactions with the environment are necessary. However, currently known open quantum walk models do not yield the ballistic propagation [24–26]. In particular, for the continuous-time open quantum walk [24], the classical evolution destroys its coherence, and

the proposed model lacks the ballistic propagation. It has been an open question whether there exists a quantum walk model which preserves the directed graph structure and whose propagation is better than the propagation observed in random walks. This may be important, for the directed graph model, for example in the case of the evolution for classical heuristic optimization algorithms like simulated annealing or Tabu Search.

There is a similar lack of generality for quantum spatial search algorithms. The quantum search algorithms are defined as the graph-restricted evolution, which aims at finding a marked node. Note that there are known examples of discrete quantum walks, yielding even a quadratic speed-up over an arbitrary Markov-chain walk [21, 27]. However, general and simple results are still missing for continuous-time quantum walks.

The first continuous-time quantum spatial search algorithm [18] has been deeply investigated for the special classes of graphs like complete graphs [18], grid graphs [18], binary trees [28], simplex of complete graphs [29], and others [30–32]. Based on these results, the special properties of quantum walks were presented. While the obtained results were an important step toward the development of quantum search algorithms, all of the graphs considered were almost regular (meaning all vertices have very similar degrees) and we can split the vertices into several classes (so-called vertex-transitivity), within which the vertices are indistinguishable.

The first approach in generalizing the above results was made for Erdős-Rényi graphs [33–37]. While these graphs are not regular, the deviations between the highest and the smallest degrees are sufficiently small to provide very tight results on the efficiency of quantum search on these graphs. Then three more general results were provided. The first one showed a quadratic speed-up compared to a general Markov-chain search [38], at the cost of larger Hilbert space. Additionally, in [39] quite general conditions for (optimal) quantum search for original continuous-time spatial search were presented. However, the application of these results required the full eigendecomposition of the graph-based Hamiltonian, which in general is a hard computational task. In fact, this task is much more demanding compared to the quantum or even the classical search itself. Finally, in [40] the authors determined the efficiency of the quantum spatial search for complex graphs. However, while the speed-up over the classical search was shown, it remains an open question whether the quadratic speed-up over the Markov search is achievable.

**Dissertation overview** In the scope of the dissertation we demonstrate that the continuous-time quantum walk models remain powerful for nontriv-

ial graph structure. The analysis was done by approaching two problems:

1. Does a time-independent continuous-time quantum walk model which is definable for general directed graphs and which maintains fast propagation exist?
2. Is the original Continuous-Time Quantum Walk based spatial search [18] powerful enough to offer the speed-up for heterogeneous graphs?

Note that for the proposed problems the context of ‘nontrivial graph structure’ changes. For the first problem, we focus on directed graphs, while for the second problem – on undirected graphs with significant deviation between the degrees of vertices. Currently, most of the results for quantum search considers almost regular graphs. Therefore, we consider heterogeneous graphs as a reasonable next step for investigation.

The first problem is approached using the formalism of quantum stochastic walks [41]. The model is a generalization of both Continuous-Time Quantum Walk [18] and continuous-time random walk. For the second problem, we analyze the CTQW-based spatial search [18] on random heterogeneous graphs and complex Barabási-Albert graphs [42]. The latter is a paradigmatic random graph model which simulates Internet network evolution.

The dissertation is organized as follows. In Chapter 2 we present a notation and preliminary information used in the dissertation. In Chapter 3 we analyze a quantum walk model presented in [41], in the context of the propagation. We improve the model into *nonmoralizing quantum stochastic walk* which is well-defined on any directed graphs. In order to achieve better than classical diffusion, we allowed a small amplitude transfer in the direction opposite to the direction of the existing arcs. In Chapter 4 we present convergence properties of the introduced model and compare it to other well-known quantum stochastic walk models. We confirm that the structure of the directed graph is indeed preserved. In Chapter 5 we improve the results for Erdős-Rényi presented in [33], in order to clarify the approach to the analysis of CTQW-based spatial search to random graphs. In Chapter 6 we present the analysis of the spatial search algorithm for heterogeneous and complex graphs. Finally, in Chapter 7 we justify the correctness of our hypothesis in the context of the results presented in the dissertation.

The results presented in Chapters 3 and 4 are based on the results from [43–45]. The results presented in chapters 5 and 6 are based on the results from [36, 37, 46, 47].

# Chapter 2

## Preliminaries

### 2.1 General preliminaries

In this chapter we introduce basic notation concepts used in the dissertation. The notation includes basics of set theory, complexity notation and linear algebra.

#### 2.1.1 Set theory notation

We will denote by  $\mathbb{Z}$ ,  $\mathbb{R}$ ,  $\mathbb{C}$  the set of integers, real numbers and complex numbers. We will use notation  $\mathbb{Z}_{\geq 0}$  to denote the set of non-negative integers, similarly for positive, negative and nonpositive, and for other sets. We will write  $|X|$  for the number of elements of the set  $X$ . We will apply the notation  $[n] := \{1, \dots, n\}$ .

Let  $X$  be an arbitrary set and  $\tilde{X} = \{Y \subseteq X\}$  be such a family of sets that for arbitrary  $Y_1, Y_2 \in \tilde{X}$  we have  $Y_1 = Y_2$  or  $Y_1 \cap Y_2 = \emptyset$ . Furthermore let

$$\bigcup_{Y \in \tilde{X}} Y = X. \quad (2.1)$$

Then we call  $\tilde{X}$  a partition of  $X$ .

#### 2.1.2 Complexity notation

Throughout the dissertation we will use the big O notation. Let  $f : \mathbb{R}_{>0} \rightarrow \mathbb{R}$  and  $g : \mathbb{R}_{>0} \rightarrow \mathbb{R}_{>0}$  be functions. We will write  $f(x) = \mathcal{O}(g(x))$  if there exists  $x_0 > 0$  and  $C > 0$  such that for all  $x > x_0$  we have

$$|f(x)| \leq Cg(x). \quad (2.2)$$

Notation	Definition
$f(x) = \mathcal{O}(g(x))$	see Sec. 2.1.2
$f(x) = \Omega(g(x))$	$g(x) = \mathcal{O}(f(x))$
$f(x) = \Theta(g(x))$	$g(x) = \mathcal{O}(f(x))$ and $f(x) = \mathcal{O}(g(x))$
$f(x) = o(g(x))$	$\lim_{x \rightarrow \infty} \frac{f(x)}{g(x)} = 0$
$f(x) = \omega(g(x))$	$\lim_{x \rightarrow \infty} \left  \frac{f(x)}{g(x)} \right  = +\infty$
$f(x) \sim g(x)$	$f(x) = g(x)(1 + o(1))$

Table 2.1: Asymptotic notations and their definitions.

In fact  $\mathcal{O}(g(x))$  is usually defined as a set of all functions  $f$  satisfying mentioned relation, so formally one should write  $f(x) \in \mathcal{O}(g(x))$ . However, in the dissertation we will follow a widely accepted computer science convention and use ‘=’ instead of ‘ $\in$ ’.

With  $\mathcal{O}(\cdot)$  notation we can define other asymptotic notations. We present them and their definition in Tab. 2.1. Note that any of these symbols hide the constant next to the leading term. For example, if  $f(x) = \mathcal{O}(n^2)$ , then at the same time  $f(x) = \mathcal{O}(2n^2)$  or  $f(x) = \mathcal{O}(\frac{1}{2}n^2)$ . In case we know the constant next to the leading term we will write  $f(x) \sim Cn^2$ , which is defined as  $f(x) = Cn^2(1 + o(1)) = Cn^2 + o(n^2)$ .

### 2.1.3 Linear algebra

Let  $X$  be a countable set. Let  $\mathbb{C}^X$  be a complex-vector space and let  $\{|x\rangle : x \in X\}$  be its orthonormal basis. Arbitrary vector  $|\psi\rangle \in \mathbb{C}^X$  has a unique representation

$$|\psi\rangle = \sum_{x \in X} \alpha_x |x\rangle, \quad (2.3)$$

where  $\alpha_x \in \mathbb{C}$ . We call  $\{|x\rangle : x \in X\}$  a computational basis and we choose them to be of the form

$$|x\rangle = \begin{bmatrix} 0 \\ \vdots \\ 0 \\ 1 \\ 0 \\ \vdots \\ 0 \end{bmatrix}, \quad (2.4)$$

where 1 appears on the  $x^{\text{th}}$  position. A conjugate transpose of  $|\psi\rangle$  is defined as

$$\langle\psi| := (|\psi\rangle)^\dagger = \sum_{x \in X} \bar{\alpha}_x \langle x|, \quad (2.5)$$

where  $\bar{\alpha}$  is a conjugate of  $\alpha$  and  $\langle x|$  is a row vector with 1 on the  $x^{\text{th}}$  position and 0 otherwise. Note that the conjugate transpose is a composition of transpose and element-wise conjugation of the vector.

If  $|\psi\rangle, |\phi\rangle \in \mathbb{C}^X$ , then  $\langle\psi|\phi\rangle$  denotes their scalar product. The outer product of vectors  $|\psi\rangle \in \mathbb{C}^X, |\phi\rangle \in \mathbb{C}^Y$  is denoted as  $|\psi\rangle\langle\phi|$ . The tensor product of states  $|\psi\rangle = \sum_{i=1}^n \alpha_{x_i} |x_i\rangle \in \mathbb{C}^X$  with  $X = \{x_1, \dots, x_n\}$  and  $|\phi\rangle \in \mathbb{C}^Y$  is defined as

$$|\psi\rangle \otimes |\phi\rangle = \begin{bmatrix} \alpha_{x_1} |\phi\rangle \\ \vdots \\ \alpha_{x_n} |\phi\rangle \end{bmatrix} \in \mathbb{C}^X \otimes \mathbb{C}^Y. \quad (2.6)$$

We will also use abbreviations  $|\psi, \phi\rangle, |\psi\phi\rangle$  instead of  $|\psi\rangle \otimes |\phi\rangle$ . Note  $\mathbb{C}^X \otimes \mathbb{C}^Y$  is isomorphic to  $\mathbb{C}^{X \times Y}$ .

Let  $B \in \mathbb{C}^{X \times Y}$  be a complex-valued matrix. Then  $B$  has a unique representation

$$B = \sum_{x \in X} \sum_{y \in Y} b_{xy} |x\rangle\langle y|. \quad (2.7)$$

The vectorization of  $B$  is defined as  $|B\rangle\rangle = \sum_{x \in X} \sum_{y \in Y} b_{xy} |xy\rangle$ . Furthermore we define a conjugate transpose of  $B$

$$B^\dagger := \sum_{x \in X} \sum_{y \in Y} \bar{b}_{xy} |y\rangle\langle x|. \quad (2.8)$$

Suppose  $B$  is a square matrix, i.e.  $B \in \mathbb{C}^{X \times X}$ . If  $B^\dagger B = BB^\dagger$ , then we call  $B$  a *normal matrix*. For such matrices an eigendecomposition can be found, i.e. there exists  $\lambda_1(B), \dots, \lambda_{|X|}(B) \in \mathbb{C}$  and orthonormal vectors  $|\lambda_1\rangle(B), \dots, |\lambda_{|X|}(B)\rangle \in \mathbb{C}^X$  such that

$$B = \sum_{i=1}^{|X|} \lambda_i(B) |\lambda_i(B)\rangle\langle\lambda_i(B)|. \quad (2.9)$$

We call  $\lambda_i(B)$  an eigenvalue and  $|\lambda_i\rangle(B)$  a corresponding eigenvector of  $B$ . Whenever it will be clear from the context, we will write shortly  $\lambda$  and  $|\lambda\rangle$  instead of  $\lambda(B)$  and  $|\lambda(B)\rangle$ . Furthermore, if all eigenvalues are real we will assume that  $\lambda_i \geq \lambda_j$  for  $j < i$ .

The space of normal matrices encapsulates many classes of matrices important for quantum mechanics. In particular if  $B^\dagger = B$ , then  $B$  is Hermitian. If  $B^\dagger B = I$ , where  $I$  is identity matrix, then we call  $B$  a unitary matrix. Eigenvalues of Hermitian operators are real, while eigenvalues of unitary matrices are complex and lie on unit circle.

Matrix  $B \in \mathbb{C}^{X \times X}$  is called nonnegative if for any vector  $|\psi\rangle \in \mathbb{C}^X$  we have  $\langle\psi| B |\psi\rangle \geq 0$ . If additionally the trace of  $B$  equals 1,

$$\text{tr}(B) := \sum_{x \in X} \langle x | B | x \rangle = 1, \quad (2.10)$$

then we call  $B$  a *density operator*. It can be shown that eigenvalues of  $B$  form a proper probability vector, i.e. they are nonnegative and they sum up to 1.

Matrix  $B$  is called stochastic if its columns are proper probability vectors.

Let  $A \in \mathbb{C}^{X \times X}$  be a matrix and  $\tilde{X} = \{X_1, \dots, X_k\}$  be a partition of  $X$ . We can construct a  $\tilde{X}$ -block representation of  $A$  as

$$\left[ \begin{array}{c|c|c|c} A_{1,1} & A_{1,2} & \dots & A_{1,k} \\ \hline A_{2,1} & A_{2,2} & \dots & A_{2,k} \\ \hline \vdots & \vdots & & \vdots \\ \hline A_{k,1} & A_{k,2} & \dots & A_{k,k} \end{array} \right], \quad (2.11)$$

where  $A_{i,j} \in \mathbb{C}^{X_i \times X_j}$  satisfies  $\langle k | A_{ij} | l \rangle = \langle k | A | l \rangle$  for any  $k \in X_i$  and  $l \in X_j$ . Note that currently a block matrix is considered to be a matrix, which elements are matrices. Such definition implies even the change of how the multiplication is defined. Our definition is used for representation purposes only. We call  $A$  a  $\tilde{X}$ -block diagonal matrix iff for all  $i \neq j$  matrix  $A_{ij}$  is a zero matrix.

In the dissertation we will oftenly choose  $X = [n]$ . In this case the vector  $|i\rangle$  will always have 1 on  $i^{\text{th}}$  position.

## 2.2 Graph theory

### 2.2.1 General concepts

We call a pair  $\vec{G} = (V, \vec{E})$  a simple directed graph (digraph), iff  $V$  is a finite set and  $\vec{E} \subseteq \{(v, w) : v, w \in V, v \neq w\}$ . We call the elements of  $V$  vertices or nodes, and of  $\vec{E}$  arcs. We call  $|V|$  the order of the digraph and  $|\vec{E}|$  the size of the digraph. Similarly we call a pair  $(V, E)$  a simple undirected graph, iff



$V$  is a finite set and  $\vec{E} \subseteq \{\{v, w\} : v, w \in V, v \neq w\}$  with order  $|V|$  and size  $|E|$ . We call the elements of  $V$  vertices or nodes and of  $E$  edges.

Note that a directed graphs can be considered as an undirected graph if for any  $(v, w) \in \vec{E}$  we have  $(w, v) \in \vec{E}$ . Thus many definitions for directed graphs can be formulated for undirected graphs as well. Because of this, unless explicitly stated, we will provide definitions for directed graphs only.

Let  $\vec{G} = (V, \vec{E})$  be a directed graph. We call  $G = (V, E)$  an underlying graph of  $\vec{G}$  iff

$$\{v, w\} \in E \iff ((v, w) \in \vec{E} \vee (w, v) \in \vec{E}). \quad (2.12)$$

Note that the undirected graph is its own underlying graph. Conversely the directed graph  $\vec{G} = (V, \vec{E})$  is an orientation of the graph  $G = (V, E)$  if each edges  $\{v, w\}$  is replaced with a either  $(v, w)$  or  $(w, v)$ . Note that we have  $2^{|E|}$  orientations of graph  $G$ , but there is single underlying graph for digraph  $\vec{G}$ .

We call set  $P(v) = \{w \in V : (w, v) \in \vec{E}\}$  a set of parents of  $v \in V$ . We define a children set of  $v \in V$  as the collection  $C(v) = \{w \in V : (v, w) \in \vec{E}\}$ . We define indegree and the outdegree of  $v$  as a sizes of these sets i.e.  $\text{indeg}(v) = |P(v)|$  and  $\text{outdeg}(v) = |C(v)|$ . If  $\text{indeg}(v) = 0$  we call  $v$  a source. If  $\text{outdeg}(v) = 0$  then we call  $v$  a sink or a leaf. A collection of all sinks (leaves) of a digraph  $\vec{G}$  is denoted by  $L(\vec{G})$ . Note that for undirected graphs we have  $\text{deg}(v) := \text{indeg}(v) = \text{outdeg}(v)$  which is simply a degree of the vertex  $v$ .

A path from  $v_1$  to  $v_{k+1}$  is a sequence  $(v_1, \dots, v_{k+1})$  such that  $(v_i, v_{i+1}) \in \vec{E}$  for each  $i = 1, \dots, k$ , and  $k$  is called a length of the path. We say a digraph (graph) is strongly connected (connected) iff for each  $v, w \in V$  there exists a path from  $v$  to  $w$ . We say that a digraph is weakly connected iff its underlying graph is connected. The distance  $d(v, w)$  from  $v$  to  $w$  is defined to be the minimum length of all paths from  $v$  to  $w$ . Note that in general for directed graphs  $d(v, w) \neq d(w, v)$ .

If a path  $(v_1, \dots, v_k)$  does not have a vertex repetition except  $v_1 = v_k$  then we call it a simple path. If  $v_1 = v_k$  then we call it a cycle. If digraph does not have a cycle of length  $k \geq 3$  then we call it acyclic. We will call undirected graph  $G$  a tree if it has no cycles and is connected.

Let  $\vec{G} = (V, \vec{E})$  be a directed graph. A directed graph  $\vec{H} = (V_H, \vec{E}_H)$  is called a subgraph iff  $V_H \subseteq V$  and  $\vec{E}_H \subseteq \vec{E}$ . We denote this fact by  $\vec{H} \subseteq \vec{G}$ . If  $\vec{E}_H$  is maximal in the number of arcs, i.e. is of the form

$$E_H = \{(v, w) \in \vec{E} : v, w \in V_H\}, \quad (2.13)$$

the we call  $\vec{H}$  an induced subgraph, which we denote  $\vec{H} \subseteq_{\text{ind}} \vec{G}$ . Note that given subset of vertices  $V_H$  there is a unique induced subgraph of  $\vec{G}$ , however

there may be multiple subgraph. Maximal connected subgraph is called a connected component.

Let  $\vec{G}_1 = (V_1, \vec{E}_1)$  and  $\vec{G}_2 = (V_2, \vec{E}_2)$  be directed graphs and  $f : V_1 \rightarrow V_2$ . We call  $f$  a graph homomorphism from  $\vec{G}_1$  to  $\vec{G}_2$  iff for each  $(v, w) \in \vec{E}_1$  we have  $(f(v), f(w)) \in \vec{E}_2$ . If  $f$  is bijection and both  $f$  and  $f^{-1}$  are homomorphisms then  $f$  is an isomorphism, and we call  $G$  and  $H$  isomorphic graphs.

Isomorphism from  $\vec{G}$  to  $\vec{G}$  is called automorphism. We call  $G = (V, E)$  a vertex-transitive graph, if for any  $v, w \in V$  there exists a automorphism  $f : V \rightarrow V$  such that  $f(v) = w$ .

Let  $A(\vec{G}) \in \mathbb{R}^{V \times V}$  be an operator defined as

$$\langle w | A(\vec{G}) | v \rangle = \begin{cases} 1, & (v, w) \in \vec{E}, \\ 0, & \text{otherwise.} \end{cases} \quad (2.14)$$

We call  $A(\vec{G})$  an adjacency matrix of  $\vec{G}$ . Note that  $A(\vec{G})$  is symmetric iff graph is undirected. Furthermore, in the literature the adjacency matrix is usually the transpose of the operator above, however our definition is more convenient based on form of evolution considered in this dissertation. If clear from the context which graphs is considered, we will write simply  $A$  instead of  $A(\vec{G})$ .

Let  $D(G) \in \mathbb{R}^{V \times V}$  be a diagonal matrix such that  $\langle v | D(G) | v \rangle = \deg(v)$ . We define (combinatorial) Laplacian as  $L(G) := D(G) - A(G)$  and normalized Laplacian as  $\mathcal{L}(G) := D(G)^{-1/2} L(G) D(G)^{-1/2} = I - D(G)^{-1/2} A(G) D(G)^{-1/2}$ . Note that the normalized Laplacian is well-defined only for graphs without isolated nodes, i.e. nodes with degree 0. Laplacian and normalized Laplacian are always nonnegative. The multiplicity of eigenvalue 0 for both equals the number of connected components of  $G$ .

We call adjacency matrix, Laplacian and normalized Laplacian *graph matrices*.

### 2.2.2 Random graphs

Random graph model  $\mathcal{G}_n$  is a probabilistic measure space defined over a set of graphs with  $n$  vertices. Precise definition requires the notion of measurable space. However, it is common to provide the sampling method instead of writing exact form of probability distribution. Each random graph model will be denoted by  $\mathcal{G}_n^{\text{LABEL}}(\nu_1, \dots, \nu_k)$ , where LABEL is the label setting the sampling method and  $\nu_1, \dots, \nu_k$  are free parameters of sampling method. Note that parameter  $\nu_i$  may depend on  $n$ .

Let us recall here the most popular random graph models. We will start with the Erdős-Rényi random graph model  $\mathcal{G}_n^{\text{ER}}(p)$ , where  $p \in [0, 1]$  [48]. The sampling method goes as follows. We start with empty graph  $G = ([n], \emptyset)$ . Then for each pair of different vertices  $v, w \in [n]$  we add edge  $\{v, w\}$  independently with probability  $p$ . Similarly for directed graphs each arc  $(v, w)$  is added independently with probability  $p$ . The random graph model is so popular that in many papers authors by ‘random graphs’ consider precisely this model. The reason for such is, beside the fact that it is the first random graph model proposed, is because for  $p = 1/2$  we have uniform distribution over all graphs with fixed vertex set.

Unfortunately, while the model is well known, it does not represent the real-world dependencies. In particular, Erdős-Rényi graphs do not have power-law degree distribution, which means that vertices with degree  $d$  are present with  $\Theta(d^{-\alpha})$  probability for some constant  $\alpha$  [42]. Real graphs usually are also small-world, which means the existence of small-length paths between all vertices, sparse (have small number of edges) and one can often observe community structures, i.e. small but dense subgraphs.

There are many graph models which may possess some of these properties. The closest to the Erdős-Rényi graph model is the Chung-Lu model  $\mathcal{G}_n^{\text{CL}}(\omega)$  [49]. This model depends on single parameter being a real-valued vector  $\omega = (\omega_1, \dots, \omega_n) \in [0, n-1]^n$ . Similarly as for the Erdős-Rényi model we start with empty graph  $G = ([n], \emptyset)$  with  $n$  vertices, and an edge between vertices  $i$  and  $j$  is added with probability  $\omega_i \omega_j / \sum_k \omega_k$ . Let us assume for now that we allow loops. Then

$$\mathbb{E} \deg(i) = \sum_{j=1}^n \mathbb{E} \mathbf{1}_{\{i,j\} \in E} = \sum_{j=1}^n \left( w_i w_j / \sum_{k=1}^n w_k \right) = w_i. \quad (2.15)$$

where  $\mathbf{1}_\varphi$  is a random variable which outputs one if  $\varphi$  is satisfied. While we will remove all self-loops at the end of sampling method, for large  $n$  this simplification has negligible impact. Note that for proper choice of  $\omega$  one obtains almost surely power-law graphs [50].

Very well known Barabási-Albert random graph model  $\mathcal{G}_n^{\text{BA}}(m_0)$  with  $m_0 \in \mathbb{Z}_{\geq 1}$ , which was designed to simulate evolution of Internet network [42]. The procedure iteratively adds vertices as long as the final graph has  $n$  vertices. There are two nonequivalent sampling procedures that share similar concept and produce graphs with similar properties. In the first, original version algorithm starts with complete graph  $K_{m_0}$ . Then new vertex  $v$  is added, and is connected to  $m_0$  already existing vertices. Already present vertex  $w$  will be a neighbor of  $v$  with probability  $\deg(w)/(2|E|)$ . With such procedure only simple, connected graphs are sampled, with power-law distribution.

Unfortunately, the very first definition provided by Barabási and Albert in [42] was not precise, and in past years many nonequivalent definitions were proposed and utilized [51–53]. Because of that, result concerning Barabási-Albert model presented in Chapter 6 will be strengthen by numerical investigations based on the model implemented in [53].

The directed version of Barabási-Albert random graph model  $\vec{\mathcal{G}}_n^{\text{BA}}(m_0)$  is defined analogically, however instead of adding edge  $\{v, w\}$  for newly added  $w$ , arc  $(v, w)$  is added [53]. For the directed version of Erdős-Rényi graph model  $\vec{\mathcal{G}}_n^{\text{ER}}(p)$  each *arc* is independently added with probability  $p$ .

Finally, random orientation of an undirected graph  $G = (V, E)$  is a digraph  $\vec{G} = (V, \vec{E})$ , where each edge  $\{v, w\} \in E$  was replaced by one of arcs  $(v, w)$  or  $(w, v)$ . Note that for random orientation of a graph we have  $|\vec{E}| = |E|$ .

## 2.3 Stochastic and quantum dynamics

### 2.3.1 Stochastic evolution

Let us consider closed system which can be in any of canonical state  $x \in X$ . Provided the system follows the rules of statistical mechanics, its state can be defined with the probability distribution over  $X$ . For finite  $X$  it has a probability vector representation  $p = \sum_{x \in X} p_x |x\rangle \in \mathbb{R}^X$ , where  $p_x$  is the probability that the system is in the state  $x$ .

We define continuous-time stochastic evolution through differential equation

$$\frac{dp(t)}{dt} = -Lp(t), \quad (2.16)$$

with  $L$  being a transition rate matrix [18] and  $t$  being the evolution time. Columns of the transition rate matrix needs to sum to 0, furthermore the diagonal elements needs to be nonnegative and out-diagonal needs to be nonpositive. Note that the matrix does not have to be symmetric.

Suppose we have two probabilistic systems that can be in canonical states  $X$  and  $Y$  respectively. Then the joint system can be defined through probabilistic vectors over  $X \times Y$ , *i.e.* on  $\mathbb{R}^X \otimes \mathbb{R}^Y$  space. In particular if the first system is in state  $p^X$  and second in  $p^Y$ , and the random these systems are independent, then the joint system's probability vector takes the form  $p^X \otimes p^Y$ .

One can also define a discrete-time stochastic evolution through stochastic matrix  $P$  and the evolution

$$p(t+1) = Pp(t). \quad (2.17)$$

Note that  $P$  has to be a stochastic matrix in this case.

### 2.3.2 Evolution in quantum systems

**Closed quantum system** Let us consider closed system which can be in any canonical state  $x \in X$ . If the the system obeys the laws of quantum mechanics, its (quantum) state has representation as a normed vector in Euclidean space  $\mathbb{C}^X$ , called a pure state.

The continuous-time quantum evolution of the state  $|\psi_t\rangle$  is defined by Schrödinger equation

$$\frac{d|\psi(t)\rangle}{dt} = -i\hbar H |\psi(t)\rangle, \quad (2.18)$$

where  $H \in \mathbb{C}^{X \times X}$  is the Hamiltonian of the system and  $\hbar$  is the reduced Planck constant. In order to defined quantum state preserving evolution one need to assume that Hamiltonian is a Hermitian operator. It is common to assume that  $\hbar = 1$ , which can be done by careful physics units change.

Suppose  $H$  does not depend on the evolution time  $t$ , and that at time  $t = 0$  we start with quantum state  $|\psi(0)\rangle$ . Then the Eq. (2.18) can be solved analytically into

$$|\psi(t)\rangle = \exp(-itH) |\psi(0)\rangle. \quad (2.19)$$

Note that  $\exp(-itH)$  is a unitary matrix.

Suppose we have two quantum systems. Furthermore, suppose the first system is in state  $|\phi_X\rangle \in \mathbb{C}^X$  and second in  $|\phi_Y\rangle \in \mathbb{C}^Y$ . Then the state of the composite system is  $|\phi_X\rangle \otimes |\phi_Y\rangle \in \mathbb{C}^X \otimes \mathbb{C}^Y$ . General state of the quantum system lies in a in  $\mathbb{C}^X \otimes \mathbb{C}^Y$  space. Similarly as for probability distribution, it may be the case that a quantum state of the composite system cannot be written in the form  $|\phi\rangle \otimes |\psi\rangle$ . Such dependence has different properties and thus earned a new term – entanglement. Entanglement takes a vital role in quantum communication, however in context of quantum computation it can be seen as an extension of superposition. Thus understanding of quantum entanglement is not vital for understanding our results.

Contrary to the statistical mechanics, measurement may affect the state of the quantum system. Suppose we have a classical system described by probability vector  $p$ . Suppose the measurement is performed but its output is ignored. Then the description of the system has not changed from our point of view—the system can still be described by the same probability vector  $p$ .

This is no longer the case for the quantum system. Suppose the system  $\mathbb{C}^X$  is in the state  $|\psi\rangle$  and we perform the measurement in the canonical

basis. Then the classical outcome of the measurement will be  $x \in X$  with probability  $|\langle \psi | x \rangle|^2$ , and the system will change into  $|x\rangle$ . In case we ignore the classical output, we can only say that the system will be a statistical mixture of quantum states  $\{|x\rangle : x \in X\}$ . The mathematical representation of such measurement outcome requires a density operator notation, which will be explained later in this chapter.

While in statistical mechanics different probabilistic vector represents different states of the system, in quantum mechanics two different vectors may be physically indistinguishable. If  $|\psi\rangle$  is the quantum state of the system, then  $\exp(-i\alpha)|\psi\rangle$  for any  $\alpha \in \mathbb{R}$  is a description of the very same state. This means, that no measurement can distinguish these two states, even in probability. The factor  $\exp(-i\alpha)$  is called a *global phase*. Because of that  $H$  and  $H + \alpha I$  represents the same quantum evolution, since

$$\exp(-it(H + \alpha I))|\psi\rangle = \exp(-itH)\exp(-it\alpha I)|\psi\rangle. \quad (2.20)$$

**Open quantum system** Suppose we have a quantum system that is in state  $|\psi\rangle \in \mathbb{C}^X$  with probability  $p$  and in  $|\varphi\rangle \in \mathbb{C}^X$  with probability  $1 - p$ . For such description we use the notion of mixed states. Such states can be represented by density matrices—the example would take the form

$$\varrho = p|\psi\rangle\langle\psi| + (1 - p)|\varphi\rangle\langle\varphi| \in \mathbb{C}^{X \times X}. \quad (2.21)$$

In general if a quantum system is in state  $|\psi_i\rangle$  with probability  $p_i$ , then the state can be described by a mixed quantum state

$$\varrho = \sum_i p_i |\psi_i\rangle\langle\psi_i|. \quad (2.22)$$

Note that if system is in a pure state  $|\psi\rangle$  with probability 1, then we have  $\varrho = |\psi\rangle\langle\psi|$ . In this representation there is no notion of global phase, and different density operators results in different quantum states. Similarly as in the case of pure quantum states, if two separable systems are in states  $\varrho_1$  and  $\varrho_2$ , then the joint system is in state  $\varrho_1 \otimes \varrho_2$ .

We can enrich the quantum evolution to open-system evolution, which assumes the existence of interactions of the quantum system with the environment. In the scope of this dissertation we will consider GKSL master equation which takes the form [54]

$$\frac{d\varrho}{dt} = -i\hbar[H, \varrho] + \sum_{L \in \mathbb{L}} \gamma_L \left( L\varrho L^\dagger - \frac{1}{2}\{L^\dagger L, \varrho\} \right). \quad (2.23)$$

Here  $H \in \mathbb{C}^{X \times X}$  is the Hamiltonian which describes coherent, closed system interaction. Set  $\mathbb{L}$  consists of Lindblad operators  $L \in \mathbb{L}$ , which may be arbitrary complex-valued  $L \in \mathbb{C}^{X \times X}$  matrices. Values  $\gamma_L$  are called intensities. Lindblad operators describe dissipative, open-system interactions. By  $[A, B] = AB - BA$  we denote the commutator, and by  $\{A, B\} = AB + BA$  the anticommutator. We assume  $\hbar = 1$  and  $\gamma_L \equiv 1$  for all  $L \in \mathbb{L}$ . Note that the GKSL master equation encapsulates both Schrödinger and stochastic equation.

Eq. (2.23) has an equivalent representation of the form [55]

$$\frac{d|\varrho_t\rangle\rangle}{dt} = S|\varrho_t\rangle\rangle, \quad (2.24)$$

where

$$S = -i(H \otimes \mathbf{I} - \mathbf{I} \otimes \bar{H}) + \sum_{L \in \mathbb{L}} \left( L \otimes \bar{L} - \frac{1}{2} L^\dagger L \otimes \mathbf{I} - \frac{1}{2} \mathbf{I} \otimes L^\top \bar{L} \right). \quad (2.25)$$

We call  $S$  an evolution generator. Assuming the Hamiltonian and Lindblad operators are time-independent, we can provide a solution of the system

$$|\varrho(t)\rangle\rangle = \exp(St)|\varrho(0)\rangle\rangle, \quad (2.26)$$

where  $\varrho(0)$  is the initial state.

Quantum measurement theory can be enriched as well, however in our case we will be satisfied with simply generalizing the notion of von Nuemann measurement into mixed states notation. Let  $\mathbb{C}^{[n]}$  be a quantum system, and let  $\{|\varphi_i\rangle\}_{i=1}^n$  be its orthonormal basis. Let  $\varrho$  be the mixed quantum state of the system being measured. Then, the measurement outputs  $i$  with probability  $\langle \varphi_i | \varrho | \varphi_i \rangle$ . In the scope of this dissertation we will ignore the quantum state coming from the measurement, and we can consider measurement as the operation destroying the quantum system.

## 2.4 Random and quantum walk theory

### 2.4.1 Typical random and quantum walks

Let  $\vec{G} = (V, \vec{E})$  be a directed graph and let  $\mathbb{R}^V$  be the space of the walker's evolution. The continuous-time random walk (CTRW) is defined through continuous-time stochastic evolution given by Eq. (2.16). The operator defining the walk has to satisfy  $\langle w | L | v \rangle = 0$  iff  $(v, w) \notin \vec{E}$ . This way the probability is not (directly) transported through nonexisting arcs. A discrete-time

equivalent is defined through Eq. (2.17) with similar condition  $\langle w|P|v\rangle = 0$  iff  $(v, w) \notin \vec{E}$ . Note that in general it is acceptable to have  $\langle w|P|v\rangle = 0$  even if  $(v, w) \in \vec{E}$ , however in this dissertation we consider only time-independent evolution, and such situation essentially excludes the arc from  $\vec{E}$ . Thus such relaxation of the definition is of no interest. We call  $p_v(t)$  a probability of state being at vertex  $v$  after time  $t$ .

There is a special class of random walks with unbiased choice of probability transfer. For such a walk, for any  $(v, w), (v, w') \in \vec{E}$  we have  $\langle w|L|v\rangle = \langle w'|L|v\rangle$ . In the case of discrete random walk, we define equivalent definition  $\langle w|P|v\rangle = \langle w'|P|v\rangle = \frac{1}{\deg v}$ . We will call this special kind of random walks a *uniform random walks*. Note that contrary to the discrete random walk, the choice of continuous-time random walk is non-unique. In this dissertation we mostly consider Laplacian matrix as an evolution operator of uniform random walk.

The continuous-time quantum walk (CTQW) is defined similarly as the continuous-time random walk [18]. Let  $G = (V, E)$  be an undirected graph and let  $\mathbb{C}^V$  be the space of the walker's evolution. The evolution is defined through the Schrödinger equation provided in Eq. (2.18), with extra condition  $\langle w|H|v\rangle = 0$  iff  $\{v, w\} \notin E$ . Since the evolution operator has to be Hermitian, CTQW is well-defined only for undirected graphs. The probability of the walker to be at a vertex  $v$  after evolution time  $t$  equals  $|\langle v|\psi(t)\rangle|^2$ . Similarly as for the continuous-time random walk, we call quantum walk a uniform CTQW iff  $\langle w|H|v\rangle = \langle w'|H|v\rangle$  for any choice of  $\{v, w\} \in E$ . Note that the normalized Laplacian defines a valid CTQW, while adjacency matrix and Laplacian define a valid uniform CTQW. Note that the evolution for  $d$ -regular graphs are equivalent independently on chosen graph matrix. Since

$$\exp(-itL) = \exp(-it(dI - A)) = \exp(-itd) \exp(-it(-A)), \quad (2.27)$$

the evolution using Laplacian is equivalent to adjacency matrix up to the global phase and sign of  $t$ . Similarly

$$\exp(-it\mathcal{L}) = \exp\left(-it\left(I - \frac{1}{d}A\right)\right) = \exp(-it) \exp\left(-i\left(-\frac{t}{d}\right)A\right), \quad (2.28)$$

hence the normalized Laplacian is equivalent to adjacency matrix up to global phase and the time rescaling  $t \mapsto -\frac{t}{d}$ . Similar equivalence for nonregular graphs does not take place, which also has impact on the application of the walk [32].

It is far more complicated to design a discrete-time quantum walk. Asserting similar condition to the above one for unitary matrix leads to pathological evolution, counter-intuitively prohibiting amplitude transfer [56]. Instead



it is common to enlarge the walker's space into  $\mathbb{C}^{[m]}$  and provide mapping  $h : [m] \rightarrow V$ . This way the probability of being at vertex  $v$  equals

$$\sum_{j \in h^{-1}(v)} |\langle j | \psi(t) \rangle|^2. \quad (2.29)$$

While discrete-time quantum walks are beyond the topic of this dissertation, system enlargement in order to guarantee special quantum properties will be of use in Chapter 3.

Finally let us define a quantum stochastic walk (QSW). This model was proposed in [41] to encapsulate the CTRW and CTQW, but also to provide new form of dynamics. Let us recall GKSL master equation

$$\frac{d\rho}{dt} = -i[H, \rho] + \sum_{L \in \mathbb{L}} \left( L\rho L^\dagger - \frac{1}{2}\{L^\dagger L, \rho\} \right). \quad (2.30)$$

Note that GKSL master equation encapsulates continuous-time stochastic and quantum evolutions [41]. Hence we can define a local environment interaction QSW as a mixture of stochastic and quantum evolution.

**Definition 2.1.** Let  $\vec{G} = (V, \vec{E})$  be a digraph and  $G = (V, E)$  be its underlying graph. Let  $H \in \mathbb{C}^{V \times V}$  be a hermitian operator such that for  $v, w \in V$  satisfying  $v \neq w$

$$\{v, w\} \notin E \iff \langle w | H | v \rangle = 0. \quad (2.31)$$

Let  $\mathbb{L} = \{c_{ij} | j \rangle \langle i | : (i, j) \in \vec{E}, c_{ij} \neq 0\}$  be a collection of Lindblad operators. Then we call a GKSL master equation with Hamiltonian  $H$  and Lindblad operators collection  $\mathbb{L}$  a *local environment interaction QSW* (LQSW).

Note that condition  $c_{ij} \neq 0$  can be relaxed to  $c_{ij} > 0$  based on the form of GKSL master equation. If  $H$  is the adjacency matrix of  $G$  and  $c_{ij} = 1$  for any  $(i, j) \in \vec{E}$ , then we call a LQSW a *standard LQSW*. If we consider a GKSL master equation of the form

$$\frac{d\rho}{dt} = -i(1 - \omega)[H, \rho] + \omega \sum_{L \in \mathbb{L}} \left( L\rho L^\dagger - \frac{1}{2}\gamma_L\{L^\dagger L, \rho\} \right). \quad (2.32)$$

with extra smooth transition parameter  $\omega \in [0, 1]$ , we call it an *interpolated LQSW*. Note that for  $\omega = 0$  and  $\omega = 1$  we recover respectively CTQW and CTRW. The LQSW has a potential to be applied in quantum computer science [14, 57].

Note that in [41] authors proposed a more complicated quantum walk model, which cannot be represented as a LQSW. We will focus on this model in the Chapter 3.

### 2.4.2 Walk quality measures

In order to quantify the ‘usefulness’ of walks, several measures can be proposed. In the scope of the dissertation, we will focus on the propagation on the graph and the search efficiency.

#### Propagation speed

A propagation of a walk is typically defined by the pace of change of the second moment of a position of the walker in time on a infinite path graph. Let  $G = (\mathbb{Z}, E)$  be an infinite path graph with  $E = \{\{k, k+1\} : k \in \mathbb{Z}\}$ . The evolution starts in a state localized at position 0, which for both CTQW and CTRW is  $|0\rangle$ . Provided  $p_k(t)$  is the probability of walker being measured in  $k$  after evolution time  $t$ , the central second moment equals

$$\mu_2(t) = \sum_{k \in \mathbb{Z}} k^2 p_k(t). \quad (2.33)$$

For time-independent walk we always have  $\mu_2(t) = \mathcal{O}(t^2)$ . It can be easily explained in term of discrete walks. After  $t$  steps the probability of finding an element at position  $k$  such that  $|k| > t$  equals zero. Thus

$$\mu_2(t) = \sum_{k=-t}^t k^2 p_k^t \leq t^2 \sum_{k=-t}^t p_k^t = t^2. \quad (2.34)$$

Provided  $\mu_2(t) = \Theta(t^\alpha)$ , we use  $\alpha$  as a measure of propagation of the walk. We distinguish the following propagation regimes:

1. if  $\alpha < 1$ , the process is sub-diffusive,
2. if  $\alpha = 1$ , the process obeys a normal diffusion regime,
3. if  $1 < \alpha < 2$ , the process is super-diffusive,
4. if  $\alpha = 2$ , the process obeys a ballistic diffusion regime.

In general, higher exponent  $\alpha$  means the walker faster propagates through a graph, which in turn may provide algorithmic speed-up. It can be shown that time-independent random walk obeys a normal diffusion regime, as the probability distribution can be approximated by Gaussian distribution. On the other hand, one can show that CTQW obeys a ballistic diffusion regime [20].

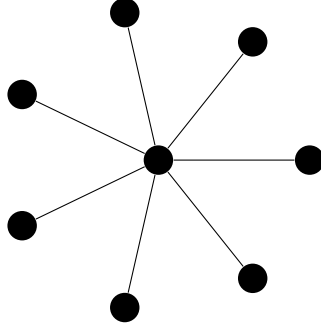


Figure 2.1: Star graph with 8 vertices.

### Search algorithms

For general search problem it is assumed that the single or multiple elements of the database are marked, and the goal is to find the elements in as short time as possible. In case of walk search, vertices plays the role of elements of the database, and the evolution has to be a walk defined by some graph. Contrary to the propagation of the walk, the way the time required to find a marked vertex is determined differs between random and quantum walks.

In case of discrete-time random walk given by stochastic matrix  $P$ , the evolution starts in its stationary distribution  $p_{\text{stat}}$ . At each step of random walk evolution walker is checked whether it is at the marked vertex. If it is the case, then the procedure stop, otherwise the step is repeated. Note that for general graph it is possible (although highly unlikely for uniform random walk) to search for a marked vertex infinitely. However expected Mean First-Passage Time  $\langle T_v \rangle$  is necessarily finite [58]. The only condition on  $G$  is to be strongly connected. Note there are known explicit formulas for uniform random walk search [58]. However, in Chapter 6 we will derive and present an alternative formula based on quantities used for quantum search [39].

Note that for the random walk search for almost all vertices  $\langle T_v \rangle = \Omega(|V|)$ , since within  $k$  steps at most  $k$  different vertices can be visited. This does not mean that some vertices cannot be found in shorter time. For example for star graph, i.e. a tree graph with single vertex connected to all the others (see Fig. 2.1), the walker either stops at step 0 or at step 1.

For the quantum walk we cannot measure the system too often, due to destructive behavior of the measurement. Instead it is necessary to understand the graph structure, and determine the optimal  $T_{\text{opt}}$  time, after which the quantum state is measured. The choice of  $T_{\text{opt}}$  has to take into account the success probability of checking the state after given evolution time. Since quantum evolution is quasi-periodic, choosing too large measurement time

may also results in  $\approx 0$  success probability, the same way as it happens for Grover search [3].

In the scope of the dissertation we will focus on the original CTQW-based quantum search algorithm. Let  $G = (V, E)$  be an undirected graph and  $w \in V$  be a marked node. The Hamiltonian defining the evolution takes the form

$$H = -\gamma H_G - |w\rangle\langle w|, \quad (2.35)$$

and originally the evolution starts in uniform superposition  $|s\rangle = \frac{1}{\sqrt{n}} \sum_{v \in V} |v\rangle$ . Here  $H_G$  is a symmetric graph matrix and  $\gamma$  is a jumping rate which has to be determined before running the algorithm.

Let us consider a complete graph  $K_n$ , *i.e.* graph with all  $n$  vertices being connected. Since the graphs is vertex-transitive, and thus regular, the choice of graph matrix and marked vertex is not relevant. Note that  $A + I = n|s\rangle\langle s|$ . Hence, despite the fact the evolution takes places in  $n$ -dimensional space, effectively it runs on a subspace spanned by  $\{|s\rangle, |w\rangle\}$ . The initial state lies in this subspace. Let  $|\bar{s}\rangle = \frac{1}{\sqrt{n-1}}(\sqrt{n}|s\rangle - |w\rangle)$ . The Hamiltonian defined as  $H_G = A$ , spanned by  $|\bar{s}\rangle$  and  $|w\rangle$ , equivalent to the above one takes the form

$$\tilde{H} = - \begin{bmatrix} \gamma(n-2) & \gamma\sqrt{n-1} \\ \gamma\sqrt{n-1} & 1 \end{bmatrix}. \quad (2.36)$$

Note for  $\gamma = \frac{1}{n-2}$  the values on the diagonal equals hence is irrelevant. For such choice of the  $\gamma$ , the simplified Hamiltonian takes the form

$$\tilde{H} = - \begin{bmatrix} 0 & \frac{\sqrt{n-1}}{n-2} \\ \frac{\sqrt{n-1}}{n-2} & 0 \end{bmatrix}. \quad (2.37)$$

For  $T_{\text{opt}} \approx \pi\sqrt{n}/2$  the Hamiltonian transforms state  $|\bar{s}\rangle$  to  $\approx |w\rangle$ . Since  $\langle s|\bar{s}\rangle = 1 - o(1)$ , the same Hamiltonian transforms  $|s\rangle$  to  $\approx |w\rangle$  as well. Hence after  $\Theta(\sqrt{n})$  evolution time there is  $1 - o(1)$  probability of finding the marked node  $w$ . Alternative derivation can be also found in [59].

Note that after  $\pi\sqrt{n}$  evolution time the Hamiltonian will transform  $|s\rangle$  to  $\approx |s\rangle$ , which gives  $\mathcal{O}(1/n)$  probability of finding the node. Hence determining the measurement time in complexity is not enough to guarantee high success probability. The situation is even worse for jumping rate, as only  $\gamma(1 + \mathcal{O}(1/\sqrt{n}))$  jumping rates would give the same result. Otherwise the diagonal elements will disturb the evolution [30, 33, 39].

To determine the actual complexity of quantum search algorithms, the cost of measurement and preparing the initial state [39, 60] should be taken into account. In this dissertation we assume that the time required for state

preparation and measurement is significantly smaller compared to the evolution time. This approach is frequently used in the literature [18, 28, 33, 36, 38, 39, 46]. It is also common to choose different initial state [39], which may depend on a chosen graph matrix  $H_G$ , but not marked vertex  $w$ .

Since we focus on the complexity of the search, we will be satisfied with obtaining  $\Theta(1)$  success probability. Note that repeating the procedure of quantum search exponentially decrease the probability of failure.

Finally let us recall recent results concerning quantum search on general graphs. In [38] authors proposed alternative continuous-time walk search, which was faster compared to any discrete random search. However, the proposed method required quadratically large linear space compared to the proposed CTQW-based search [18]. Finally in [39] authors proposed very general results concerning the optimality of the CTQW-based quantum search. However in this case full eigendecomposition of  $H_G$  has to be known in order to apply their results, which in general is a computationally difficult problem compared to quantum or even random search. Finally, the case of Erdős-Rényi graph was considered in [33–35]

## 2.5 Numerical analysis and tools

In this section we describe a numerical procedure for determining exponent  $\alpha$  for function  $f = \Theta(n^\alpha)$ . Furthermore, in order to simplify the reproduction of our numerical results, we described tools used in our numerical experiment and provide the link where the code can be found.

### 2.5.1 Exponent estimation

Suppose  $f(t) = Ct^{\alpha \pm \varepsilon}$ . Then we have

$$\log(f(t)) = (\alpha \pm \varepsilon) \log(t) + \log(C + o(1)). \quad (2.38)$$

Note  $\alpha$  is a slope of  $\log(\mu_2(t))$  versus  $\log(t)$ . Several approaches can be proposed in order to estimate  $\alpha$ . First, one can estimate the slope of linear regression of pairs  $(\log t_i, \log f(t_i))$ . This approach was satisfactory in case of walk search analysis, however for propagation the values for small  $t$  disturbed the actual value.

In case of walk propagation, the estimation of  $\alpha$  goes as follows. For time-points  $t_1, \dots, t_k$  we calculate  $f(t_1), \dots, f(t_k)$ . We choose batch size  $l \ll k$  and calculate the slope  $\alpha_i$  based on  $(t_i, f(t_i)), \dots, (t_{i+l-1}, f(t_{i+l-1}))$  in a way described in previous paragraph. Thus we obtained  $k - l + 1$  approximations of  $\alpha$ . It is expected that the larger the values of time-points are, the better

the estimation of  $\alpha$  is. For convenience we choose  $(t_{i+l-1} + t_i)/2$  to be the time-point corresponding to the estimated  $\alpha_i$  when plotting the results.

### 2.5.2 Software used

Numerical analysis presented in this dissertation was generated with Julia programming language version 1.5.2 [61]. The simulation was done using in particular Expokit.jl [62], LightGraphs.jl [53] and QSWalk.jl [63]. The latter package is the package co-developed by the author of this dissertation. The code is available on GitHub under <https://doi.org/10.5281/zenodo.4548423>.

## Chapter 3

# Non-moralizing Quantum Stochastic Walk

Despite the evolution formula for CTRW and CTQW are very similar, the stochastic and quantum evolution exhibits very different properties. For random walks, based on the Perron-Frobenius theorem, the evolution converges to a fixed distributions for connected undirected graphs. In the case of quantum walk, we observe quasi-periodic evolution.

**Lemma 3.1** ([23]). *Let  $|\psi\rangle \in \mathbb{C}^X$  be vector of a finite-dimensional linear space and let  $U \in \mathbb{C}^{X \times X}$  be a unitary matrix. For any  $\varepsilon > 0$  there exists  $n \geq 1$  such that*

$$|\langle \psi | U^n | \psi \rangle| > 1 - \varepsilon. \quad (3.1)$$

Based on the lemma we can see that by choosing proper  $n \geq 1$  we can be arbitrarily close to the initial state. The proof of the lemma was based on the theorem provided in [64] for continuous-time evolution.

The lemma shows why it is complicated to define a quantum walk formula for the directed graphs. Traditionally the space of the walk is splitted into orthogonal subspaces, each attached to a different vertex. However based on the lemma above, if we start at the sink vertex  $v$ , then based on the graph topology we cannot move outside the sink because of the graph topology. Algebraically, it means that  $\langle v | U | v \rangle = 1$ . However this means that  $\langle v | U | w \rangle = 0$  for any choice of  $w \neq v$ . From this we can see that one cannot amplify amplitude on a sink vertex with the unitary evolution. For continuous-time evolution, another obstacle is that Hamiltonian has to be a Hermitian matrix.

In this chapter we overcome the limitation by utilizing stochastic quantum walks. However, this kind of walk does not obey ballistic propagation (see Fig. 3.1b). Hence despite the fact that the LQSW may be a well-defined

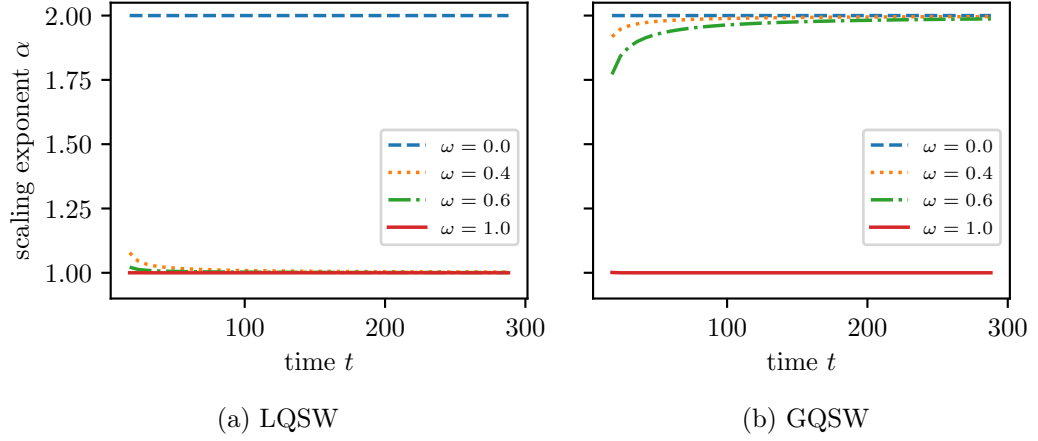


Figure 3.1: Numerical investigation of the propagation for (a) interpolated standard GQSW and (b) interpolated standard LQSW. We can see that for  $\omega < 0.75$  scaling exponent approaches 2, while decreases in time. The calculations were made for interpolating parameters  $\omega = 0, 0.4, 0.6, 1$  for path graph with time-points  $t = 6, 12, \dots, 300$ .

evolution preserving the digraph topology (which in fact we will prove in the next Chapter), it does not obey super-diffusive regime. However, the quantum stochastic walk is not limited to Lindblad operators of the form  $|v\rangle\langle w|$  [41].

**Definition 3.2.** Let  $\vec{G} = (V, \vec{E})$  be a digraph and  $G = (V, E)$  be its underlying graph. Let  $H \in \mathbb{C}^{V \times V}$  be a hermitian operator, and  $\mathcal{L} = \{L_1, \dots, L_k\}$  with  $L_i \in \mathbb{C}^{V \times V}$  of the form

$$H = \sum_{\{v,w\} \in E} c_{\{v,w\}} |v\rangle\langle w| + \bar{c}_{\{v,w\}} |w\rangle\langle v|, \quad (3.2)$$

$$L_i = \sum_{(v,w) \in \vec{E}} c_{(v,w),i} |w\rangle\langle v|, \quad (3.3)$$

where  $c_{\{v,w\}}, c_{(w,v),i} \in \mathbb{C}_{\neq 0}$ . Then we call a GKSL master equation with Hamiltonian  $H$  and proposed Lindblad operators a *global environment interaction QSW* (GQSW).

We propose equivalent standard and interpolated GQSW. If  $H$  is the adjacency matrix of  $G$  and  $L$  is the adjacency matrix of  $\vec{G}$ , then we call a GQSW with  $H$  and  $\{L\}$  a *standard GQSW*. We define an interpolated GQSW analogously to an interpolated LQSW.



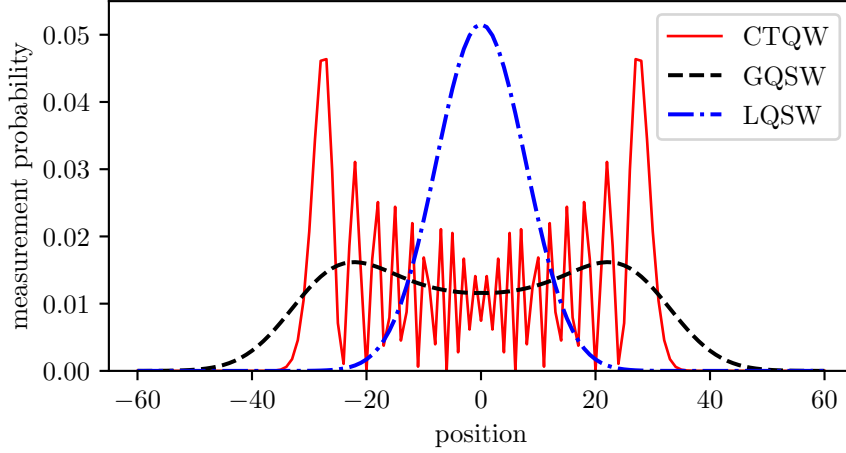


Figure 3.2: Probability distribution of CTQW with Hamiltonian being adjacency matrix (red line), standard LQSW (black dashed line), and standard GQSW (blue dash-dotted line). We can see that the LQSW is highly concentrated around 0, contrary to other models. The computation were made for evolution time  $t = 15$  and path graph with 121 vertices. The evolution started in state  $|0\rangle\langle 0|$ .

GQSW is a quantum walk based on open system evolution, but yielding different evolution than LQSW (see Fig. 3.2). As we will see it obeys a ballistic propagation. However this is achieved at cost of introducing extra edges not existing even in the underlying graph. Thus in this chapter we start with analytical justification of why the ballistic propagation for the GQSW. Next we propose a modification which preserves at least superdiffusive propagation and removed the undesired edges. The new quantum walk model will be called *nonmoralizing quantum stochastic walk*.

### 3.1 Ballistic propagation for GQSW

In this section we will show that the GQSW model obeys ballistic propagation. Let us consider the GQSW on path graph  $P_n = ([n], E_n)$ , where for  $i, j \in [n]$  we have  $i, j \in E_n \iff |i - j| = 1$ . Let  $A$  be an adjacency matrix of  $P_n$ . Then the GQSW takes the form.

$$\frac{d\rho}{dt} = -i(1 - \omega)[A, \rho] + \omega \left( A\rho A^\dagger - \frac{1}{2}\{A^\dagger A, \rho\} \right). \quad (3.4)$$

We start the evolution in  $\rho(0) = |0\rangle\langle 0|$ . Based on numerical results presented in Fig. 3.1b, we can see that for  $\omega \neq 1$  the scaling exponent approaches 2.

Below we will present the analytical derivation confirming our numerical investigations. Let  $\mu_m(t)$  be the  $m$ -th central moment of the probability distribution of the computational measurement of  $\varrho(t)$ . We will derive  $\alpha$  for which  $\mu_2(t)/t^\alpha \rightarrow c \neq 0$ .

The proofs consists of several parts. First we derive the probability distribution  $p_t$  fo  $\varrho(t)$  defined over path graph  $P_n$ . Since the adjacency matrix of the path graph is a Toeplitz matrix, its eigendecomposition is known, which in turns gives us the following theorem.

**Theorem 3.3.** *Given a interpolated standard GQSW on a path graph of order  $n$  with initial state  $\varrho(0) = |l\rangle\langle l|$  for some  $l \in \{1, \dots, n\}$ , the quantum state  $\varrho(t)$  at time  $t$  satisfies*

$$\begin{aligned} \langle k | \varrho(t) | k \rangle &= \left( \frac{2}{n+1} \right)^2 \sum_{i,j=1}^n \sin \left( \frac{ki\pi}{n+1} \right) \sin \left( \frac{kj\pi}{n+1} \right) \sin \left( \frac{li\pi}{n+1} \right) \sin \left( \frac{lj\pi}{n+1} \right) \times \\ &\times \exp \left[ -\frac{t}{2} \omega (\lambda_i - \lambda_j)^2 \right] \exp [-it(1 - \omega)(\lambda_i - \lambda_j)], \end{aligned} \quad (3.5)$$

where

$$\lambda_i = 2 \cos \left( \frac{i\pi}{n+1} \right). \quad (3.6)$$

The proof of the theorem can be found in Appendix A.1

By increasing the order of the graph we obtain the limit of the probability distribution. Note that in order to consider  $n \rightarrow \infty$ , we consider path graph with  $2n + 1$  vertices labeled by  $-n, \dots, n$ , and we start at vertex 0. we determine the probability distribution of the interpolated standard GQSW on infinite path by taking  $n \rightarrow \infty$ . The limiting probability distribution in  $n \rightarrow \infty$  takes the following form.

**Theorem 3.4.** *Given an interpolated standard GQSW on an infinite path with initial state  $\varrho(0) = |0\rangle\langle 0|$ , the quantum state  $\varrho(t)$  at time  $t$  satisfies*

$$\begin{aligned} \langle k | \varrho(t) | k \rangle &= \frac{1}{4\pi^2} \int_{-\pi}^{\pi} \int_{-\pi}^{\pi} \cos(kx) \cos(ky) \exp [-2\omega t (\cos(x) - \cos(y))^2] \\ &\times \exp [2it(1 - \omega)(\cos(x) - \cos(y))] dx dy. \end{aligned} \quad (3.7)$$

The proof can be found in Appendix A.1.2.

Despite we have not found a simple analytical formula for the integral above, we were able to find its Taylor expansion of the formula above. By proper summing it turns out that the moments are simply a polynomials in

$t$ , which provides the values of their scaling exponent directly. The results are concluded with following theorem.

**Theorem 3.5.** *Given a interpolated standard GQSW on an infinite path with initial state  $\varrho(0) = |0\rangle\langle 0|$ , for odd  $m$  the  $m$ -th moment equals zero. For even  $m$  we have*

$$\mu_m(t) = \begin{cases} \left(\frac{m}{2}\right)(\omega - 1)^m(1 + o(1))t^m, & \omega \in [0, 1), \\ \frac{m!}{(m/2)!8^{m/2}} \binom{m}{m/2}(1 + o(1))t^{m/2}, & \omega \in 1. \end{cases} \quad (3.8)$$

The case  $\omega > 0$  is proven in Appendix A.2, the  $\omega = 0$  is a standard CTQW evolution and the proof can be found in [20]. Formally in [20] author shown that for even  $m = 2k$

$$\lim_{t \rightarrow \infty} \mu_m(t)/t^m \rightarrow \frac{(2k-1)!!}{(2k)!!} = \frac{(2k)!}{((2k)!!)^2} = \binom{2k}{k} \frac{1}{2^{2k}} = \binom{m}{m/2} \frac{1}{2^m}. \quad (3.9)$$

The difference in factor  $1/2^m$  results from time rescaling  $t \leftarrow \frac{t}{2}$ .

As we mentioned before, the  $m$ -th moments are in fact polynomials in  $t$  and we were able to find closed formula. The formula can be used to determine the precise form of  $\mu_m(t)$  for any  $\omega$ . In particular for  $\omega \in (0, 1)$  we have  $\mu_2(t) = 2\omega t + 2(1 - \omega)^2 t^2$ .

Thanks to the theorem above we can confirm the ballistic propagation of interpolated standard GQSW with the following theorem, which is the main results of this section.

**Theorem 3.6.** *Let  $\alpha(\omega)$  be the scaling exponent of interpolated standard GQSW on infinite path with initial state  $\varrho(0) = |0\rangle\langle 0|$ , given the transition parameter  $\omega \in [0, 1]$ . Then*

$$\alpha(\omega) = \begin{cases} 2, & \omega \in [0, 1), \\ 1, & \omega = 1. \end{cases} \quad (3.10)$$

## 3.2 Spontaneous moralization in GQSW

In previous section we considered a GQSW and we shown, that despite of the presence of dissipation evolution, we observe the ballistic propagation. At the same time Lindblad operators do not need to be symmetric, thus GKSL master equation is a natural choice for evolution model of fast quantum walk definable on arbitrary directed graph.

Let  $\vec{G} = (V, \vec{E})$  be a directed graph and  $G = (V, E)$  be its underlying graph. Let  $\vec{A}$  be an adjacency matrix of the digraph and  $A$  be an adjacency

matrix of the underlying graph. Let us start with the interpolated standard GQSW of the form

$$\frac{d\varrho}{dt} = -i(1 - \omega)[A, \varrho] + \omega \left( \vec{A}\varrho\vec{A}^\dagger - \frac{1}{2}\{\vec{A}^\dagger\vec{A}, \varrho\} \right). \quad (3.11)$$

Note that for  $\omega \in (0, 1)$ , we expect to observe the backward propagation. This fact is unavoidable if we plan to utilize the coherent evolution for fast propagation. Unexpectedly, this is not the only effect that can be observed.

Let us consider the graph presented in Fig. 3.3 with interpolating parameter  $\omega = 1$  case, i.e. evolution with dissipative part only. The Lindblad operator takes the form

$$L = \vec{A} = |v_3\rangle\langle v_1| + |v_3\rangle\langle v_2| = |v_3\rangle(\langle v_1| + \langle v_2|). \quad (3.12)$$

Let us consider the evolution starting at state  $\varrho(0) = |v_1\rangle\langle v_1|$ . Since Hamiltonian is not present in the evolution and we expect that the Lindblad operator will follow the digraph topology, one should expect that  $\langle v_2|\varrho(t)|v_2\rangle = 0$  independently of chosen  $t \geq 0$ . This is not the case, as calculations shows

$$\begin{aligned} \varrho(t) = & \frac{1}{4}(e^{-t} + 1)^2 |v_1\rangle\langle v_1| + \frac{1}{4}(e^{-2t} - 1) |v_1\rangle\langle v_2| \\ & + \frac{1}{4}(e^{-2t} - 1) |v_2\rangle\langle v_1| + \frac{1}{4}(e^{-t} - 1)^2 |v_2\rangle\langle v_2| \\ & + e^{-t} \sinh(t) |v_3\rangle\langle v_3|. \end{aligned} \quad (3.13)$$

In a time limit we have

$$\lim_{t \rightarrow \infty} \varrho(t) = \frac{1}{4} |v_1\rangle\langle v_1| - |v_1\rangle\langle v_2| - |v_2\rangle\langle v_1| + |v_2\rangle\langle v_2| + \frac{1}{2} |v_3\rangle\langle v_3|, \quad (3.14)$$

which gives as 1/4 probability for measuring the vertex  $v_2$ .

Two explanations of the phenomena can be proposed. First, let us recall the evolution operator  $S$  given in Eq. (2.25)

$$S = -i(H \otimes \mathbf{I} - \mathbf{I} \otimes \bar{H}) + \sum_L \left( L \otimes \bar{L} - \frac{1}{2} L^\dagger L \otimes \mathbf{I} - \mathbf{I} \otimes L^\top \bar{L} \right). \quad (3.15)$$

Let us consider propagation from  $|a\rangle\langle\alpha|$  to  $|b\rangle\langle\beta|$ . We have

$$\begin{aligned} \langle b\beta| S |a\alpha\rangle = & \delta_{\alpha\beta} \langle a| \left( -iH - \frac{1}{2} \sum_L L^\dagger L \right) |b\rangle + \delta_{ab} \langle\beta| \left( iH - \frac{1}{2} \sum_L L^\top \bar{L} \right) |\alpha\rangle \\ & + \langle b| L |a\rangle \langle\beta| \bar{L} |\alpha\rangle. \end{aligned} \quad (3.16)$$

In our case we consider only real valued operator, thus conjugation can be added or remove without change on the operator. Thus we replace  $L^T$  with  $L^\dagger$  and  $\bar{L}$  with  $L$  to get

$$\begin{aligned} \langle b|\beta|S|a\alpha\rangle &= \delta_{\alpha\beta} \langle a|\left(-iH - \frac{1}{2} \sum_L L^\dagger L\right)|b\rangle \\ &+ \delta_{ab} \langle \beta|\left(iH - \frac{1}{2} \sum_L L^\dagger L\right)|\alpha\rangle \\ &+ \sum_L \langle b|L|a\rangle \langle \beta|L|\alpha\rangle. \end{aligned} \quad (3.17)$$

Let us simplify the equation part by ignoring the parts that fit the graph topology. In particular note that  $\langle b|L|a\rangle \langle \beta|L|\alpha\rangle$  is nonzero if  $(\alpha, \beta) \in \vec{E}$  and  $(a, b) \in \vec{E}$  which fits the graph topology. Furthermore, Hamiltonian has nonzero impact iff  $\alpha = \beta$  and  $\{a, b\} \in E$ . This introduces the backward propagation if only one direction is allowed of complex graph. However, Hamiltonian part introduces ballistic propagation as was shown in Sec. 3.1, thus we allow such not-along the graph propagation. Moreover, this does not explains our example, where the Hamiltonian was absent.

Let us consider the remaining part

$$-\frac{1}{2} \delta_{\alpha\beta} \sum_L \langle a|L^\dagger L|b\rangle + \frac{1}{2} \delta_{ab} \sum_L \langle \beta|L^\dagger L|\alpha\rangle. \quad (3.18)$$

We will consider only the first addend, the second can be considered analogically. Note that  $\delta_{\alpha\beta}$  implies that the problem appears only for propagation from  $|a\rangle\langle\alpha|$  to  $|b\rangle\langle\alpha|$  (or  $|a\rangle\langle\alpha|$  to  $|a\rangle\langle\beta|$ ). On the other hand for standard GQSW we have

$$\begin{aligned} \sum_L \langle a|L^\dagger L|b\rangle &= \langle a|\vec{A}^\dagger \vec{A}|b\rangle = \sum_{v \in V} \langle a|\vec{A}^\dagger|v\rangle \langle v|\vec{A}|b\rangle \\ &= |\{v : (a, v) \in \vec{E}, (b, v) \in \vec{E}\}|. \end{aligned} \quad (3.19)$$

Note that this is precisely the situation observed in our example, visualized in Fig. 3.3. Here  $a = v_1$ ,  $b = v_2$  and  $\alpha = \beta = v_3$ . Thus an additional connection is introduced between every vertices that have common child. While this would be acceptable in case of undirected edges, as we would introduce extra connection within radius 2, it is not acceptable in the case of directed graphs. Due to the similarities between graph moralization that occurs in machine learning [65], we call our phenomena *spontaneous moralization* or simply moralization.

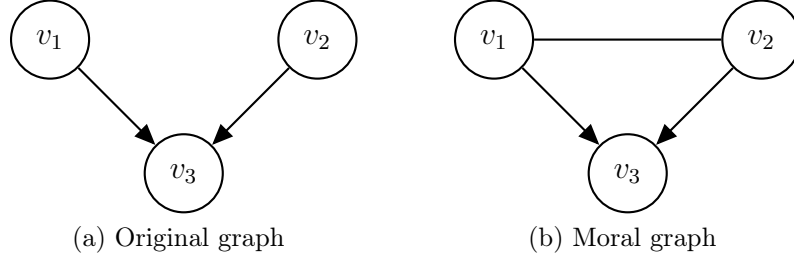


Figure 3.3: Visualization of (a) a directed graph and its (b) moral graph.

The first explanation provides the sufficient and necessary condition for when the moralization occurs. Second, simpler explanation suggests how to correct this effect. Let us consider again the example provided in Fig. 3.3a. The Lindblad operator takes the form

$$L = |v_3\rangle (\langle v_1| + \langle v_2|). \quad (3.20)$$

Note that arbitrary state of the form  $\alpha |v_1\rangle + \beta |v_2\rangle$  have a decomposition in the basis  $\{\frac{1}{\sqrt{2}}(|v_1\rangle + |v_2\rangle), \frac{1}{\sqrt{2}}(|v_1\rangle - |v_2\rangle)\}$ . Thus the Lindblad operator projects that part related to  $\frac{1}{\sqrt{2}}(|v_1\rangle + |v_2\rangle)$  onto  $|v_3\rangle$ , while leaves  $\frac{1}{\sqrt{2}}(|v_1\rangle - |v_2\rangle)$  unchanged. We can observe this in a quantum state as well

$$\begin{aligned} \varrho(t) = & \frac{1}{2} \frac{|v_1\rangle - |v_2\rangle}{\sqrt{2}} \frac{\langle v_1| - \langle v_2|}{\sqrt{2}} + \frac{e^{-2t}}{2} \frac{|v_1\rangle + |v_2\rangle}{\sqrt{2}} \frac{\langle v_1| + \langle v_2|}{\sqrt{2}} \\ & + \frac{1}{2} e^{-t} |v_1\rangle \langle v_1| + \frac{1}{2} e^{-t} |v_2\rangle \langle v_2| + e^{-t} \sinh(t) |v_3\rangle \langle v_3|. \end{aligned} \quad (3.21)$$

We can see that the only part spanned by  $|v_1\rangle, |v_2\rangle$  that remains unchanged is the part connected to  $\frac{1}{\sqrt{2}}(|v_1\rangle - |v_2\rangle)$  as predicted. This suggests that we need to change the operator in such a way that whole subspace spanned by the parents for each vertex is projected on the child subspace.

### 3.2.1 Spontaneous moralization removal

In this section we provide new QSW model called *nonmoralizing global interaction QSW* (NGQSW). Similarly to GQSW we construct single Lindblad operator which describes the structure of directed graph. However in this model we will remove the undesired moralization effect.

Let  $\vec{G} = (V, \vec{E})$  be a directed graph. We will construct new directed graph  $\underline{\vec{G}} = (\underline{V}, \underline{\vec{E}})$  homomorphic to  $\vec{G}$ . For consistency every graph object or operator that is connected to  $\underline{\vec{G}}$ , and thus nonmoralizing evolution, will be underlined as  $\underline{(\cdot)}$ .

Let for each  $v \in V$  define  $\underline{V}_v = \{\underline{v}^0 \dots, \underline{v}^{\text{indeg}(v)-1}\}$  iff  $\text{indeg}(v) > 0$ . If  $\text{indeg}(v) = 0$ , then let  $\underline{V}_v = \{\underline{v}^0\}$ . We choose

$$\underline{V} = \bigcup_{v \in V} \underline{V}_v. \quad (3.22)$$

Furthermore, let  $\vec{E}_{vw} = \{(\underline{v}, \underline{w}) : \underline{v} \in \underline{V}_v, \underline{w} \in \underline{V}_w\}$ . Then

$$\vec{E} = \bigcup_{(v,w) \in E} \vec{E}_{vw}. \quad (3.23)$$

Note that  $f : \underline{V} \rightarrow V$  of the form  $f : \underline{v} \mapsto v$  is a proper homomorphism from  $\vec{G}$  to  $\vec{G}$ . We call  $\vec{G}$  *demoralizing graph* and  $f$  a *natural homomorphism* from  $\vec{G}$  to  $\vec{G}$ . Note that  $f$  is also a proper homomorphism from underlying graphs of  $\vec{G}$  to  $G$ .

Let  $\underline{\varrho} \in \mathbb{C}^{\underline{V} \times \underline{V}}$  be a mixed state. We define a natural measurement in terms of the vertices of the original graph  $\vec{G}$  as

$$p(v) = \sum_{\underline{v} \in \underline{V}_v} \langle \underline{v} | \underline{\varrho} | \underline{v} \rangle. \quad (3.24)$$

Our goal is to define QSW on  $\vec{G}$  that will simulate the nonmoralizing evolution on  $\vec{G}$ . We cannot use simply an adjacency matrix of  $\vec{G}$  as it will lead to exactly the same moralization effect. The solution is to choose the orthogonal vectors for columns  $\underline{L}$  in such a way that  $\langle \underline{w} | \underline{L}^\dagger \underline{L} | \underline{v} \rangle = 0$  and  $\langle \underline{w} | \underline{L} | \underline{v} \rangle = 0$  for  $(v, w), (w, v) \notin \vec{E}$ .

**Lemma 3.7.** *Let  $\vec{G} = (V, \vec{E})$  be a directed graph and  $\vec{G}$  be its demoralizing graph. Let  $L_v \in \mathbb{C}^{\underline{V}_v \times P(v)}$  be such a matrix that columns are orthogonal, i.e.  $\langle u | L_v^\dagger L_v | w \rangle = 0$  for  $u \neq w$ , where  $u, w \in P(v)$ . Let*

$$\langle \underline{v}^k | \underline{L} | \underline{w}^l \rangle := \begin{cases} \langle \underline{v}^k | L_v | w \rangle, & (w, v) \in \vec{E}, \\ 0, & \text{otherwise.} \end{cases} \quad (3.25)$$

*Then for arbitrary  $\underline{v}, \underline{w}$  such that  $v \neq w$  we have  $\langle \underline{v} | \underline{L}^\dagger \underline{L} | \underline{w} \rangle = 0$ .*

*Proof.* Let  $v, w \in V$  be arbitrary different vertices and  $\underline{v}^k$  and  $\underline{w}^l$  respective

vertices from  $\vec{G}$ . We have

$$\begin{aligned}
\langle \underline{v}^k | \underline{L}^\dagger \underline{L} | \underline{w}^l \rangle &= \sum_{\underline{u} \in V} \langle \underline{v}^k | \underline{L}^\dagger | \underline{u} \rangle \langle \underline{u} | \underline{L} | \underline{w}^l \rangle \\
&= \sum_{\underline{u} \in V} \sum_{\underline{u}^i \in V_u} \overline{\langle \underline{u}^i | \underline{L} | \underline{v}^k \rangle} \langle \underline{u}^i | \underline{L} | \underline{w}^l \rangle \\
&= \sum_{\underline{u} \in C(v) \cap C(w)} \sum_{\underline{u}^i \in V_u} \overline{\langle \underline{u}^i | L_u | v \rangle} \langle \underline{u}^i | L_u | w \rangle. \\
&= \sum_{\underline{u} \in C(v) \cap C(w)} \sum_{\underline{u}^i \in V_u} \langle v | L_u^\dagger | \underline{u}^i \rangle \langle \underline{u}^i | L_u | w \rangle. \\
&= \sum_{\underline{u} \in C(v) \cap C(w)} \langle v | L_u^\dagger L_u | w \rangle.
\end{aligned} \tag{3.26}$$

Since  $v \neq w$  we have  $\langle v | L_u^\dagger L_u | w \rangle = 0$ , which ends the proof.  $\square$

A simple remark of the lemma is that the  $\underline{L}^\dagger \underline{L}$  impact on the evolution between the vertices is removed. Note that  $\underline{L}^\dagger \underline{L}$  part still have impact on the internal evolution. However, this does not imply that the amplitude is transferred not along the digraph, only within the space defined for a single vertex in  $\vec{G}$ .

Let us recall the example the example given in Fig. 3.3a. Its nonmoralizing version is presented in Fig. 3.4. We chose  $L_v$  to be Fourier matrices  $F_{|V_v|} \in \mathbb{C}^{|V_v| \times |V_v|}$ , i.e.

$$\langle j | F_{|V_v|} | k \rangle = \omega_{|V_v|}^{jk}, \tag{3.27}$$

where  $\omega_n = \exp(2\pi i/n)$ . The Lindblad operator takes the form

$$\underline{L} = |v_3^0\rangle\langle v_1^0| + |v_3^1\rangle\langle v_1^0| + |v_3^0\rangle\langle v_2^0| - |v_3^1\rangle\langle v_2^0|. \tag{3.28}$$

One can verify that, if  $\underline{\varrho}(0) = |v_1^0\rangle\langle v_1^0|$ , then the state takes the form

$$\underline{\varrho}(t) = e^{-2t} |v_1^0\rangle\langle v_1^0| + \frac{1}{2} (1 - e^{-2t}) (|v_3^0\rangle + |v_3^1\rangle)(\langle v_3^0| + \langle v_3^1|). \tag{3.29}$$

Note that for arbitrary  $t \geq 0$  we have  $\langle v_2^0 | \underline{\varrho}(t) | v_2^0 \rangle = 0$ , which confirms that our correction scheme fixes the moralization effect.

### 3.2.2 Premature localization

Through numerical analysis of the introduced model we noticed undesired phenomenon: premature localization. For example, let us consider the graph



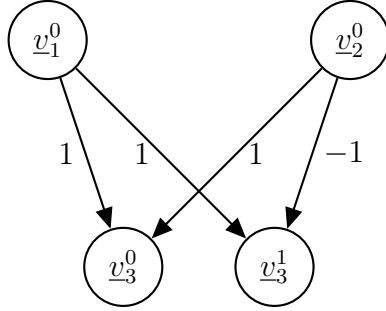


Figure 3.4: Visualization of the Lindblad operator in new model. The original graph is presented in Fig. 3.3a.

presented in Fig. 3.5a. In our model the Lindblad operator will represent the graph presented in Fig. 3.5b. Its Lindblad operator  $\underline{L}$  has the form

$$\underline{L} = \begin{bmatrix} 0 & 1 & 1 & 0 & 0 & 1 & 1 \\ 1 & 0 & 1 & 0 & 1 & 0 & 1 \\ 1 & 1 & 0 & 0 & 1 & 1 & 0 \\ 1 & 0 & 0 & 0 & 1 & 0 & 0 \\ 0 & 1 & -1 & 0 & 0 & 1 & -1 \\ 1 & 0 & -1 & 0 & 1 & 0 & -1 \\ 1 & -1 & 0 & 0 & 1 & -1 & 0 \end{bmatrix}, \quad (3.30)$$

with order  $v_1^0, v_2^0, v_3^0, v_4^0, v_1^1, v_2^1, v_3^1$ . It is expected that starting from arbitrary proper mixed state (at least in a vertex, *i.e.*  $\underline{\varrho}(0) = |\underline{v}_i^j\rangle\langle v_i^j|$ ), we should obtain  $\underline{\varrho}(\infty) := \lim_{t \rightarrow \infty} \underline{\varrho}(t) = |\underline{v}_4^0\rangle\langle v_4^0|$ . Oppositely, through numerical simulation one can verify that

$$\underline{\varrho}(\infty) = \frac{1}{16} \begin{bmatrix} 5 & 1 & 1 & 0 & -5 & -1 & -1 \\ 1 & 1 & 1 & 0 & -1 & -1 & -1 \\ 1 & 1 & 1 & 0 & -1 & -1 & -1 \\ 0 & 0 & 0 & 2 & 0 & 0 & 0 \\ -5 & -1 & -1 & 0 & 5 & 1 & 1 \\ -1 & -1 & -1 & 0 & 1 & 1 & 1 \\ -1 & -1 & -1 & 0 & 1 & 1 & 1 \end{bmatrix}, \quad (3.31)$$

is a stationary state of the evolution, when starting from a state  $\underline{\varrho}(0) = |\underline{v}_1^0\rangle\langle v_1^0|$ .

To correct this problem, we propose to add the Hamiltonian  $\underline{H}_{\text{rot}} \in \mathbb{C}^{V \times V}$  which changes the state within the subspace corresponding to single vertex, Let  $H_{\text{rot},v} \in \mathbb{C}^{V_v \times V_v}$  be arbitrary Hamiltonian. Then  $H_{\text{rot}}$  will be a  $V$ -block

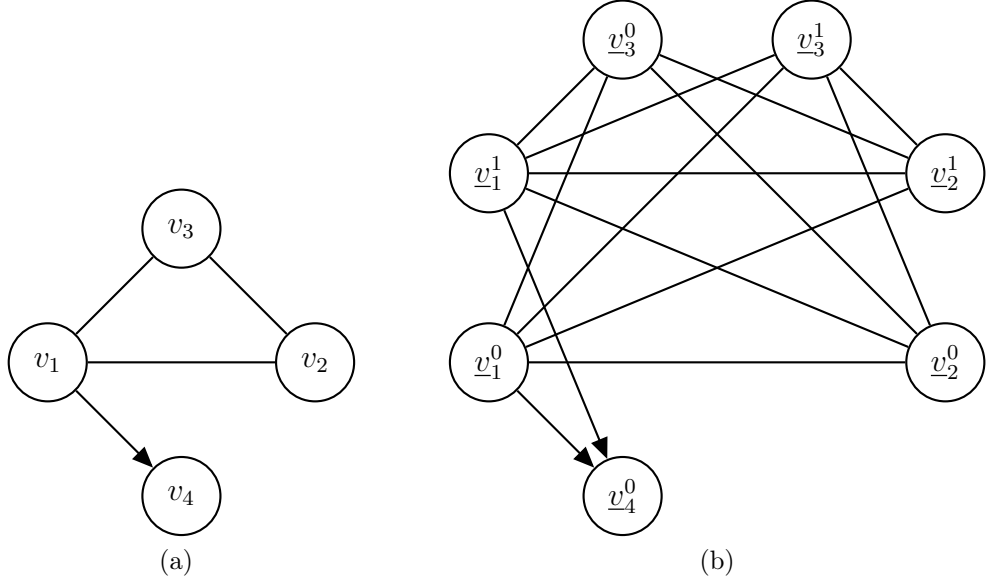


Figure 3.5: The original graph with the premature localization 3.5a, and the graph  $\underline{G}$  based on the original graph 3.5b. Starting from  $|\underline{v}_1^0\rangle\langle\underline{v}_1^0|$  we obtain a stationary state which is not fully localised in the vertex  $\underline{v}_4^0$ .

diagonal operator

$$H_{\text{rot}} = \begin{bmatrix} H_{\text{rot},v_1} & & & \\ & H_{\text{rot},v_2} & & \\ & & \ddots & \\ & & & H_{\text{rot},v_{|V|}} \end{bmatrix}. \quad (3.32)$$

Now the evolution takes the form

$$\frac{d}{dt}\underline{\varrho} = -i[\underline{H}_{\text{rot}}, \underline{\varrho}] + \underline{L}\underline{\varrho}\underline{L}^\dagger - \frac{1}{2}\{\underline{L}^\dagger\underline{L}, \underline{\varrho}\}. \quad (3.33)$$

We call this Hamiltonian the *locally rotating Hamiltonian*, since it acts only locally on the subspaces corresponding to single vertex. We have verified numerically that the appropriate Hamiltonian corrects the premature localisation. In particular, if we choose the locally rotating Hamiltonian based on

$$\langle\underline{v}^k| \underline{H}_{\text{rot},v} |\underline{v}^l\rangle = \begin{cases} i, & l = k + 1 \pmod{\text{indeg}(v_i)}, \\ -i, & l = k - 1 \pmod{\text{indeg}(v_i)}, \\ 0, & \text{otherwise,} \end{cases} \quad (3.34)$$

the evolution on the graph presented in Fig. 3.5b results in a unique stationary state  $|\underline{v}_4^0\rangle\langle\underline{v}_4^0|$ .

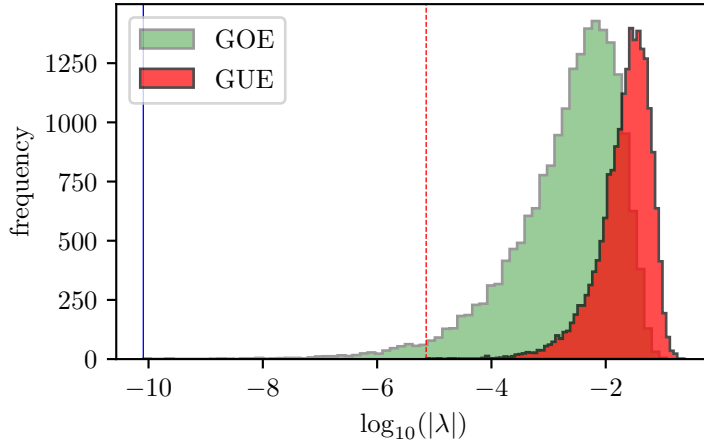


Figure 3.6: The analysis of impact of the form of locally rotating Hamiltonians on the uniqueness of the stationary state for graph presented in Fig. 3.5. GOE (GUE) denotes evolution where each block of the Hamiltonian was sampled independently from GOE (GUE) distribution. The  $\log_{10}(|\lambda|)$  the logarithm of the absolute value of the second smallest (in absolute value) eigenvalue of the evolution generator. For each GOE and GUE we sampled 20 000 Hamiltonians. Vertical blue solid (red dashed) line denotes the minimum obtained value for GOE (GUE).

Note that the quantum state of the form  $|\underline{v}_4^0\rangle\langle\underline{v}_4^0|$  is a stationary state for any choice of locally-rotating Hamiltonian. This can be shown by calculating  $\frac{d\rho}{dt}$  for the given state (we will elaborate more on this problem in Chapter 4). However in case of a locally-rotating Hamiltonian being a zero matrix, we show that also other mixed states are proper stationary states of the evolution.

To exemplify the impact of the Hamiltonians on the convergence, we analyzed the spectrum of the evolution generator. Since there is always at least one stationary state, it means that the multiplicity of 0 eigenvalue is at least 1. Then the second smallest eigenvalue (ordered in absolute value) gives us insight into the convergence property of the walk. Based on the results presented in Fig. 3.6 we see that both random real- and complex-valued rotating Hamiltonian with high probability produce high separation between smallest eigenvalues. However, in the case of complex-valued Hamiltonians far larger eigenvalues are obtained. Thus a random GUE Hamiltonian may be a good candidate to be a block for the locally rotating Hamiltonian.

### 3.2.3 Final model and correction cost

Let us now sum up all considered corrections and define a nonmoralizing QSW. We start with introducing a formal definitions of nonmoralizing operators. Let  $\vec{G} = (V, \vec{E})$  be an arbitrary directed graph. Then  $\underline{\vec{G}} = (\underline{V}, \underline{\vec{E}})$  will be a demoralizing graph of  $G$ . Furthermore  $G$  and  $\underline{G} = (\underline{V}, \underline{E})$  will be the underlying graphs of  $\vec{G}$  and  $\underline{\vec{G}}$ . Let  $f$  will be a natural homomorphism from  $\underline{\vec{G}}$  to  $\vec{G}$ .

**Definition 3.8.** Let  $\vec{G} = (V, \vec{E})$  be an arbitrary directed graph. Hermitian operator  $\underline{H} \in \mathbb{C}^{\underline{V} \times \underline{V}}$  is nonmoralizing Hamiltonian of QSW on  $\vec{G}$  if for all  $\underline{v}, \underline{w} \in \underline{V}$  we have

$$\{\underline{v}, \underline{w}\} \notin \underline{E} \iff \langle \underline{w} | \underline{H} | \underline{v} \rangle = 0. \quad (3.35)$$

In other words, if vertices are not connected in the underlying graph of  $\underline{G}$ , then the corresponding Hamiltonian element vanishes. Note that amplitude transfer along the  $\{\underline{v}, \underline{w}\}$  edge in  $\underline{G}$  corresponds to a transfer between  $|\underline{V}_v|$ -dimensional and  $|\underline{V}_w|$ -dimensional space. Thus, for each edge we have  $2|\underline{V}_v| \cdot |\underline{V}_w|$  real degrees of freedom for each edge  $e \in E$ . For LQSW and GQSW we have two real degree of freedom per edge. We say that a nonmoralizing Hamiltonian is standard if  $\{\underline{v}, \underline{w}\} \in \underline{E}$  implies  $\langle \underline{w} | \underline{H} | \underline{v} \rangle = 1$ . Note that in  $\underline{V}$ -block representation, if blocks correspond to non-connected vertices in  $V$ , then the block is a zero matrix.

**Definition 3.9.** Let  $\vec{G} = (V, \vec{E})$  be arbitrary directed graph. An operator  $\underline{L} \in \mathbb{C}^{\underline{V} \times \underline{V}}$  is nonmoralizing Lindblad operator of QSW on  $\vec{G}$  if for all  $\underline{v}, \underline{w} \in \underline{V}$  we have

$$(\underline{v}, \underline{w}) \notin \underline{\vec{E}} \iff \langle \underline{w} | \underline{L} | \underline{v} \rangle = 0, \quad (3.36)$$

and for any  $\underline{v}, \underline{w} \in \underline{V}$  satisfying  $f(\underline{v}) \neq f(\underline{w})$  we have

$$\langle \underline{v} | \bar{\underline{L}}^\dagger \bar{\underline{L}} | \underline{w} \rangle = 0. \quad (3.37)$$

Note that Lemma 3.7 provides a simple construction method. The method requires a mapping  $v \mapsto L_v$ , where each  $L_v$  is a matrix with pairwise orthogonal columns. While the number of degrees of freedom depends on the choice of  $\vec{G}$ , clearly the free-parameter space is larger comparing to LQSW and GQSW. For LQSW we have only one real degree of freedom, for the GQSW for the Lindblad operator collection  $\mathcal{L}_{\text{GQSW}}$  we have  $|\mathbb{L}_{\text{GQSW}}|$  degrees of freedom. We say that the nonmoralizing Lindblad operator is standard if it is constructed according to Lemma 3.7 with  $L_v$  being a Fourier matrix. Similarly as is for nonmoralizing Hamiltonian, in  $\underline{V}$ -block representation if there is no  $(v, w)$  arc, then the block corresponding to this arc is a zero matrix.

**Definition 3.10.** Let  $\vec{G} = (V, \vec{E})$  be an arbitrary directed graph. Hermitian operator  $\underline{H}_{\text{rot}} \in \mathbb{C}^{V \times V}$  is locally rotating Hamiltonian of QSW on  $\vec{G}$  if we have

$$f(\underline{v}) \neq f(\underline{w}) \implies \langle \underline{w} | \underline{H}_{\text{rot}} | \underline{v} \rangle = 0 \quad (3.38)$$

for all  $\underline{v}, \underline{w} \in \underline{V}$ .

Note that locally rotating Hamiltonian introduces  $2|\underline{V}_v|^2 - |\underline{V}_v|$  real degrees of freedom for each vertex  $v \in V$ . We say that locally rotating Hamiltonian is standard iff block are defined as in Eq. (3.34).

Finally we define a nonmoralizing global interaction QSW as follows.

**Definition 3.11.** Let  $\vec{G} = (V, \vec{E})$  be an arbitrary directed graphs. Let  $\underline{H}$  be a nonmoralizing Hamiltonian,  $\underline{\mathbb{L}}$  be a collection of nonmoralizing Lindblad operators and  $\underline{H}_{\text{rot}}$  be a locally rotating Hamiltonian. Then the evolution

$$\frac{d}{dt}\underline{\varrho} = -i[\underline{H} + \underline{H}_{\text{rot}}, \underline{\varrho}] + \sum_{\underline{L} \in \underline{\mathcal{L}}} \left( \underline{L}\underline{\varrho}\underline{L}^\dagger - \frac{1}{2}\{\underline{L}^\dagger \underline{L}, \underline{\varrho}\} \right), \quad (3.39)$$

is called a nonmoralizing global interaction QSW (NGQSW).

We say that a NGQSW is standard if all operators defining the evolution are standard.

In the previous section we introduced a interpolating parameter  $\omega$ , which was responsible for adjusting a relative strength of closed- and open-system evolution. Note that for the model defined above locally rotating Hamiltonian should be introduced only in the presence of open-system evolution. Hence an interpolated NGQSW with the parameter  $\omega$  will be of the form

$$\frac{d}{dt}\underline{\varrho} = -i[(1 - \omega)\underline{H} + \omega\underline{H}_{\text{rot}}, \underline{\varrho}] + \omega \sum_{\underline{L} \in \underline{\mathbb{L}}} \left( \underline{L}\underline{\varrho}\underline{L}^\dagger - \frac{1}{2}\{\underline{L}^\dagger \underline{L}, \underline{\varrho}\} \right). \quad (3.40)$$

The presented correction scheme enlarges the Hilbert space used. We can bound from above the dimension of the constructed space. If the original graphs consists of  $n$  vertices, with indegree  $\text{indeg}(v)$  for vertex  $v$ , then the dimension of enlarged Hilbert space equals  $\sum_{v \in V} \text{indeg}(v) + |\{v : \text{indeg}(v) = 0\}| = |\vec{E}| + |\{v : \text{indeg}(v) = 0\}|$ . Note that in the worst case scenario of a complete digraph, the dimension of the enlarged Hilbert space is  $\mathcal{O}(|V|^2)$ . In the term of number of qubits the additional qubit number is  $\mathcal{O}(\log n)$ , hence in our opinion the correction scheme is efficient. Comparing to other models [66], where for each vertex there is corresponding qubit, size of our Hilbert space is still small.

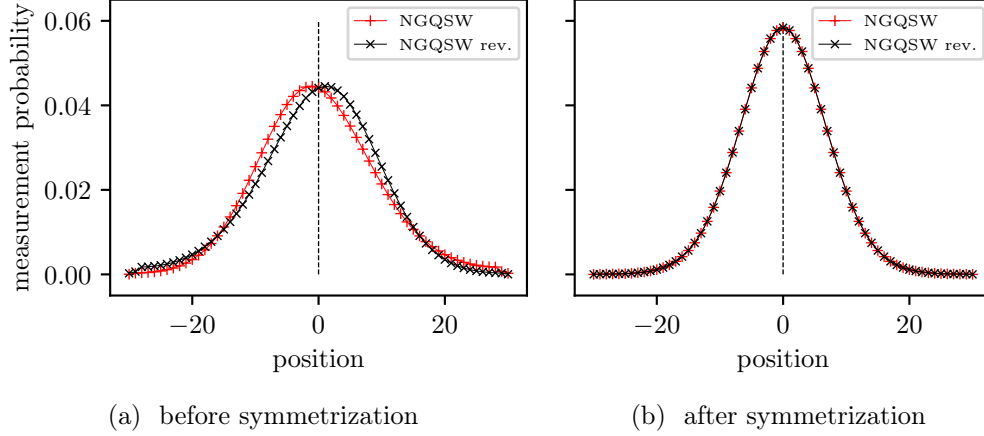


Figure 3.7: Probability distribution of the measurement in the standard basis and its reflection by the initial position for  $t = 100$  on the line segment of length 61, (a) before procedure application and (b) after procedure application described in Sec. 3.3.1. In both cases we start in  $\frac{1}{2}(|\psi_0^0\rangle\langle\psi_0^0| + |\psi_0^1\rangle\langle\psi_0^1|)$ .

### 3.3 Propagation of standard NGQSW

In Chapter 3.1 we have shown that standard GQSW yields a ballistic propagation. However, because of the spontaneous moralization, the graph which was actually analysed was an undirected line with additional edges between every two vertices as in Fig. 3.8. Hence, in this section we analyze NMQSW, to verify if the fast propagation recorded in moralizing quantum stochastic walk for the global interaction case is due to the additional amplitude transitions or due to the global interactions.

#### 3.3.1 Lack of symmetry on infinite path

Let us analyse the standard NGQSW on undirected path graph. A further undesired effect has occurred for some symmetric graphs, where we observe the lack of symmetry of the probability distribution. In Fig. 3.7a we present the probability distribution of the position measurement and the reflection of distribution according to the initial position. We observe that probability distribution is not symmetric with respect to the initial position.

Removing the locally rotating Hamiltonian does not remove the asymmetry and the nonmoralizing Hamiltonian is a symmetric operator. Hence, the lack of symmetry comes from asymmetry of nonmoralizing Lindblad operators. Since by construction the columns of matrices  $L_v$  need to be orthogonal,

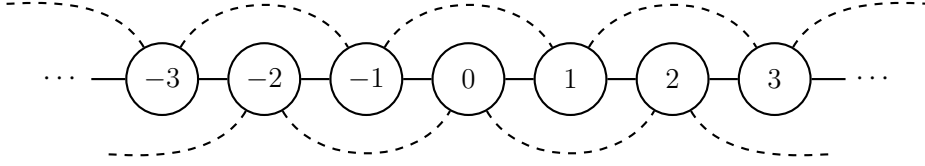


Figure 3.8: Line graph. Dashed lines correspond to additional amplitude transitions every two nodes coming from the GKSL model.

the matrices  $L_v$  will not be symmetric in general.

We propose to add another global interaction Lindblad operator, with different  $L_v$  matrices which will remove the side-effect. In the case of undirected segment, we choose  $\underline{L} = \{\underline{L}_1, \underline{L}_2\}$  defined through matrices  $L_v^{(1)}$  and  $L_v^{(2)}$  for the vertex  $v$ . For  $\underline{L}_1$  we choose for each vertex

$$L_v^{(1)} = \begin{bmatrix} 1 & 1 \\ 1 & -1 \end{bmatrix} \quad (3.41)$$

and for  $\underline{L}_2$  we choose for each vertex

$$L_v^{(2)} = \begin{bmatrix} 1 & 1 \\ -1 & 1 \end{bmatrix}. \quad (3.42)$$

The evolution takes the form

$$\frac{d}{dt} \underline{\varrho} = -i[\underline{H}_{\text{rot}}, \underline{\varrho}] + \sum_{\underline{L} \in \{\underline{L}_1, \underline{L}_2\}} \left( \underline{L} \underline{\varrho} \underline{L}^\dagger - \frac{1}{2} \{ \underline{L}^\dagger \underline{L}, \underline{\varrho} \} \right). \quad (3.43)$$

Note that the evolution operator is defined through two asymmetric, correcting each other Lindblad operators. Thus, the state has to be symmetric for the whole evolution. Numerical analysis confirms this conclusion (see Fig. 3.7b).

### 3.3.2 Propagation analysis

In this section we present a numerical analysis of interpolated standard NGQSW. To do so we analyse use the scaling exponent  $\alpha$  of the variance  $\mu_2(t) = \Theta(n^\alpha)$ . In Section 3.1 we have analytically shown that the scaling exponent in time limit equals 2.

We consider the model based on the symmetrized quantum stochastic walk given by Eq. (3.43). We use a standard nonmoralizing Hamiltonian  $\underline{H}$  and locally rotating Hamiltonian  $\underline{H}_{\text{rot}}$ . We choose  $\underline{L} = \{L_1, L_2\}$  to be a

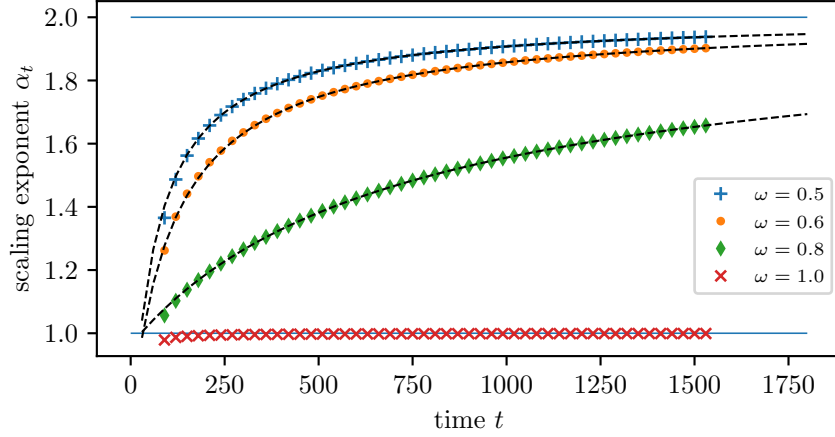


Figure 3.9: Slope of the local regression line for various values of  $\omega \leq 1$  for interpolated standard NGQSW. The scaling plots were computed for timepoints  $t = 30, 60, \dots, 1590$  and we chose batch size  $l = 5$ , according to the method presented in Sec. 2.5.1. Vertical solid lines represents values  $\alpha = 1, 2$ . Dashed lines for  $\omega < 1$  presents fit line according to model  $f(t; p) := p_1 - p_2 \frac{1}{(t-p_3)^{p_4}}$ . The fit was calculated using Levenger-Marquardt algorithm implemented in `LsqFit.jl` based on 30 estimations  $\alpha_t$  for largest values of  $t$ .

collection of two Lindblad operator defined in previous section. The evolution takes the form

$$\frac{d}{dt} \underline{\varrho} = -i(1 - \omega)[\underline{H}, \underline{\varrho}] + \omega \left( i[\underline{H}_{\text{rot}}, \underline{\varrho}] + \sum_{\underline{L} \in \{\underline{L}_1, \underline{L}_2\}} \left( \underline{L} \underline{\varrho} \underline{L}^\dagger - \frac{1}{2} \{ \underline{L}^\dagger \underline{L}, \underline{\varrho} \} \right) \right). \quad (3.44)$$

To determinate the scaling exponent we used a method presented in Sec. 2.5.1. The scaling exponents were derived for  $\omega = 0.5, 0.6, 0.8, 1.0$ . Results are shown in Fig. 3.9. We can see that for  $\omega = 1$  the scaling exponent converged to 1. On the other hand for  $\omega < 1$  the slope increases in time and exceeds 1, which is the upper bound for classical propagation. To determine the limiting value of  $\alpha_t$ , we fitted pairs  $(t, \alpha_t)$  to model function  $f(t; p) := p_1 - p_2 \frac{1}{(t-p_3)^{p_4}}$ . Note that  $\lim_{t \rightarrow \infty} f(t; p) = p_1$  for positive values of  $p_4$ , which was assumed during the optimization. For value  $\omega = 0.5, 0.6, 0.8$  we obtained values  $p_1 = 2.00, 2.01, 2.04$ , which shows that the propagation is in fact ballistic.

The results confirm that the fast propagation (ballistic or at least super-diffusive) is the property of global interactions present in quantum stochastic



walks and not from the fact that the original model allows additional transitions not according to the graph structure. It remains an open question, whether the evolution is convergent to a subspace corresponding to sink vertices. In the next chapter, we will show that this convergence occurs, and in fact, it is stronger compared to LQSW.



## Chapter 4

# Convergence of quantum stochastic walks

In chapter 3 we proposed a new model of quantum stochastic walk. We showed that in the case of absence of the Hamiltonian, which defines the walk on the underlying graph, the structure of the directed graph is perfectly preserved. However in order to introduce superdiffusive propagation, one need to introduce the Hamiltonian. Thus the model in fact may present a trade-off between the preservation of the arcs direction and the propagation speed. Furthermore NGQSW may have different converging property comparing to LQSW and GQSW.

In this chapter we investigate the directed-graph preservation for various QSW models. We analyze the direction preservation for standard LQSW, standard GQSW, and standard NGQSW. We achieve this by analyzing the limiting behavior of the quantum walks.

Various convergence classes can be considered. We will say that the evolution is convergent, if for arbitrary initial state  $\varrho_0$  there exists stationary state  $\varrho_\infty$  such that  $\varrho_0$  will converge to  $\varrho_\infty$  according to the evolution. Otherwise we say that the model is not convergent. Note that any evolution based on a time-independent GKSL master equation has at least one stationary state [67]. Hence, it is not possible to define an evolution that does not converge for any initial state.

Evolution may have a special property called *relaxing property*. It is defined as an evolution which has a unique stationary state. Uniqueness of the stationary states implies that the evolution is convergent for any choice of initial state [68].

All this properties can be checked without the simulation of the GKSL master equation. Let us recall the GKSL master equation presented in

Eq. (2.23)

$$\frac{d\varrho}{dt} = -\hbar[H, \varrho] + \sum_{L \in \mathbb{L}} \left( \gamma_L L \varrho L^\dagger - \frac{1}{2} \gamma_L \{L^\dagger L, \varrho\} \right). \quad (4.1)$$

Since we consider time-independent Hamiltonian and Lindblad operators, the solution to the equation above takes the form

$$|\varrho_t\rangle\rangle = \exp(St)|\varrho_0\rangle\rangle, \quad (4.2)$$

where  $S$  is an evolution generator of the form presented in Eq. (2.25). It can be shown that the eigenvalues  $\lambda$  of  $S$  satisfies  $\text{Re } \lambda \leq 0$ . Since there exists at least one stationary state,  $S$  possess at least one zero eigenvalue. Furthermore,  $S$  has single zero eigenvalue iff the evolution represented by  $S$  is relaxing [68]. Finally, if  $S$  possess purely imaginary eigenvalues, then one can suspect the existence of an initial state that result in periodic or quasi-periodic evolution.

## 4.1 Convergence of LQSW

### Strongly connected digraphs and single sink condensation graphs

The local environment interaction case is relaxing for all connected undirected graphs and arbitrary Hamiltonian [69]. The proof presented therein is based on the Spohn theorem [67], which requires the self-adjointness of the set of Lindblad operators  $\mathbb{L}$ , hence its applications is limited to the undirected graphs case. Nevertheless we show, that the result can be extended to strongly connected digraphs and weakly connected graphs with single sink vertex. Our proofs utilize Conditions 2. and 3. from [68], recalled below as Lemma 4.1 and 4.2. By the interior we mean set of density matrices with full rank.

**Lemma 4.1** ([68]). *Let  $\mathcal{H}$  be a Hilbert space. If there is no proper subspace  $S \subsetneq \mathcal{H}$ , that is invariant under all Lindblad generators  $L \in \mathbb{L}$  then the system has a unique steady state in the interior.*

**Lemma 4.2** ([68]). *If there do not exists two orthogonal proper subspaces of  $\mathcal{H}$  that are simultaneously invariant under all Lindblad generators  $L \in \mathbb{L}$ , then the system has unique fixed point, either at the boundary or in the interior.*

**Theorem 4.3.** *Let  $\vec{G} = (V, \vec{E})$  be a strongly connected digraph and let  $\mathbb{L} = \{L_{vw} = c_{(v,w)} |w\rangle\langle v| : (v, w) \in \vec{E}, c_{(v,w)} > 0\}$ . Then the LQSW with  $\mathcal{L}$  is relaxing for arbitrary Hamiltonian  $H$  with stationary state in the interior.*

*Proof.* Let  $\mathcal{H}$  be a Hilbert space spanned by  $\{|v\rangle : v \in V\}$  and  $S \neq \{0\}$  be arbitrary subspace of  $\mathcal{H}$  invariant under  $\mathbb{L}$ . We will show that  $S = \mathcal{H}$ , which by Lemma 4.1 will end the proof.

Let  $v \in V$  be arbitrary vertex. Let  $|\psi\rangle \in S$  be a nonzero vector. Since  $G$  is strongly connected, for each  $w$  there is a directed path  $P_{vw} = (v_1 = v, v_2, \dots, v_k, w)$ . Then

$$c_w |w\rangle = L_{v_k w} L_{v_{k-1} v_k} \cdots L_{v_2, v_1} |\psi\rangle \quad (4.3)$$

for some  $c_w \in \mathbb{C}_{\neq 0}$ . Hence we have  $|w\rangle \in S$  for all  $w \in V$ . Hence  $S \supseteq \text{span}(\{|w\rangle : w \in V\}) = \mathcal{H}$  and by this,  $S = \mathcal{H}$ .  $\square$

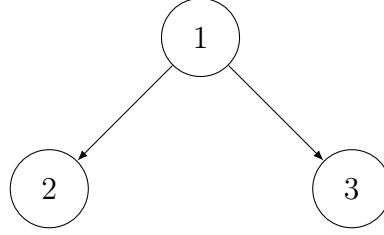
Let  $\vec{G} = (V, \vec{E})$  be an arbitrary weakly connected digraph. Let  $V' \subset V$  be such a set that for each  $v, w \in V'$  there exist paths from  $v$  to  $w$  and from  $w$  to  $v$ . Let any superset of  $V'$  does not have this property. Then we call induced subgraph  $\vec{G}' = (V', \vec{E}')$  a strongly connected component.

We define a *condensation graph*  $\vec{G}^c = (V^c, \vec{E}^c)$  as follows. Let  $V^c = \{V_1, \dots, V_k\}$  be a partition of  $V$  such that each  $V_i$  constructs a strongly connected component of  $\vec{G}$ . Furthermore let  $(V_i, V_j) \in \vec{E}^c$  iff there exist  $v_i \in V_i$  and  $v_j \in V_j$  such that  $(v_i, v_j) \in \vec{E}$ . Then we call  $\vec{G}^c$  a condensation graph of  $\vec{G}$ . Note that  $\vec{G}^c$  is a directed acyclic graph. Let us denote  $L(\vec{G})$  the collection of leaves (sinks) of a digraph  $\vec{G}$ .

**Theorem 4.4.** *Let  $\vec{G} = (V, \vec{E})$  be a weakly connected digraph such that  $|L(\vec{G}^c)| = 1$  and let  $\mathbb{L} = \{c_{(v,w)} |w\rangle\langle v| : (v,w) \in \vec{E}\}$  for some  $c_{(v,w)} > 0$ . Then the LQSW with  $\mathbb{L}$  is relaxing for arbitrary Hamiltonian  $H$ .*

*Proof.* Suppose  $S_1 \neq \{0\}, S_2 \neq \{0\}$  are two subspaces of  $\mathcal{H}$  and let  $|\psi_1\rangle \in S_1, |\psi_2\rangle \in S_2$ . Let  $w$  be an element from the sink vertex of  $\vec{G}^c$ . Similarly to method in Theorem 4.3 one can show that there exist  $L_1^1, \dots, L_k^1 \in \mathbb{L}$  and  $L_1^2, \dots, L_{k'}^2 \in \mathbb{L}$  such that  $c_w^1 |w\rangle = L_k^1 L_{k-1}^1 \cdots L_1^1 |\psi_1\rangle$  and  $c_w^2 |w\rangle = L_{k'}^2 L_{k'-1}^2 \cdots L_1^2 |\psi_2\rangle$  for some  $c_w^1, c_w^2 \in \mathbb{C}_{\neq 0}$ . Hence  $S_1$  and  $S_2$  are not orthogonal and by Lemma 4.2 the theorem holds.  $\square$

Several interesting things can be pointed. First note that since strongly connected digraphs satisfies the assumptions of Theorem 4.4, the Theorem 4.3 can be considered as a special case of the former one. However Theorem 4.3 provides that the stationary state has full rank. This is not achievable in general for directed graphs that are not strongly connected and such with  $L(\vec{G}^c) = \{V_i\}$  being a singleton. Let us consider an evolution with no Hamiltonian. Then the evolution is a CTRW, and the stationary state is spanned by vertices from the sink from the condensation graph.

Figure 4.1: An oriented  $K_{1,2}$ .

Note that the Hamiltonian has no influence on the for of the convergence. However it does have an impact on a form of stationary state. Let us consider a directed path graph  $P_2 = (\{1, 2\}, \{(1, 2)\})$ . Let us take a Lindblad operator collection  $\mathbb{L} = \{|2\rangle\langle 1|\}$ . If there is no Hamiltonian, then  $\begin{bmatrix} 0 & 0 \\ 0 & 1 \end{bmatrix}$  is the unique stationary state. However if we apply Hamiltonian  $H = \frac{1}{2} \begin{bmatrix} 0 & 1 \\ 1 & 0 \end{bmatrix}$ , then the stationary state changes into  $\frac{1}{3} \begin{bmatrix} 1 & -i \\ i & 2 \end{bmatrix}$ .

**Multi-sink condensation graphs** The remaining class of weakly connected graphs is those for which  $|L(\vec{G}^c)| > 1$ . Note that in this case one cannot expect relaxing property for a general Hamiltonian. In particular, let us consider a purely classical CTRW on an oriented  $K_{1,2}$  as in Fig. 4.1. Note that both  $|2\rangle\langle 2|$  and  $|3\rangle\langle 3|$  are a proper stationary states.

Let  $\vec{G} = (V, \vec{E})$  be digraph. Let us consider a CTRW with Lindblad operators  $\mathcal{L} = \{|w\rangle\langle v| : (v, w) \in \vec{E}\}$  and Hamiltonian  $H$  being an adjacency matrix of its underlying graph  $G$ . Let us consider an interpolated LQSW with interpolating parameter  $\omega \in [0, 1]$ . Note that for  $\omega = 0$  we obtain a Schrödinger equation, thus if  $H \neq 0$  we have a non-convergent evolution. For  $\omega = 1$  we have a CTRW, hence states localized in different strongly connected components which are sinks will converge to two different stationary states. However the evolution will be in general convergent.

We conclude our analysis with numerical investigation. We have analyzed a standard LQSW on various random graph models in context of its convergence properties. We have chosen only graphs with multi-sink condensation graph. The results of the numerical experiment can be found in Fig. 4.2. The red bar presents an amount of graphs which yield a relaxing evolution. Black bar presents an amount of graphs which does not yield a relaxing evolution, but were still convergent. Finally blue bar (not present in given figure) yielded the graph for which evolution generator had purely imaginary eigenvalues.

We haven't found a single graph for which the evolution operator had a purely imaginary eigenvalues, which would suggest quasi-periodic evolution.

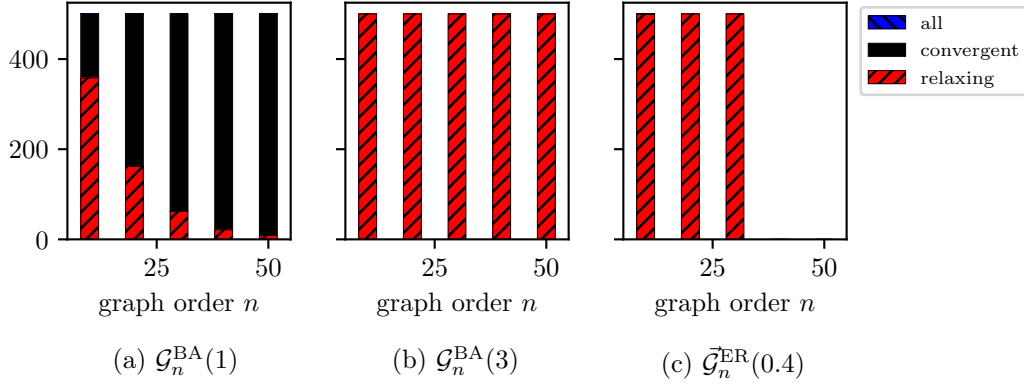


Figure 4.2: The convergence statistics of LQSW for various directed random graph models. For each  $\mathcal{G}_n^{\text{BA}}(m_0)$  models a sample  $G$  was chosen, then its random orientation  $\vec{G}$  was chosen. For randomly directed Erdős-Rényi graphs only weakly connected were considered. We have chose at random 500 graphs for each model and  $n$  s.t. the corresponding condensation graph has at least two sinks. Since it was extremely difficult to find such for Erdős-Rényi graphs, numerical results are limited to at most 30 nodes. The analysis was done through analysis of eigenvalues of evolution generator  $S$ . We considered eigenvalue  $\lambda$  to be 0 if  $|\lambda| < 10^{-10}$ . We assumed  $\lambda$  to be purely imaginary if  $|\Re \lambda| < 10^{-10}$  and  $|\Im \lambda| > 10^{-10}$ .

For randomly oriented  $\mathcal{G}_n^{\text{BA}}$  models and  $\vec{\mathcal{G}}_n^{\text{ER}}(0.4)$  all graphs yield relaxing property. Contrary, for randomly oriented trees the number of graphs yielding relaxing evolution decreases with the order of the graph.

## 4.2 Convergence of GQSW

### Undirected graphs

We start this section with providing the general result for the commuting operators.

**Proposition 4.5.** *Let us consider GKSL master equation in the case of commuting Lindbladian operators  $\mathbb{L}$  and Hamiltonian  $H$ . Then the evolution operation is of the form*

$$(U \otimes \bar{U}) D_S (U \otimes \bar{U})^\dagger, \quad (4.4)$$

where

$$D_S = -i(D_H \otimes I - I \otimes D_H) + \sum_{L \in \mathcal{L}} \left( D_L \otimes \bar{D}_L - \frac{1}{2} \bar{D}_L D_L \otimes I - \frac{1}{2} I \otimes D_L \bar{D}_L \right) \quad (4.5)$$

is a diagonal matrix. Here we assume that  $U$  is a unitary operator and  $D_H, D_L$  are diagonal operators such that  $H = U D_H U^\dagger$  and  $L = U D_L U^\dagger$ .

*Proof.* The proof comes directly from the eigendecompositions of the operators. Since all operators commute, it is possible to find common eigendecomposition with the same unitary matrix. By this we can easily find the result.  $\square$

The standard GQSW on undirected graphs is a special case of the evolution described in the theorem above, where we choose only single Lindbladian operator  $L = H$ .

**Theorem 4.6.** *The stationary states of the standard interpolated GQSW are precisely the stationary states of the CTQW. The evolution is convergent for  $\omega \in (0, 1]$ , but not relaxing iff the system size is greater than one.*

*Proof.* By the model construction we can choose  $\mathbb{L} = \{\sqrt{\omega}A\}$  and  $H = (1 - \omega)A$  and apply the Theorem 4.5. The diagonal matrix takes the form

$$D_{S_\omega} = -i(1 - \omega)(D \otimes I - I \otimes D) + \omega \left( D \otimes D - \frac{1}{2} D^2 \otimes I - \frac{1}{2} I \otimes D^2 \right). \quad (4.6)$$

Here we assume  $A = U D U^\dagger$ . Since  $A$  is hermitian, operator  $D$  is a real-valued diagonal matrix. The diagonal entries of operator  $D_{S_\omega}$  are eigenvalues which characterize the evolution. Let  $d_i := \langle i | D | i \rangle$ . Then we have

$$\begin{aligned} \langle i, j | D_{S_\omega} | i, j \rangle &= -i(1 - \omega)(d_i - d_j) + \omega \left( d_i d_j - \frac{1}{2} d_i^2 - \frac{1}{2} d_j^2 \right) \\ &= -i(1 - \omega)(d_i - d_j) - \frac{\omega}{2} (d_i - d_j)^2. \end{aligned} \quad (4.7)$$

Here  $-i(1 - \omega)(d_i - d_j)$  corresponds to purely Hamiltonian evolution, and hence to CTQW. Since 0-eigenvalues of  $S_\omega$  correspond to 0-eigenvalues of Hamiltonian part of the system, which furthermore correspond to the stationary states of the CTQW, we obtained the first part of the theorem.

Note that  $S_\omega$  does not have purely imaginary eigenvalues for  $\omega > 0$ . Hence, we have that the evolution is convergent. Since the set of stationary states of CTQW for graph with  $n$  vertices has at least  $n$  elements, we obtain that the presented evolution is never relaxing.  $\square$

The result from the above theorem implies that we can generate the stationary states of the CTQW by adding proper Lindbladian operator.



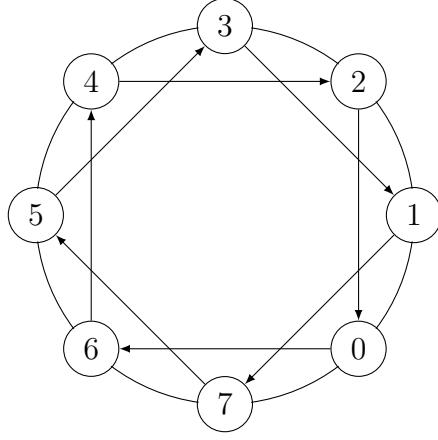


Figure 4.3: An example of strongly connected directed graph, for which the global interaction case evolution is not convergent.

### Directed graphs

In this section we provide an example of standard GQSW on a directed graph for which the evolution is no longer convergent.

**Theorem 4.7.** *There exist an infinite number of digraphs  $\vec{G}$  with corresponding initial states  $\varrho_0$  for which the interpolated standard GQSW is non-convergent for an arbitrary value of the smoothing parameter  $\omega$ .*

*Proof.* Case  $\omega = 0$  comes directly from the properties of continuous-time quantum evolution. Let us consider  $\omega > 0$ . We choose a circulant graph of size  $4k$  for  $k > 1$  and with extra jump every two vertices. An example for  $k = 2$  is presented in Fig. 4.3. The graph and its underlying graph are circulant matrices. Therefore, we can use Eq. (4.5) to find out that there exists an eigenvalue of the form  $2(1 - \omega)i$  with corresponding eigenvector  $|C_k\rangle |C_{2k}\rangle$ , where  $|C_i\rangle$  is the  $i$ -th eigenvector of a circulant matrix of the form [70]

$$|C_i\rangle = \frac{1}{2\sqrt{k}} \sum_{j=0}^{4k} \exp\left(\frac{2\pi i j}{4k-1}\right) |i\rangle. \quad (4.8)$$

The initial state takes the form

$$\varrho(0) = \frac{1}{2}(|C_k\rangle + |C_{2k}\rangle)(\langle C_k| + \langle C_{2k}|), \quad (4.9)$$

and the  $\varrho(t)$  takes the form

$$\varrho(t) = \frac{1}{2}(|C_k\rangle\langle C_k| + |C_{2k}\rangle\langle C_{2k}| + e^{2i(1-\omega)t} |C_k\rangle\langle C_{2k}| + e^{-2i(1-\omega)t} |C_{2k}\rangle\langle C_k|). \quad (4.10)$$

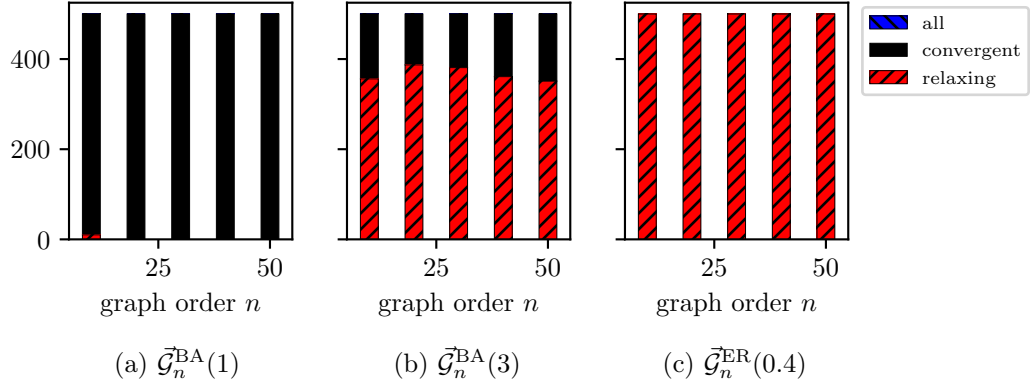


Figure 4.4: The convergence statistics of GQSW for various directed random graph models. Only weakly connected Erdős-Rényi graphs were considered. We applied the same conditions for eigenvalues as in Fig. 4.2.

Since  $\varrho(t)$  is periodic with period  $\frac{\pi}{(1-\omega)}$ , we obtain the result.  $\square$

Note, that for different  $t$  we can obtain different state in the sense of possible measurement output. For example we have  $\langle 0 | \varrho(0) | 0 \rangle = \frac{1}{2k}$ , but at the same time we have  $\langle 0 | \varrho(\frac{\pi}{2(1-\omega)}) | 0 \rangle = 0$ .

Circulant graphs provide an infinite collection of directed graphs for which the convergence does not hold. Note that the example used in the proof of Theorem 4.7 is a strongly connected directed graph. This shows that the convergence in the local interaction case does not imply the convergence in the global interaction case.

We finalize our analysis of standard GQSW with numerical investigations of random digraphs. We have sampled 500 weakly connected directed graphs for each model and order of the graph. The statistics are presented in Fig. 4.4. As in LQSW, none of sample graphs had a purely imaginary eigenvalue, although based on the theorem above we know such graphs exist. Almost all  $\vec{\mathcal{G}}_n^{\text{BA}}(3)$  and  $\vec{\mathcal{G}}_n^{\text{ER}}(0.4)$  graphs yielded relaxing evolution. For  $\vec{\mathcal{G}}_n^{\text{BA}}(1)$  the number of relaxing GQSW decreased with the graph order, as it was in LQSW model. Thus GQSW and LQSW have statistically similar convergence properties.

### 4.3 Convergence of standard NGQSW

Contrary to previous results, NGQSW is nonconvergent evolution even for an undirected graphs.

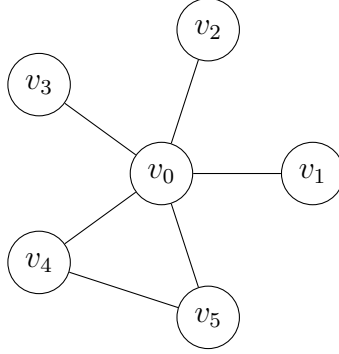


Figure 4.5: An example of graph for which non-moralizing global interaction evolution is not convergent.

**Theorem 4.8.** *Let us consider the standard NGQSW. Then there exists a digraph  $\vec{G}$  and initial state  $\varrho(0)$  for which the evolution is periodic in time for an arbitrary value of the smoothing parameter  $\omega \in (0, 1]$ .*

*Proof.* Let us consider a graph presented in Fig. 4.5. Using the scheme presented in Chapter 3, new graph will consist of 5 copies of vertex  $v_0$ , two copies of vertices  $v_4$  and  $v_5$ , and single copy of other vertices. Let us consider standard NGQSW

Let us choose two eigenvectors of the standard rotating Hamiltonian

$$|\varphi\rangle = \frac{1}{2\sqrt{3}} |v_0^0\rangle - \frac{i}{2} |v_0^1\rangle - \frac{1}{\sqrt{3}} |v_0^2\rangle + \frac{i}{2} |v_0^3\rangle + \frac{1}{2\sqrt{3}} |v_0^4\rangle, \quad (4.11)$$

$$|\psi\rangle = \frac{1}{2\sqrt{3}} |v_0^0\rangle - \frac{i}{2} |v_0^1\rangle - \frac{1}{\sqrt{3}} |v_0^2\rangle + \frac{i}{2} |v_0^3\rangle + \frac{1}{2\sqrt{3}} |v_0^4\rangle. \quad (4.12)$$

One can show that the vectors  $|\varphi\rangle \overline{|\varphi\rangle}$ ,  $|\varphi\rangle \overline{|\psi\rangle}$ ,  $|\psi\rangle \overline{|\varphi\rangle}$ ,  $|\psi\rangle \overline{|\psi\rangle}$  are eigenvectors of the increased evolution operator  $S_{t,\omega}$  for arbitrary  $\omega \in (0, 1]$ . Corresponding eigenvalues are respectively  $0, -2i\sqrt{3}\omega, 2i\sqrt{3}\omega, 0$ . Similarly to the example presented in the previous section, the state

$$\tilde{\varrho}_0 = \frac{1}{2} (|\varphi\rangle + |\psi\rangle) (\langle\varphi| + \langle\psi|) \quad (4.13)$$

is the required initial state. The state after time  $t$  takes the form

$$\tilde{\varrho}_t = \frac{1}{2} \left( |\varphi\rangle \langle\varphi| + e^{-2it\sqrt{3}\omega} |\varphi\rangle \langle\psi| + e^{2it\sqrt{3}\omega} |\psi\rangle \langle\varphi| + |\psi\rangle \langle\psi| \right). \quad (4.14)$$

The function  $\tilde{\varrho}_t$  is periodic with period  $\frac{\pi}{\sqrt{3}\omega}$ , hence we obtained the result.  $\square$

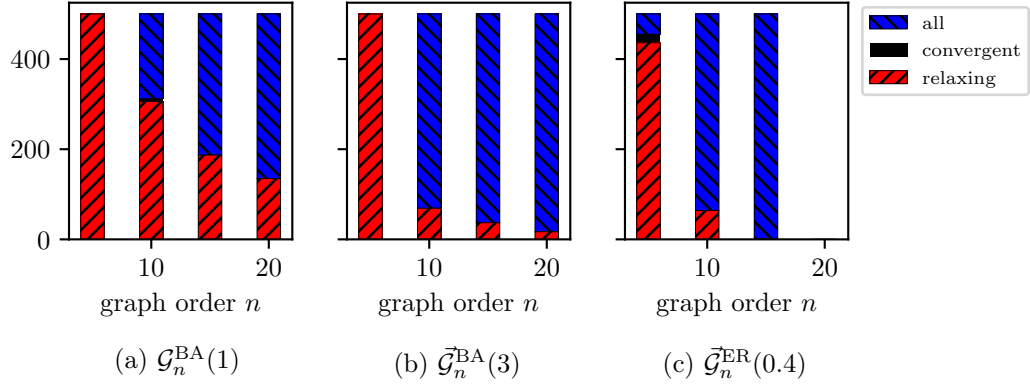


Figure 4.6: The convergence statistics of NGQSW for various directed random graph models. Only weakly connected Erdős-Rényi graphs were considered. We applied the same conditions for eigenvalues as in Fig. 4.2. We were not able to perform the statistics for the Erdős-Rényi model for  $n = 20$ , due to the size of the evolution generator.

Contrary to the LQSW and GQSW, it seems that such situation may occur quite frequently for standard NGQSW, see Fig. 4.6. It turns out that for majority of graphs the evolution generator have a purely imaginary eigenvalues which suggest that the evolution will be periodic. However, provided there is no imaginary eigenvalues, the evolution turned out to be relaxing.

Note that in the example above the probability distribution coming from the measurement in canonical basis in the enlarged Hilbert space will differ. However, independently on the chosen measurement time, the probability distribution coming from the natural measurement of NGQSW remains unchanged. This suggests that different measure of convergence has to be chosen.

Let  $p(t; \underline{\varrho})$  be a probability distribution of measurement of the NGQSW with initial state  $\underline{\varrho}$  after evolution time  $t$ , according to its natural measurement. We will be interested, whether given initial state, its probability distribution will converge. Formally, we are interested whether there exists  $p(\infty; \underline{\varrho})$  s.t.

$$\lim_{t \rightarrow \infty} \|p(t; \underline{\varrho}) - p(\infty; \underline{\varrho})\| = 0. \quad (4.15)$$

The spectral analysis is no longer useful here, as imaginary eigenvalues may imply local evolution within subspace attached to  $\underline{V}_v$ . Instead, we made numerical analysis for a special choice of input state of the form

$$\underline{\varrho} = \frac{1}{|V|} \sum_{v \in V} \frac{1}{|V_v|} \sum_{\underline{v} \in V_v} |\underline{v}\rangle \langle \underline{v}|. \quad (4.16)$$

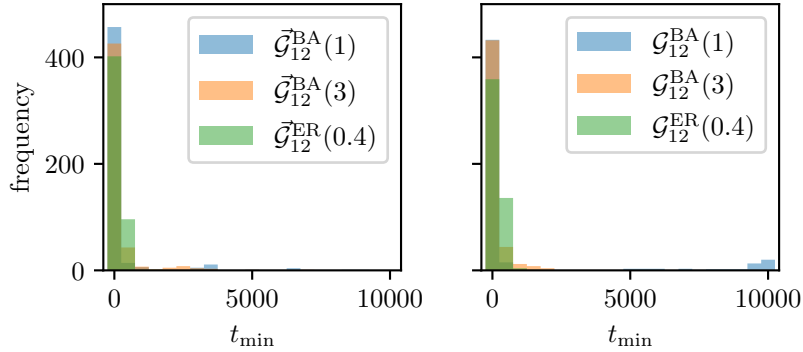


Figure 4.7: Convergence for various directed random graph models for standard NGQSW. For (directed) Erdős-Rényi models only (weekly) connected graphs were chosen. For  $t = 0, 100, \dots, 10\,000$  we calculated  $p(t, \varrho)$  with  $\varrho$  define as in Eq. (4.16). Then for given  $p$  looked for minimal  $t_{\min}$  such that for all  $t' \geq t_{\min}$  we have  $\|p(t' + 100, \varrho) - p(10\,000, \varrho)\| \leq \|p(t', \varrho) - p(10\,000, \varrho)\|$ . We repeated the procedure for 500 graphs for each graph model. Note that for some graphs we observed that the convergence were monotonic starting from very large values of  $t$ . However, for this samples the difference in norms for last 30 pairs of timepoints were (except single case) below  $10^{-10}$ . Hence, we claim that this deviations are due to a numerical error of estimating  $p(t, \varrho)$ .

It turns out that difference between  $p(t; \underline{\varrho})$  and  $p(10\,000; \underline{\varrho})$  was almost monotonically decreasing as  $t$  approached 10 000, see Fig. 4.7. Hence we conclude that at least for the proposed initial state the evolution was convergent in probability.

The limit probability distribution depends in general on the initial state. Let us analyse the graph presented in Fig. 4.8. For the standard NGQSW and two initial states, we see that the limiting probability distribution differ.

## 4.4 Digraph structure observance

Let us consider standard interpolated QSW models with  $\omega = 1$ , *i.e.* evolution defined for a digraph. Let  $\vec{G} = (V, \vec{E})$  be a digraph and let  $v \in V$  be a sink vertex. Independently of chosen QSW model, mixed state defined over the

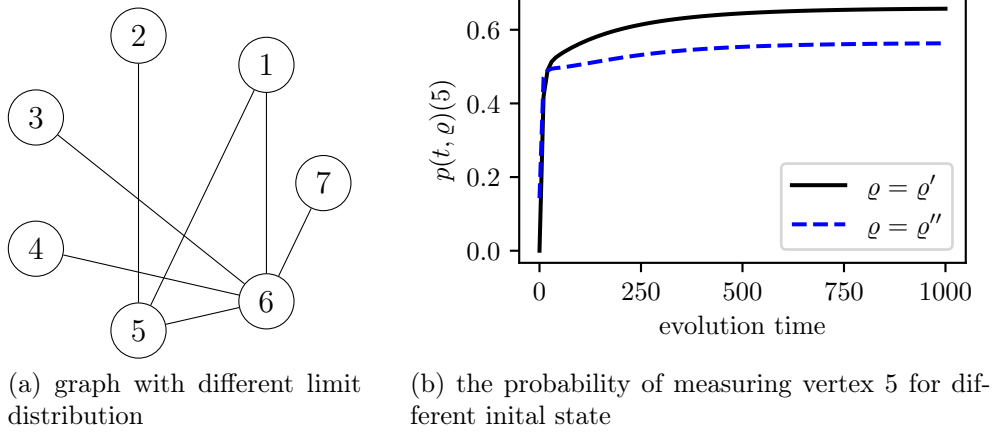


Figure 4.8: Graph for which there exists two different stationary states in the sense of the natural measurement for NGQSW. The states can be obtained by starting in the state  $\varrho' = \frac{1}{3} \sum_{v \in V_s} |v\rangle\langle v|$  and the  $\varrho''$  defined in Eq. (4.16).

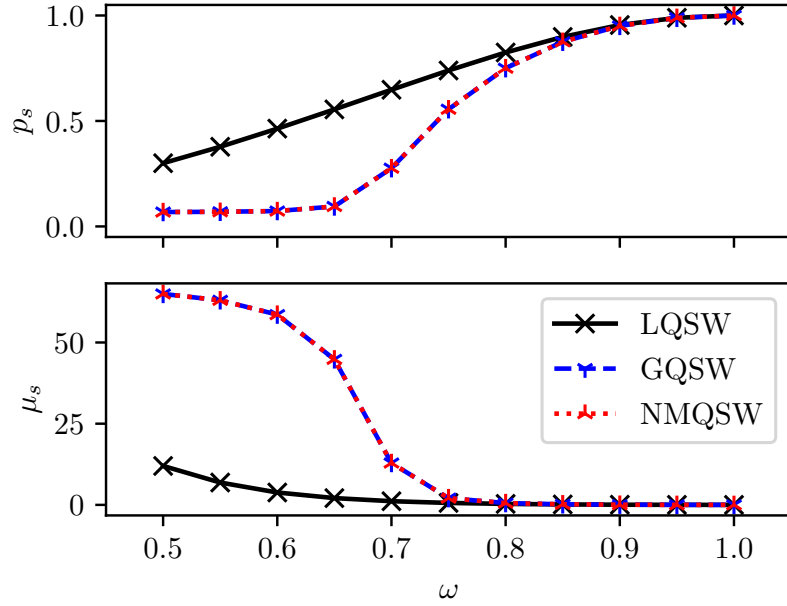


Figure 4.9: Measures  $p_s$  and  $\mu_s$  in term of  $\omega = .5, .55, \dots, 1$ . for directed path with 15 vertices. The evolution starts in the initial state described in Eq. (4.16), and the evolution time equals 10 000. Note that the plots for GQSW and NGQSW coincides – this comes from the fact that for each vertex in directed path the indegree is at most 1, hence the standard GQSW and NGQSW are indistinguishable

space of  $v$  is a stationary state. For LQSW we have

$$\begin{aligned} \frac{d|v\rangle\langle v|}{dt} &= \sum_{(i,j) \in \vec{E}} \left( |c_{i,j}|^2 |j\rangle\langle i| \cdot |v\rangle\langle v| \cdot |i\rangle\langle j| - \frac{1}{2} |c_{i,j}|^2 \{ |i\rangle\langle j| \cdot |j\rangle\langle i|, |v\rangle\langle v| \} \right) \\ &= \sum_{(v,j) \in \vec{E}} (|c_{v,j}|^2 |j\rangle\langle j| - |c_{v,j}|^2 |v\rangle\langle v|) = 0, \end{aligned} \quad (4.17)$$

because there is no arc of the form  $(v, j)$ . Similarly, for GQSW with set  $\mathbb{L}$  of Lindblad operators we have

$$\frac{d|v\rangle\langle v|}{dt} = \sum_{L \in \mathbb{L}} \left( L |v\rangle\langle v| L^\dagger - \frac{1}{2} \{ L^\dagger L, |v\rangle\langle v| \} \right) = 0, \quad (4.18)$$

because  $L|v\rangle$  is a zero vector.

The case of NGQSW is more complicated because the subspace connected to the sink vertex is  $\text{indeg}(v)$ -dimensional. Hence, based on the results from Sec. 4.3, we should allow the state to evolve within the subspace  $S_v$  attached to  $\underline{V}_v$ . Let  $\underline{v} \in \underline{V}_v$ . Note that  $H_{\text{rot}}|\underline{v}\rangle$  is a vector spanned by  $S_v$ , and for any nonmoralizing Lindblad operator  $L$  we have  $L|\underline{v}\rangle = 0$ . This means, by linearity, that for any mixed state defined over  $S_v$  is evolving within the space spanned by  $\underline{V}_v$ , hence the probability distribution coming from the natural measurement is stationary.

However, as it was shown in Sec. 4.1, even for a very simple directed path  $(\{1, 2\}, \{(1, 2)\})$  the amplitude for stationary state may be localized outside the sink vertices in the presence of the Hamiltonian. Still we expect, that as  $\omega \rightarrow 1$ , the more amplitude should be localized in the subspaces attached to the sink vertices.

Let  $\vec{G}$  be a directed graph and let  $\vec{G}^c = (V^c, \vec{E}^c)$  be its condensation graph with unique sink vertex  $V_s^c \in V^c$ . We propose two measures of how much the state is localized in the sink vertex or its neighborhood. First, we can determine the probability of being at any vertex from  $V_s^c$ , *i.e.*

$$p_s(t; \varrho) = \sum_{v \in V_s^c} p(t; \varrho_0)(v). \quad (4.19)$$

Similarly we proposed measure based on the second moment. Let  $w \in V$  and  $v \in V_s^c$ . Let  $d(w, V_s^c) = \min_{v \in V_s^c} d(w, v)$ . Note that the function  $d$  is well-defined if there is a unique sink vertex in the digraph  $\vec{G}^c$ .

$$\mu_s(t; \varrho) = \sum_{v \in V} d^2(v, w) p(t; \varrho_0)(v). \quad (4.20)$$

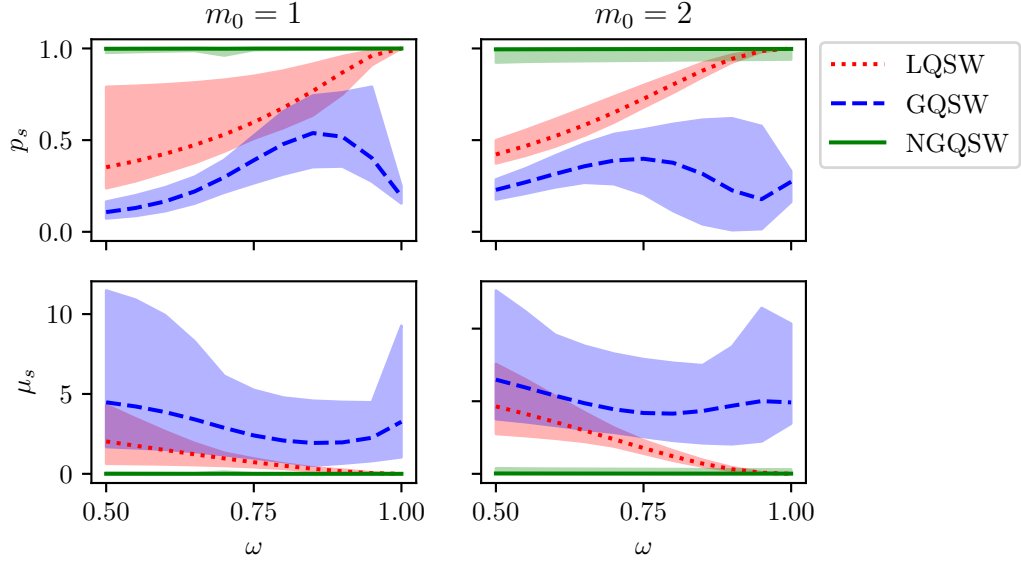


Figure 4.10: Measures  $p_s$  and  $\mu_s$  in term of  $\omega = .5, .55, \dots, 1$ . for Barabási-Albert random digraphs with 15 vertices for  $m_0 = 1, 2$ . For each value of parameter  $m_0$  and each QSW model we sampled 50 graphs. The evolution starts in the initial state described in Eq. (4.16), and the evolution time equals 10 000. For NGQSW we chosen random rotating Hamiltonian, s.t. for each block we sampled independently  $X + X^\top + i(Y - Y^\top)$ , where  $X, Y$  are random matrices with entry sampled independently according to uniform distribution over  $[0, 1]$ .

For the evolution preserving the digraph structure, we expect  $p_s(\infty; \varrho) = 1$  and  $\mu_s(\infty; \varrho) = 0$ . In the case of QSW walk we expect  $p_s \rightarrow 1$  and  $\mu_s \rightarrow 0$  as  $\omega \rightarrow 1$ . As we can observe on Fig. 4.9, the measures converge to proper values for all QSW models as  $\omega \rightarrow 1$ .

We repeated the experiment for  $\vec{\mathcal{G}}_n^{\text{BA}}(1)$  and  $\vec{\mathcal{G}}_n^{\text{BA}}(2)$ , see Fig. 4.10. For GQSW model, independently of  $\omega$  the values of  $p_s$  and  $\mu_s$  were far from their optimal values 1 and 0. This is expected, as even for the undirected graphs the model is projecting the initial state to stationary state of the unitary evolution. Note that as  $\omega \rightarrow 1$ , LSQW model acquire  $p_s = 1$  and thus  $\mu_1 = 1$ . However, for  $\omega < 1$  there is a clear gap between obtained and limit value. For NGQSW we observe that independently of chosen  $\omega$  the model converged almost fully to the vertices from sink of the condensation graph. However, for 3 out of 50 graphs the value  $p_s$  was below .99. This may be due to invalid choice of the rotating Hamiltonian.



## Chapter 5

# Hiding vertices for quantum spatial search

In Sec. 2.4.2 we analyzed a complete graph in the context of efficiency of quantum search. The analysis was simple, because the procedure does not depend on the marked node. This comes from the fact that complete graphs are vertex-transitive, *i.e.* the vertex can be distinguished only by its label.

However, in general one could expect that the transition rate and measurement time may depend not only on the chosen graph, but also on the marked vertex. Let us consider an adjacency matrix of a star graph  $K_{n-1,1}$ , with vertex 0 being connected to all the other vertices. The eigenvalues of the adjacency matrix of the graph are  $-\sqrt{n-1}$ , 0,  $\sqrt{n-1}$  with multiplicity 1,  $n-2$ , and 1 respectively check numbers. The eigenvectors corresponding to  $-\sqrt{n-1}$  and  $\sqrt{n-1}$  are:

$$|-\sqrt{n-1}\rangle = \frac{1}{\sqrt{2}}|0\rangle - \frac{1}{\sqrt{2(n-1)}} \sum_{v=1}^n |i\rangle, \quad (5.1)$$

$$|\sqrt{n-1}\rangle = \frac{1}{\sqrt{2}}|0\rangle + \frac{1}{\sqrt{2(n-1)}} \sum_{v=1}^n |i\rangle. \quad (5.2)$$

Let us consider an initial state  $|\psi_0\rangle = |\sqrt{n-1}\rangle$ . If  $w = 0$  is the marked vertex, then the success probability at time  $t = 0$  of  $w$  is  $1/2$ . This shows that the optimal choice is to not move at all, which gives the complexity  $\mathcal{O}(1)$ .

Since the full eigendecomposition is known, one can estimate manually the proper measurement time to find any of the sink vertex. However, it is possible to use a lemma proved in [33] and improved in [39] instead.

**Lemma 5.1** ([33, 39]). *Let  $H$  be a Hamiltonian with eigenvalues  $\lambda_1 \geq \dots \geq \lambda_n$  satisfying  $\lambda_1 = 1$  and  $c := \max_{i \geq 2} |\lambda_i| < 1$  for all  $i > 1$  with corresponding eigenvectors  $|\lambda_1\rangle, |\lambda_2\rangle, \dots, |\lambda_n\rangle$  and let  $|w\rangle$  be another state lying in the same quantum system. For an appropriate choice of  $r \in [-\frac{c}{1+c}, \frac{c}{1-c}]$ , the starting state  $|\lambda_1\rangle$  evolves by the Schrödinger's equation with the Hamiltonian  $(1+r)H + |w\rangle\langle w|$  for time  $t = \Theta(\frac{1}{\langle \lambda_1 | w \rangle})$  into the state  $|f\rangle$  satisfying  $|\langle w | f \rangle|^2 \geq \frac{1-c}{1+c} + o(1)$ .*

The adjacency matrix  $A = A(K_{n-1,1})$  does not fulfill the requirement of the lemma, because the largest eigenvalue is not equal to 1. In order to satisfy  $\lambda_1 = 1$  one can simply take  $\frac{1}{\sqrt{n-1}}A$ , however still one does not have a separation between  $\lambda_1$  and  $\lambda_i$ , since  $\lambda_n = -1$  and by this  $c = 1$ . However, adding a scaled identity matrix does not change the quantum evolution. By this, transformation  $\frac{2}{3\sqrt{n-1}}(A + \frac{\sqrt{n-1}}{2}I)$  maps eigenvalues  $-\sqrt{n-1}, 0, \sqrt{n-1}$  to  $-1/3, 1/3, 1$  giving  $c = 1/3$ . In general, applying a shifting and rescaling transformation

$$H_G \mapsto H'_G := \frac{H_G - \frac{\lambda_2(H_G) + \lambda_n(H_G)}{2}I}{\lambda_1(H_G) - \frac{\lambda_2(H_G) + \lambda_n(H_G)}{2}} \quad (5.3)$$

transforms  $H_G$  to a new Hermitian operator with  $|\lambda_2(H'_G)| = |\lambda_n(H'_G)|$  and  $\lambda_1(H'_G) = 1$ .

Using this fact we can finally show the optimality of the star graph for leaves. Using the shifting and rescaling transformation we have  $c = 1/3$ . Based on Lemma 5.1 after time  $T = \Theta(2\sqrt{n-1}) = \Theta(\sqrt{n})$  we obtain a state with the probability of measuring the marked state at least  $|\langle w | f \rangle|^2 \geq \frac{1-c}{1+c} + o(1) = \frac{1}{2} + o(1)$ .

The star graph is an example of a graph where all vertices can be found within the time  $\mathcal{O}(\sqrt{N})$ , except the single vertex which can be found in  $\mathcal{O}(1)$  time. Note that it does not violate the  $\Omega(\sqrt{N})$  bound for quantum search [3, 71], as there is only  $1 = o(n)$  vertex with the time complexity below the bound. On the other hand, the result from [71] is applicable only for uniformly random chosen vertex, and in such case for the star graph, the vertices can still be found in expected time  $\Theta(\sqrt{n})$ .

It is also possible to find an opposite example, where some of the vertices require significantly more time to be found. Let us consider a complete graph  $K_n^+$  with an extra leaf as in Fig. 5.1. The eigenvalues of the normalized Laplacian matrix  $\mathcal{L}$  are

$$0, \frac{n-1}{n-2}, \frac{1}{n-2} \left( 2n-3 \pm \frac{\sqrt{23-19n+4n^2}}{\sqrt{n-1}} \right), \quad (5.4)$$

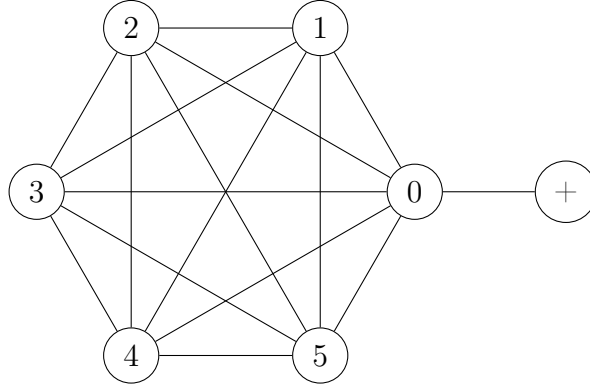


Figure 5.1: An example of a graph for all vertices except ‘+’ can be found in  $\Theta(\sqrt{n})$  time. The vertex ‘+’ requires  $\Theta(n)$  time.

with multiplicity 1,  $n - 3$ , 1. The eigenvalues converge to 0, 1, and 2, respectively. By this we have a constant spectral gap between 0 and 1 for operator  $I - \mathcal{L}$ , hence by applying the shift and rescaling transformation we have that the overlap  $\langle \lambda_1 | \omega \rangle$  gives the required time in complexity. For the graph matrix  $I - \mathcal{L}$ , the the eigenvector corresponding to the largest eigenvalue takes the form

$$|\lambda_1\rangle = \sqrt{\frac{2}{|E|}} \sum_{v \in V} \sqrt{\deg(v)} |v\rangle. \quad (5.5)$$

Note that for  $K_n^+$  we have  $|E| = \binom{n-1}{2} + 1 = \Theta(n^2)$ . Furthermore, for all vertices except vertex ‘+’, the degree is  $\Theta(n)$ . Using Lemma 5.1 for these vertices we have computational complexity  $T = \Theta(\sqrt{n})$ . For the vertex ‘+’ the complexity is  $\Theta(n)$ . This gives us the opposite situation compared to the star graph. Another example where some vertices require more time compared to others can be found in [28].

These simple examples show what we can expect when considering random graphs. In [33], the authors show that for almost all Erdős-Rényi graphs we can find a vertex in optimal  $\Theta(\sqrt{n})$  time. However, one could expect that even for a simple Erdős-Rényi model, some vertices may require significantly more or less time compared to the typical scenario. In the following sections we focus on the Erdős-Rényi model to show that this is not the case. However, we propose that instead of using an adjacency matrix, which is far more robust, it seems to be more convenient to use the Laplacian matrix.

## 5.1 Adjacency matrix

### 5.1.1 Issues found in the paper of Chakraborty et al.

In this section, we start by pointing the issues found in paper [33] regarding the efficiency of quantum spatial search on random Erdős-Rényi graphs. The authors showed three results. First, they demonstrate that the quantum spatial search considered in this dissertation is optimal on random Erdős-Rényi graphs. Then they show the application for creating Bell pairs and state transfer on the same graphs. Our comments concern the first part of the results. We would like to emphasize that the comments concern mostly the quality aspects instead of the conceptual aspect, and do not diminish the results given in [33].

Let us start with the results. In the paper, the authors claim that

*CTQW is almost surely optimal as long as  $p \geq \log^{3/2}(n)/n$ . Consequently, we show that quantum spatial search is in fact optimal for almost all graphs, meaning that the fraction of graphs of  $n$  vertices for which this optimality holds tends to one in the asymptotic limit.*

The authors show it through a simplified version of Lemma 5.1, which we recall below

**Lemma 5.2.** *Let  $H_1$  be a Hamiltonian with eigenvalues  $\lambda_1, \geq \lambda_2 \geq \dots \lambda_n$  (satisfying  $\lambda_1 = 1$  and  $|\lambda_i| \leq c < 1$  for all  $i > 1$ ) and eigenvectors  $|v_1\rangle = |s\rangle, |v_2\rangle, \dots, |v_n\rangle$ , and let  $H_2 = |w\rangle\langle w|$  with  $|\langle w|s\rangle| = \varepsilon$ . For an appropriate choice of  $r = \mathcal{O}(1)$ , applying the Hamiltonian  $(1+r)H_1 + H_2$  to the starting state  $|s\rangle$  for time  $\Theta(1/\varepsilon)$  results in a state  $|f\rangle$  with  $|\langle w|f\rangle|^2 \geq \frac{1-c}{1+c} + o(1)$ .*

Here,  $|s\rangle$  denotes the superposition of states in canonical basis. From now we assume that  $\lambda_i \geq \lambda_j$  for  $j < i$ . The main difference between Lemmas 5.1 and 5.2 is the form of the principal eigenvector. In the latter the eigenvector has to be an uniform superposition, while in the former it can be an arbitrary vector. While both lemmas are correct, the authors overused them when applying to random graphs.

The authors presented a proof suggesting  $|\langle \lambda_1|s\rangle| = 1 - o(1)$  provided that  $p \geq \log^{3/2} n/n$ . The authors claimed that based on this it is enough to show the optimality of the CTQW. However, based on the example from the introduction of this chapter,  $K^+$  graph, we can see that a large overlap is not a guarantee of optimal search for *all* nodes. In fact, one can show that at most  $n(1 - o(n))$  nodes can be found optimally.

**Proposition 5.3** ([37]). *Let  $|\varphi_n\rangle = \sum_{i=0}^{n-1} a_{i,n} |i\rangle \in \mathbb{R}^{\mathbb{Z}_{\geq 0}}$  and  $|s_n\rangle = \frac{1}{\sqrt{n}} \sum_{i=0}^{n-1} |i\rangle$ . Suppose  $\langle \varphi_n | s_n \rangle \rightarrow 1 - o(1)$ . Then there exists  $I_n \subseteq \{1, \dots, n\}$  such that  $|I_n| = n(1 - o(1))$  and*

$$\max_{i \in I_n} |\sqrt{n}a_{i,n} - 1| = o(1). \quad (5.6)$$

Furthermore  $|I_n| = n(1 - o(1))$  is tight in the worst case scenario.

*Proof.* Let  $|\varphi_n\rangle = \alpha_n |s_n\rangle + \beta_n |s_n^\perp\rangle$ , with  $|s_n^\perp\rangle = \sum_{i=0}^{n-1} b_{i,n} |i\rangle$  being a normed vector. Let  $I_\varepsilon^c(n) := \{i \in \{1, \dots, n\} : |\sqrt{n}a_{i,n} - \alpha_n| > \varepsilon\}$ . Since  $\sqrt{n}a_{i,n} - \alpha_n = \sqrt{n}\beta_n b_{i,n}$ , we have

$$1 = |\langle s_n^\perp | s_n^\perp \rangle|^2 = \sum_{i=0}^{n-1} |b_{i,n}|^2 \geq \sum_{i \in I_\varepsilon^c(n)} |b_{i,n}|^2 > \frac{\varepsilon^2}{n\beta_n^2} |I_\varepsilon^c(n)|, \quad (5.7)$$

hence  $|I_\varepsilon^c(n)| < n\beta_n^2/\varepsilon^2$ . Let  $I_n := \{1, \dots, n\} \setminus I_{\sqrt{\beta_n}}^c(n)$ . Then since  $\beta_n = o(1)$ , we have  $|I_n| = n(1 - o(1))$

$$\begin{aligned} \max_{i \in I_n} |\sqrt{n}a_i - 1| &\leq \max_{i \in I_n} |\sqrt{n}a_i - \alpha_n| + |1 - \alpha_n| \\ &\leq \sqrt{\beta_n} + |1 - \alpha_n| = o(1). \end{aligned} \quad (5.8)$$

Let us now show that  $|I_n| = n(1 - o(1))$  is tight. Let  $f(n) = o(n)$  and let  $|\varphi_n\rangle = \frac{1}{\sqrt{n-f(n)}} \sum_{i=0}^{n-f(n)-1} |i\rangle$ . Vector  $|\varphi_n\rangle$  satisfies the assumptions of the theorem, yet the maximal  $|I_n|$  is of order  $n - f(n)$ .  $\square$

A simple example for which the scenario described by the proposition above occurs is a graph over  $n$  vertices, where  $n - f(n)$  vertices form a complete graph, and the remaining  $f(n)$  vertices are isolated. For such graphs,  $n - f(n)$  vertices can be still found optimally in time  $\sqrt{n - f(n)} = \sqrt{n}(1 - o(1))$ , while the isolated vertices need  $\Theta(n)$  time to be found.

Furthermore, the authors incorrectly derived the condition on  $p$ . In the paper, they used Theorem 1.4 from [72] and the result from [73], which states that

$$\max_{i \geq 1} |\lambda_i| \leq 2\sqrt{p(1-p)n}(1 + o(1)), \quad (5.9)$$

and for sufficiently large  $n$

$$\lambda_1/(np) \sim \mathcal{N}\left(1, n\sqrt{\frac{1-p}{p}}\right), \quad (5.10)$$

where  $\mathcal{N}(\mu, \sigma)$  is a Gaussian distribution with mean  $\mu$  and variance  $\sigma^2$ . However, the first one requires  $p(1-p) = \Omega(\log^4 n/n)$ , while the latter requires

$p \in (0, 1]$  to be a fixed number. Hence, the proof presented in [33] was correct only for the fixed nonzero  $p$ .

Finally, the authors falsely approximated transition rate  $\gamma$  by  $\frac{1+r}{\lambda_1} \approx 1/(np)$  to Erdős-Rényi graphs. They took the Hamiltonian of the form

$$-|\lambda_1\rangle\langle\lambda_1| - |w\rangle\langle w| + \frac{1}{\lambda_1}\tilde{A}, \quad (5.11)$$

where  $\tilde{A} + \lambda_1 |\lambda_1\rangle\langle\lambda_1| = A$ , hence the transition rate  $\gamma$  equals  $\frac{1}{\lambda_1}$ . Provided with high probability  $|\lambda_1/(np) - 1| \leq \delta = \frac{1}{\sqrt{n}}$ , using perturbation theory similarly as in [33] one can have

$$p(t) = \frac{1}{1 + n\delta^2/4} \sin^2 \left( \frac{\sqrt{\delta^2/4 + 1/n}}{2} t \right). \quad (5.12)$$

The formula implies that by choosing proper  $T = \Theta(\sqrt{n})$  we can achieve the constant success probability. This derivation was proven by approximating  $|\lambda_1\rangle\langle\lambda_1|$  with  $|s\rangle\langle s|$ . However, approximation  $|\lambda_1\rangle = \alpha|s\rangle + \beta|s^\perp\rangle$  allows only the approximation of the form  $|\lambda_1\rangle\langle\lambda_1| = |\alpha|^2|s\rangle\langle s| + o(1)H_{\lambda_1}$ , where  $\|H_{\lambda_1}\| = \mathcal{O}(1)$ . Hence, the new transition rate would equal  $\frac{1}{|\alpha|^2 np}$ , and it is not obvious how good is the approximation of  $\alpha$ . Furthermore, part  $o(1)H_{\lambda_1}$  should have the spectral norm of order  $\mathcal{O}(1/\sqrt{n})$  so that we could use the perturbation theory.

For these reasons, we will try to provide similar results concerning the optimality of quantum spatial search on random Erdős-Rényi graphs, by using the adjacency matrix. We will consider the efficiency in two contexts:

1. When can the quantum search find almost all nodes optimally?
2. When can the quantum search find *all* nodes optimally (no-hiding property)?

The first objective requires  $|\langle s|\lambda_1\rangle| = 1 - o(1)$ , and  $\max_i |\lambda_i| = o(\lambda_1)$ . Then by using Lemma 5.1 and Proposition 5.3 we can find  $n(1 - o(1))$  nodes in  $\Theta(\sqrt{n})$  with  $\Theta(1)$  success probability. The second objective requires also  $\| |s\rangle - |\lambda_1\rangle \|_\infty = o(1/\sqrt{n})$ . Here, the application of Lemma 5.1 is straightforward.

### 5.1.2 Quantum search is almost always optimal

First, let us show the convergence of eigenvalues. We will use the theorems from [50], originally defined for Chung-Lu model  $\mathcal{G}_n^{\text{CL}}(\omega)$ , written here for  $\omega$  being all- $np$  vector.

**Theorem 5.4** ([50]). *Let  $A$  be an adjacency matrix of a random Erdős-Rényi graph with parameter  $p$ . If  $p > \frac{8}{9} \ln(\sqrt{2n})/n$ , then, with the probability at least  $1 - 1/n$  we have*

$$|\lambda_1(A) - np| \leq \sqrt{8np \ln(\sqrt{2n})}, \quad (5.13)$$

$$\max_{i \geq 2} |\lambda_i(A)| \leq \sqrt{8np \ln(\sqrt{2n})}. \quad (5.14)$$

Before proving  $|\langle \lambda_1 | s \rangle| = 1 - o(1)$ , we require another technical lemma.

**Lemma 5.5** ([50]). *Let  $A$  be an adjacency matrix of a random Erdős-Rényi graph with parameter  $p$ . Let for  $n$  sufficiently large  $p > \frac{8}{9} \ln(n)/n$ . Then, with the probability at least  $1 - o(1/n)$ , for  $n$  sufficiently large we have*

$$\|A - \mathbb{E}A\| \leq \sqrt{8np \ln(n)}. \quad (5.15)$$

The lemma comes from the proof of Theorem 1 [50] by choosing  $\varepsilon = 2/n$  therein.

**Lemma 5.6.** *Let  $A$  be an adjacency matrix of a random Erdős-Rényi graph with parameter  $p$ . Provided  $p = \omega(\log n/n)$ , we have asymptotically almost surely  $|\langle \lambda_1(A) | s \rangle| = 1 - o(1)$ .*

*Proof.* The proof goes similar as in [33]. Let  $|\lambda_1\rangle = \alpha |s\rangle + \beta |s^\perp\rangle$ . it is sufficient to show that  $\alpha \geq 1 - o(1)$ . Note that we have

$$\begin{aligned} (A - \mathbb{E}A) |\lambda_1\rangle &= \sum_i \lambda_i |\lambda_i\rangle \langle \lambda_i| - np |s\rangle \langle s| = \lambda_1 |\lambda_1\rangle - np\alpha |s\rangle \\ &= (\lambda_1 - np\alpha^2) |\lambda_1\rangle - np\alpha\beta |s^\perp\rangle, \end{aligned} \quad (5.16)$$

and by this  $\|(A - \mathbb{E}A) |\lambda_1\rangle\|^2 \geq (\lambda_1 - np\alpha^2)^2$ . Since  $\|B|\varphi\rangle\| \leq \|B\|$  for any choice of  $B$  and  $|\varphi\rangle$ , by Lemma 5.5 we have

$$(\lambda_1 - np\alpha^2)^2 \leq 8np \ln(n), \quad (5.17)$$

and by this

$$\alpha^2 \geq \frac{2\sqrt{np \ln(n)}}{np} - \frac{\lambda_1}{np} = 2\sqrt{\frac{\ln n}{np}} - \frac{np(1 - o(1))}{np} = 1 - o(1), \quad (5.18)$$

where the transformations are valid a.a.s., and the first inequality comes from Lemma 5.4. By  $\alpha^2 = 1 - o(1)$  we have  $\alpha = 1 - o(1)$ .  $\square$

Taking all into account, by Lemma 5.1 and Proposition 5.3, provided  $p = \omega(\log(n)/n)$ , almost all nodes can be found optimally in time  $\Theta(\sqrt{n})$  with constant success probability. Note that since  $|\langle \lambda_1 | s \rangle| = 1 - o(1)$ , we can start the evolution in  $|s\rangle$  instead of  $|\lambda_1\rangle$ .

### 5.1.3 No-hiding theorem

In this section we will show that if  $p = \omega(\log^3(n)/(n \log^2 \log n))$ , the quantum search is optimal for *all* nodes for almost all graphs. We will show this by proving  $\| |\lambda_1\rangle - |s\rangle \| = o(1/\sqrt{n})$  a.a.s. Then, by the direct application of the Lemma 5.1 we obtain the result.

Here we follow the proof shown by Mitra [74] which assumed  $p \geq \log^6 n/n$ . The proof of the following proposition can be found in App. B.1.1.

**Proposition 5.7** ([36]). *Let  $|\lambda_1\rangle$  be a principal eigenvector of an adjacency matrix of a random Erdős-Rényi graph with parameter  $p$ . For the probability  $p = \omega(\log^3(n)/(n \log^2 \log n))$  and some constant  $c > 0$  we have*

$$\| |\lambda_1\rangle - |s\rangle \|_\infty \leq c \frac{1}{\sqrt{n}} \frac{\ln^{3/2}(n)}{\sqrt{np} \ln(np)} \quad (5.19)$$

with probability  $1 - o(1)$ .

### 5.1.4 Conclusions for adjacency matrix

In Sections 5.1.2 and 5.1.3 we have shown two significant thresholds for  $p$  which determine the known behaviour of quantum search based on CTQW for adjacency matrices. For  $p = \omega(\log n/n)$ , almost all nodes can be found in optimal time with constant success probability. Under stronger condition  $p = \omega(\log^3(n)/(n \log^2 \log(n)))$ , all vertices can be found in optimal  $\Theta(\sqrt{n})$  time.

One could ask what happens below these two thresholds. Erdős-Rényi graph is a very special model, with the connectivity threshold at  $\ln n/n$ . This means that for any  $\varepsilon > 0$ , for  $p < (1 - \varepsilon) \ln(n)/n$  there is almost surely at least one isolated vertex. For such a vertex, the amplitude does not change, hence the success probability is  $1/n$  independently on the evolution time. Furthermore, if  $np < 1$  then all connected components are of order at most  $\mathcal{O}(\log(n))$ , hence one cannot expect the success probability better than  $\mathcal{O}(\log(n)/n)$ .

Still, when  $p > (1 + \varepsilon) \ln n/n$ , the graphs are almost surely connected. Hence, there is a gap between the derived threshold and the connectivity threshold. Unfortunately, for the adjacency matrix we have to take care of all three parameters required in Lemma 5.1: largest eigenvalue, spectral gap, and principal eigenvector. In the next section, we will provide a better result using the Laplacian matrix instead of the adjacency matrix.



## 5.2 Laplacian matrix

Let us consider the Laplacian matrix  $L = D - A$ . Provided the graph  $G$  is connected, its Laplacian is a nonnegative matrix with a single zero eigenvalue  $\lambda_n = 0$ , with the corresponding eigenvector being an uniform superposition  $|s\rangle$ . Hence, not only  $\langle \lambda_n(L) | s \rangle = 1$ , but also  $\| |\lambda_n(L)\rangle - |s\rangle \|_\infty = 0$ . Therefore, the conditions for optimality for almost all nodes in fact already imply the optimality for all nodes, provided the graph is almost surely connected.

Note that for the Laplacian matrix we will consider  $H_G = I - \gamma L$  matrix, in order to provide a spectral gap next to the largest eigenvalue as required by Lemma 5.1. Since  $-L$  is a nonpositive matrix, a shifting and rescaling procedure will always be required.

Let us now show that all nodes can be found in  $\Theta(\sqrt{n})$  time using the Laplacian matrix as long as  $p = \Omega(\log n/n)$ . We will demonstrate it in two parts, first assuming  $p = \omega(\log n/n)$ , then for  $p = p_0 \ln n/n$  for  $p_0 \in \mathbb{R}_{\geq 0}$ .

### 5.2.1 Case $p = \omega(\log n/n)$

Under the condition  $p = \omega(\log n/n)$  we have  $\lambda_2(L/(np)) = 1 + \mathcal{O}\left(\sqrt{\frac{\log n}{np}}\right) \sim 1$  [75]. To show that  $H_G = -\gamma L$  for a proper choice of  $\gamma$  satisfies Lemma 5.2, it is enough to show that  $\lambda_n/(np) \rightarrow 1$  as well. By Theorem 1.5 from [76], if  $\tilde{L}$  is a symmetric matrix whose off-diagonal elements have two-points distribution with mean 0 and variance  $p(1-p)$  and  $\tilde{L}_{ii} = \sum_{j \neq i} \tilde{L}_{ij}$ , then

$$\lim_{n \rightarrow \infty} \frac{\|\tilde{L}\|}{\sqrt{2np(1-p) \log n}} = 1. \quad (5.20)$$

Note that  $p$  may depend on  $n$ . Hence, we can extend the Corollary 1.6 from the same paper.

Let  $L = \tilde{L} + \mathbb{E}L$ , where  $\mathbb{E}L$  is an expectation of a random Erdős-Rényi Laplacian matrix.  $\mathbb{E}L$  has a single 0 eigenvalue and all of the others equal  $np$ . By this we have  $\|\mathbb{E}L\| = np$ . Then we have

$$\left| \frac{\lambda_1(L)}{np} - \frac{\|\mathbb{E}L\|}{np} \right| \leq \frac{\|L - \mathbb{E}L\|}{np} = \frac{\|\tilde{L}\|}{np} \rightarrow 0 \quad (5.21)$$

where the limit comes from Eq. (5.20), assuming  $p = \omega(\log n/n)$ .

We have shown that  $\lambda_1(L) \sim np$ ,  $\lambda_{n-1}(L) \sim np$ , and  $\lambda_n = 0$ . Note that for  $H_G = I - L/(np)$ , we have  $\lambda_1(H_G) = 1$ ,  $\lambda_2(H_G) = o(1)$ , and  $\lambda_n = o(1)$ . Since the principal eigenvector of  $H_G$  is a uniform superposition, we have that for the combinatorial Laplacian *all vertices* can be found in optimal  $\Theta(\sqrt{n})$  time with  $1 + o(1)$  success probability.

### 5.2.2 Case $p = p_0 \ln n/n$

Suppose  $G$  is a random graph chosen according to  $\mathcal{G}_n^{\text{ER}}(p_0 \frac{\ln(n)}{n})$  distribution, for  $p_0 > 1$  being a constant. Let  $\delta_{\min}$  ( $\delta_{\max}$ ) be a minimal (maximal) degree of a sampled graph. Based on [75] we can show that the algebraic connectivity  $\lambda_{n-1}(L) \sim \delta_{\min}$ . Below we show similar results for the largest eigenvalue. The proof can be found in App. B.1.2.

**Theorem 5.8.** *Let  $G$  be a random graph chosen according to  $\mathcal{G}_n^{\text{ER}}(p)$ . Let  $p_0 > 0$  be such that  $np \geq p_0 \ln(n)$ . Let  $\delta_{\max} \sim cnp$  for some  $c > 0$  almost surely. Then almost surely  $\lambda_1(L(G)) \sim cnp$ .*

Based on [77] it can be shown that

$$\delta_{\min} \sim (1 - p_0) \left( W_{-1} \left( \frac{1 - p_0}{ep_0} \right) \right)^{-1} \ln(n) \quad (5.22)$$

and

$$\delta_{\max} \sim (1 - p_0) \left( W_0 \left( \frac{1 - p_0}{ep_0} \right) \right)^{-1} \ln(n). \quad (5.23)$$

Here  $W_{-1}$  and  $W_0$  are Lambert W functions.

Note that  $\lambda_1(L) = \Theta(\lambda_{n-1}(L))$ , which is sufficient to show the optimality of the search. Indeed, let us consider graph matrix  $H_G = I - L/\lambda_1(L)$ . Its largest eigenvalue equals 1, and the smallest one equals 0. Since  $\lambda_1(L)$  and  $\lambda_{n-1}(L)$  grows with the same complexity, the spectral gap for  $H_G$  equals  $1 - \lambda_{n-1}(L)/\lambda_1(L)$ , which is constant. Applying Lemma 5.2 we obtain a lower bound for success probability

$$\sim \frac{1 - \frac{\lambda_{n-1}(L)}{\lambda_1(L)}}{1 + \frac{\lambda_{n-1}(L)}{\lambda_1(L)}} = \frac{\lambda_1(L) - \lambda_{n-1}(L)}{\lambda_1(L) + \lambda_{n-1}(L)} \sim \frac{W_{-1} \left( \frac{1-p_0}{ep_0} \right) - W_0 \left( \frac{1-p_0}{ep_0} \right)}{W_{-1} \left( \frac{1-p_0}{ep_0} \right) + W_0 \left( \frac{1-p_0}{ep_0} \right)}. \quad (5.24)$$

Note that the lower bound can be improved. Adding the identity matrix has no impact on the quantum evolution, and rescaling of the form  $H/b$  can be compensated by the proper transformation of transition rate  $\gamma$ .

Without loss of generality, let  $H'$  be a Hamiltonian with the largest eigenvalue equal to 1. Let  $H(a) = (H' + aI)/b$ . We will search for such  $a, b \in \mathbb{R}$  that  $H(a)$  will have a spectral gap as required in Lemma 5.1, and so that  $\frac{1-c}{1+c}$  is maximized. Note that  $b > 0$  so that the order of eigenvalue is preserved. Furthermore,  $b = 1 + a$ , as  $H(a)$  should still have the largest eigenvalue equal to 1.

Let  $\lambda_2, \lambda_n$  be the second largest and smallest eigenvalues of  $H'$ . Note that the  $c$  of  $H(a)$  is defined as  $c(a) := \frac{\max\{|\lambda_2+a|, |\lambda_n+a|\}}{1+a}$ . Since the success

probability  $\frac{1-c}{1+c} = \frac{2}{1+c} - 1$  decreases in  $c$ , maximizing the lower bound on the success probability is equivalent to minimizing  $c$ . Note that for  $a_{\text{thr}} = -\frac{\lambda_2 + \lambda_n}{2}$  we have  $c(a) = \frac{\lambda_2 - \lambda_n}{2 - \lambda_2 - \lambda_n}$ . For  $a > a_{\text{thr}}$ , the  $\lambda_2 + a$  plays a dominant role in the maximum in  $c(a)$ , hence

$$c(a) = \frac{\lambda_2 + a}{1 + a} = 1 + \frac{\lambda_2 - 1}{1 + a}, \quad (5.25)$$

is a function decreasing in  $a$  because  $\lambda_2 - 1 < 0$ . For  $a < a_{\text{thr}}$ , the  $\lambda_n + a$  plays a dominant role and we have

$$c(a) = -\frac{\lambda_n + a}{1 + a} = -1 + \frac{\lambda_n - 1}{1 + a}, \quad (5.26)$$

which increases in  $a$ . This confirms that  $c(a)$  has the global maximum at  $a_{\text{thr}}$ , which gives the optimal shifting and rescaling parameter. Note that for optimal  $a$  we have the success probability

$$\sim \frac{1 - c(a_{\text{thr}})}{1 + c(a_{\text{thr}})} = \frac{1 - \frac{\lambda_2 - \lambda_n}{2 - \lambda_2 - \lambda_n}}{1 + \frac{\lambda_2 - \lambda_n}{2 - \lambda_2 - \lambda_n}} = \frac{1 - \lambda_2}{1 - \lambda_n}. \quad (5.27)$$

Let us consider the Laplacian of Erdős-Rényi graphs, where  $\lambda_{n-1}(L) \sim (1-p_0) \left( W_{-1} \left( \frac{1-p_0}{ep_0} \right) \right)^{-1} \ln n$  and  $\lambda_1(L) \sim (1-p_0) \left( W_0 \left( \frac{1-p_0}{ep_0} \right) \right)^{-1} \ln n$ . Then for  $H_G = I - L/\lambda_1$  we have

$$\lambda_1(H_G) = 1, \quad (5.28)$$

$$\lambda_2(H_G) \sim 1 - \frac{W_0 \left( \frac{1-p_0}{ep_0} \right)}{W_{-1} \left( \frac{1-p_0}{ep_0} \right)}, \quad (5.29)$$

$$\lambda_n(H_G) = 0. \quad (5.30)$$

Using the optimal shift-and-rescaling technique we have that the success probability can be upperbounded almost surely by

$$\sim \frac{1 - c(a)}{1 + c(a)} = \frac{1 - \lambda_2(H_G)}{1 - \lambda_n(H_G)} = \frac{W_0 \left( \frac{1-p_0}{ep_0} \right)}{W_{-1} \left( \frac{1-p_0}{ep_0} \right)}. \quad (5.31)$$

The function changes smoothly from 0 for  $p_0 = 1$  to 1 for  $p_0 \rightarrow \infty$ , see Fig 5.2. This coincides with the intuition behind the random Erdős-Rényi graphs. For probability  $p < \frac{(1-\varepsilon) \ln n}{n}$ , the graphs are almost surely disconnected, hence the Laplacian has multiple zero eigenvalues, giving no spectral gap. On the other

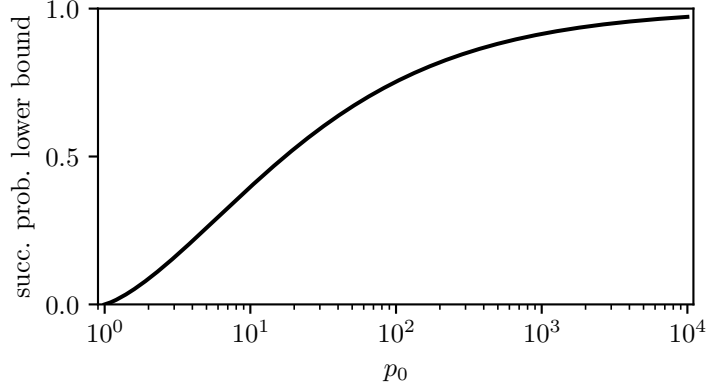


Figure 5.2: The limit lower bound of success probability of finding nodes for Erdős-Rényi graphs with parameter  $p = p_0 \frac{\ln n}{n}$ . Note that the function changes smoothly from 0 for  $p_0 = 1$  to 1 for  $p_0 \rightarrow \infty$ .

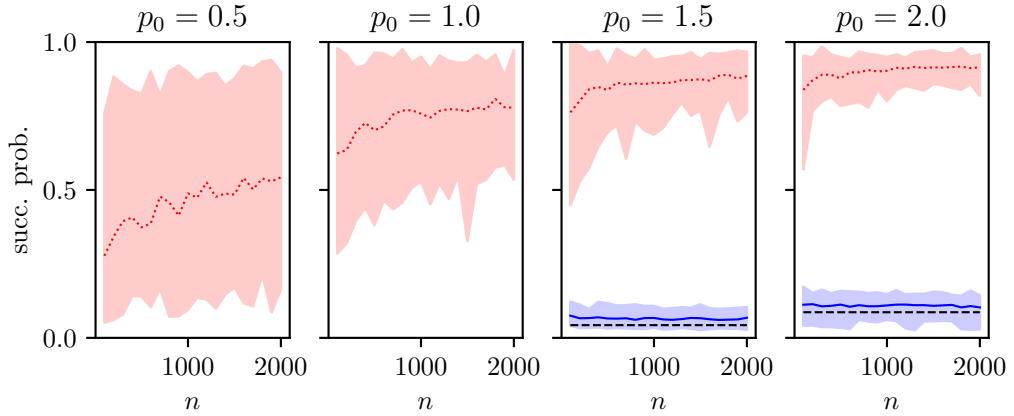


Figure 5.3: The success probability and its lower bound for Erdős-Rényi graphs with  $p = p_0 \ln n / n$  with  $H_G = I - L / \mu_1$ . Dotted red line denote the mean success probability with  $\gamma = \sum_{i \geq 2} \frac{|\langle w | \lambda_1 \rangle|^2}{1 - \lambda_i} / \sum_{i \geq 2} |\langle w | \lambda_1 \rangle|^2$ , which is a transition rate proposed in [33]. The evolution time equals  $\pi \sqrt{n} / 2$ . The blue solid line denotes  $\frac{1-c}{1+c}$  where  $c$  is the second maximal eigenvalue in absolute value of the optimally shifted and rescaled Laplacian. The dashed black line denotes the limit lower bound on the success probability computed according to the formula  $W_0 \left( \frac{1-p_0}{ep_0} \right) / W_{-1} \left( \frac{1-p_0}{ep_0} \right)$ . Note that it is well-defined only for  $p_0 > 1$ . For each  $p_0$  and  $n = 100, 200, \dots, 2000$ , we sampled 50 graphs and its largest giant component was chosen. The areas span the minimum and maximum values obtained.

hand, when  $p_0$  approaches  $\infty$ , the value of  $p$  becomes ‘closer’ to  $\omega(\log n/n)$  case which was proved to attain full success probability. Thus  $p_0 \frac{\ln n}{n}$  is a smooth transition case for the Laplacian matrix.

The derived value  $\frac{W_0\left(\frac{1-p_0}{ep_0}\right)}{W_{-1}\left(\frac{1-p_0}{ep_0}\right)}$  is only a lower bound. The analysis of  $p = p_0 \frac{\ln n}{n}$  for  $p_0 = 0.5, 1, 1.5, 2$  shows that not only for  $p_0 > 1$  the success probability is high, but even the nodes from a giant component retain high success probability, see Fig. 5.3. However, for  $p_0 \leq 1$  almost surely there are isolated vertices which cannot be found in  $o(n)$  time.

### 5.3 Conclusions

In this section we analyzed the efficiency of CTQW spatial search for random Erdős-Rényi graphs. Our analysis considered both adjacency matrix and the Laplacian matrix, however the obtained results favour the latter graph matrix. For adjacency matrix,  $p = \omega(\log^3(n)/n)$  is required at the moment to guarantee that all vertices can be found in optimal  $\Theta(\sqrt{n})$  time with the constant success probability. Relaxing the condition on  $p$  to  $p = \omega(\log n/n)$ , we can still find most of them.

For the Laplacian matrix, we can achieve constant success probability for *all* vertices already for  $p > (1 + \varepsilon) \ln n/n$  for any  $\varepsilon > 0$ . This is tight as for  $p < (1 - \varepsilon) \ln n/n$  sampled graphs almost surely have isolated vertices which cannot be found by any reasonable quantum-walk based search. While the results obtained for the adjacency matrix give only sufficient conditions and could be theoretically improved, our consideration shows considerable advantage of applying the Laplacian matrix over the adjacency matrix.



## Chapter 6

# Quantum spatial search on heterogeneous graphs

At this moment the state-of-the-art results concerning Childs and Goldstone quantum spatial search can be found in [39]. Let  $H_G$  be a graph matrix with eigenvalues  $\lambda_1 = 1 \geq \lambda_2 \geq \dots \geq \lambda_n = 0$ . Let  $|\lambda_i\rangle$  be an eigenvector corresponding to eigenvalue  $\lambda_i$ . Let  $\Delta := \lambda_1 - \lambda_2$  be a spectral gap. Let  $w$  be a marked node and  $\varepsilon := |\langle w|\lambda_1\rangle|^2$ . Finally, let

$$S_k := \sum_{i=2}^n \frac{|\langle w|\lambda_i\rangle|^2}{(1 - \lambda_i)^k}. \quad (6.1)$$

Based on Theorem 2 from [39], if

$$\sqrt{\varepsilon} < c \min \left( \frac{S_1 S_2}{S_3}, \Delta \sqrt{S_2} \right) \quad (6.2)$$

for sufficiently small  $c$ , then applying Hamiltonian  $S_1 H_G + |w\rangle\langle w|$  for time  $T = \Theta(\frac{1}{\sqrt{\varepsilon}} \frac{\sqrt{S_2}}{S_1})$  transforms the initial state  $|\lambda_1\rangle$  into  $|f\rangle$  satisfying  $|\langle w|f\rangle|^2 = \Theta(S_1^2/S_2)$ .

Note that not all graphs satisfy the condition given in Eq. (6.2) [39]. Furthermore, the condition, estimation on  $T$  and  $\gamma = S_1$  requires knowledge about the marked node based on the definition of  $S_k$ . Based on the introduction from the previous chapter and [28, 32], the optimal measurement time and transition rate may depend on the marked node. While the same situation occurs in Lemmas 5.1 and 5.2, statistics  $S_k$  are not required in general for estimating the optimal measurement time or to detect the validity of the condition from Eq. (6.2).

In the following sections, we consider the choice of graph matrix  $H_G$  and the measurement time  $T$ . In particular, we consider a normalized Laplacian,

which was not widely considered in the theory of quantum search, except for a brief recall in [33,39]. Finally, we propose an educated-guess method which does not require knowledge on the value of optimal  $T$ .

One should note that there exists a continuous-time quantum walk model which was proven to attain the quadratic speed-up over the corresponding markov random walk [38]. However, the model requires a quadratically larger quantum system.

## 6.1 Choice of $H_G$ for heterogeneous graphs

Neither adjacency matrix nor the Laplacian seems to be a good choice for governing the efficiency of quantum spatial search. While there are known results concerning the spectral gap for the adjacency matrix, the principal eigenvector takes usually a complicated form. The principal eigenvector of the Laplacian matrix of a connected graph is always an equal superposition, although there is a serious issue with the spectral gap. Note that the largest eigenvalue satisfies  $\delta_{\max} \leq \lambda_1(L) \leq 2\delta_{\max}$  [78,79], thus  $\lambda_1(L) = \Theta(\delta_{\max})$ . However, it is known that the second smallest eigenvalue satisfies  $\lambda_{n-1} \leq \delta_{\min}$  [78]. Thus, for the typical choice  $I - L/\lambda_1$ , we find out that the spectral gap is at most  $\mathcal{O}\left(\frac{\lambda_{n-1}(L)}{\lambda_1(L)}\right)$ , which is at most  $\mathcal{O}\left(\frac{\delta_{\min}}{\delta_{\max}}\right)$ . This bound can decrease very rapidly. For example for Barabási-Albert graphs, where the minimum degree equals  $m_0$  and the maximum degree grows like  $\Theta(\sqrt{n})$  [52], the spectral gap decreases like  $\mathcal{O}\left(\frac{1}{\sqrt{n}}\right)$ . This implies that the necessary conditions from Lemmas 5.1 and 5.2 are not satisfied.

There are significant problems with using the adjacency matrix and the Laplacian as a graph matrix. Before considering the normalized Laplacian, let us consider a uniform random walk defined through matrix  $P = D^{-1}A$ . If the graph is connected the mean first hitting time to vertex  $v$  equals  $\langle T_v \rangle = \frac{|E|}{\deg(v)} S_1$ , see App. B.3 for derivation. Provided the spectral gap  $\lambda_1(P) - \lambda_2(P)$  is constant, we have  $\langle T_v \rangle = \Theta\left(\frac{|E|}{\deg v}\right)$ . This is optimal, as  $\langle T_v \rangle \geq \frac{|E|}{d_j} - \frac{1}{2}$  for any choice of a connected graph and  $v$ .

Closely correlated to the stochastic matrix  $P$  is the normalized Laplacian  $\mathcal{L} = I - D^{-1/2}AD^{-1/2}$ . The normalized Laplacian is a nonnegative matrix with the spectrum lying in  $[0, 2]$  interval. Furthermore, provided the graph is connected, the matrix has a single 0-eigenvalue with the corresponding eigenvector

$$|\lambda_1\rangle = \frac{1}{\sqrt{2|E|}} \sum_{v \in V} \sqrt{\deg(v)} |v\rangle. \quad (6.3)$$



Note that for a connected graph  $D$  is invertible and

$$D^{-1/2} \mathcal{L} D^{1/2} = I - D^{-1} A = I - P, \quad (6.4)$$

hence the normalized Laplacian is similar to the corresponding stochastic matrix up to transformation  $x \mapsto 1 - x$ . Hence the spectral gap is the same for  $I - \mathcal{L}$  and  $P$ . Furthermore, by Lemma 5.1 one can find vertex  $v$  for the normalized Laplacian in time  $\Theta(1/\sqrt{\varepsilon}) = \Theta(\sqrt{\frac{|E|}{\deg v}})$  which is the square root of classical hitting time.

One could expect that similarly as it was for the Laplacian graph, the constant spectral gap occurs very rarely. In the next subsection, we show that the constant spectral gap occurs for heterogeneous random graph models, including the paradigmatic Barabási-Albert model.

## 6.2 Special random graph models

### 6.2.1 Chung-Lu graphs

In this section we will provide analytical evidence why the normalized Laplacian may be a better graph matrix compared to the adjacency matrix. Since the parametrization of Chung-Lu graphs lies in the  $n$ -dimensional space for  $n$ -vertex graph, in this section we will consider a special parameter class  $\omega_i = n^{a+\frac{i}{n}b}$  for  $i = 1, \dots, n$  and  $0 < a < a + b \leq 1$ . Note we assume  $b > 0$ , hence our parametrization *does not* generalize Erdős-Rényi model.

Let us first consider the adjacency matrix based graph matrix  $\frac{1}{\lambda_1(A)} A$ . In order to apply Lemma 5.1, one has to ensure there is a constant gap between the largest eigenvalues of  $H_G$  (equal to 1 in here), and the maximum in absolute value over the remaining eigenvalues. Let  $\tilde{d} = \frac{\|\omega\|_2^2}{\|\omega\|_1}$ . Given the maximum expected degree  $\omega_{\max} := \max_i \omega_i > \frac{8}{9} \ln(\sqrt{2}n)$ , one can show that asymptotically almost surely [50]

$$|\lambda_1 - \tilde{d}| \leq \sqrt{8\omega_{\max} \ln(\sqrt{2}n)}, \quad (6.5)$$

$$\max_{i \geq 2} |\lambda_i| \leq \sqrt{8\omega_{\max} \ln(\sqrt{2}n)}. \quad (6.6)$$

Given  $\sqrt{\omega_{\max} \ln(n)}/\tilde{d} = o(1)$  one has a constant spectral gap for  $\frac{1}{\lambda_1(A)} A$ . It is difficult to analyse the fraction in general, since the behaviour of  $\tilde{d}$  strongly depends on the form of  $\omega$ . In the case of the proposed  $\omega$  parameter class, for any valid  $a, b$  we have  $\omega_{\max} = n^{a+b}$  and  $\tilde{d} = \frac{n^{1+2a+2b}}{2b \log n} \frac{b \log n}{n^{1+a+b}} = \frac{1}{2} n^{a+b} =$

$\omega(\sqrt{n^{a+b} \ln n})$ , see App. B.2.1. Hence, based on Lemma 5.1, the time required to maximize the success probability for vertex  $w$  is of order  $\Theta(1/|\langle w|\lambda_1\rangle|)$ .

Let  $|\omega\rangle = \frac{1}{\|\omega\|_2} \sum_i |\omega_i\rangle$ . Similarly as it was for Erdős-Rényi graphs [33], it can be shown that provided  $\sqrt{\omega_{\max} \ln(n)}/\tilde{d} = o(1)$  we have  $\langle \omega|\lambda_1\rangle = 1 - o(1)$ . Based on this fact one can show that in the case of the chosen parametrization, as long as  $a < 3b$ , for almost all nodes  $i$  we have  $\langle i|\lambda_1\rangle \sim n^{a+\frac{i}{n-1}b}/\|\omega\|_2$ , see App. B.2.4. Hence for almost all vertices we have the time complexity

$$\|\omega\|_2/n^{a+\frac{i}{n-1}b} \sim \sqrt{\frac{n^{1+2a+2b}}{2b \log n}} \frac{1}{n^{a+\frac{i}{n}b}} = \Theta\left(\sqrt{\frac{n}{\log n}} n^{b(1-\frac{i}{n})}\right). \quad (6.7)$$

The complexity strongly depends on  $i$ , hence the marked vertex. For  $i = n$ , *i.e.* the node with maximal expected degree, we have complexity  $\Theta(\sqrt{\frac{n}{\log n}})$ .

Contrary for  $i = 1$  we have time complexity  $\Theta(\sqrt{\frac{n}{\log n}} n^b)$  (note  $n^{\frac{1}{n}} \sim 1$ ).

In the case of the normalized Laplacian, as long as the minimum expected degree  $\omega_{\min} := \min_i \omega_i = \omega(\log n)$ , positive eigenvalues satisfy

$$\max_{i \geq 2} |\lambda_i - 1| \leq 3\sqrt{\frac{6 \ln(2n)}{\omega_{\min}}} = o(1). \quad (6.8)$$

For the considered parameter family we have  $\omega_{\min} > n^a = \omega(\log n)$ . Furthermore, for the normalized Laplacian the minimum eigenvalue equals 0, hence  $I - \mathcal{L}$  satisfies the requirements from Lemma 5.1. Hence the complexity of finding the marked node is  $\Theta(\sqrt{|E|/\deg(w)})$ , where  $|E|$  and  $\deg(w)$  are the number of edges and the degree of  $w$  of *sampled* graph. However, with probability  $1 - o(1)$  for the considered  $\omega$  we have almost surely  $|E| \sim \mathbb{E}E = \frac{n^{1+a+b}}{b \log n}$  and for the degree we have almost surely  $\deg(i) \sim \omega_i = n^{a+\frac{i}{n}b}$ , see App. B.2.2 and B.2.3. Hence the complexity for the normalized Laplacian is

$$\sqrt{\frac{|E|}{\deg(i)}} \sim \sqrt{\frac{n^{1+a+b}}{b \log n}} \frac{1}{n^{a+\frac{i}{n}b}} = \Theta\left(\sqrt{\frac{n}{\log n}} \sqrt{n^{b(1-\frac{i}{n})}}\right) \quad (6.9)$$

For  $i = n$  we have complexity  $\Theta(\sqrt{\frac{n}{\log n}})$  while for  $i = 1$  the complexity equals  $\Theta(\sqrt{\frac{n}{\log n}} \sqrt{n^b})$  hence it is better by  $\sqrt{n^b}$  compared to the adjacency matrix. According to our derivation presented in the previous section, the classical search is quadratically slower compared to quantum search using the normalized Laplacian.

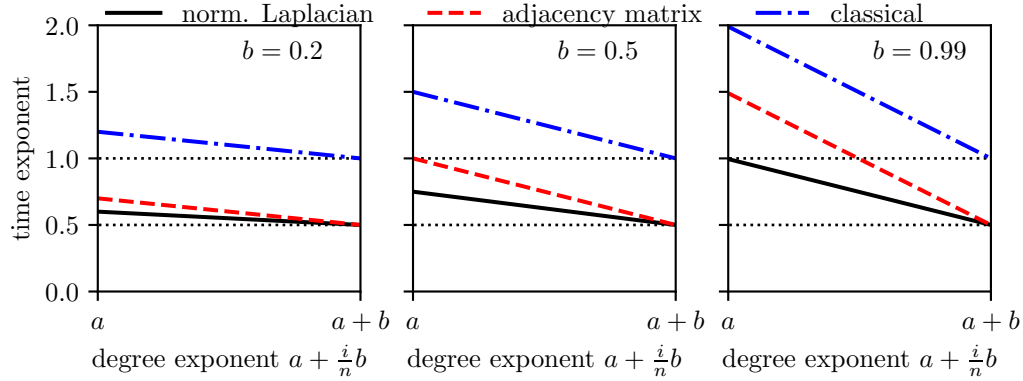


Figure 6.1: The visualization for time complexity depending on the expected degree of the vertex. The visualization is made for  $b = 0.2, 0.5, 0.99$ , for we can choose  $a = 0.01$ . Note that independently on the model chosen the time complexity decrease with the increase of the degree. Horizontal dotted lines are for readability only and are placed for general optimal quantum and classical search.

In Fig. 6.1 we present a visualization of complexities for various values of  $a$  and  $b$ . Note that for any node the complexity for quantum search with the adjacency matrix is between the quantum search with the normalized Laplacian and the classical search. However, the worst case scenario for the normalized Laplacian is at worst equal to the optimal measurement time of the classical search. This is not the case for the adjacency matrix. For  $b > 0.5$  the hardest to find node yields the complexity worse than many nodes for the classical search. In the extreme case for  $b \approx 1$  the complexity is worse for almost half of the nodes.

This example shows that the choice of the graph matrix has a crucial impact on the efficiency of CTQW-based quantum search. Furthermore, we found a large nonregular family of graphs, for which the quantum search is proved to be quadratically faster than the classical random walk search.

### 6.2.2 Barabási-Albert graphs

In this subsection we consider a Barabási-Albert graph model which is the paradigmatic random graph model for sampling complex networks. Let us consider the efficiency of quantum search using the normalized Laplacian. Let us start with proving the existence of a spectral gap. According to [51], we have  $\frac{h^2}{2} \leq \lambda_{n-1}(\mathcal{L}) \leq 2h$ , with  $h \geq 0$  defined as in Section 6.2 in [51]. Since  $\frac{h^2}{2} \leq 2h$ , we have  $h \leq 4$ . Hence if  $h = \Omega(1)$  we immediately have

$\lambda_{n-1} = \Theta(1)$ . In the case of Barabási-Albert model we have  $h \geq \frac{\iota_a}{2m_0 + \iota_a}$  with  $\iota_a$ , see Section 6.4 in [51]. By Lemma 6.4.4 from [51] we have  $\iota_a = \Omega(1)$  for  $m_0 > 1$ . All the inequalities above show that indeed  $\lambda_{n-1}(\mathcal{L}) = \Theta(1)$  which gives a constant spectral gap. This is sufficient to apply Lemma 5.1.

Now let us analyse the number of edges and degrees of nodes. By the very construction, for any fixed  $m_0$  the number of edges for  $n$ -vertex Barabási-Albert graph is at most  $nm_0$ . Since Barabási-Albert graphs are connected, the number of edges is at least  $n - 1$ . From this we have  $|E| = \Theta(n)$ . The last added vertex has the degree between 1 and  $m_0$ , hence for fixed  $m_0$  the smallest degree is constant. Contrary, the largest degree grows like  $\Theta(\sqrt{n})$  [52]. Hence the search complexity varies between  $\Theta(\sqrt{n})$  for constant degree nodes and  $\Theta(\sqrt[4]{n})$  for the highest degree nodes.

In the case of Barabási-Albert we obtained a complexity below  $\Theta(\sqrt{n})$  lower bound for high degree vertices. However, since there are only  $\Theta(n)$  edges, then almost all nodes would have a fixed degree. Hence better-than-optimal complexity happens only in rare cases.

For the classical search we obtain analogical results: the time complexity goes from  $\Theta(\sqrt{n})$  for high-degree nodes to  $\Theta(n)$  for constant degree nodes.

In the case of the adjacency matrix there is a lack of analytical derivation of a spectral gap. For the Laplacian, following the reasoning presented previously we can show that the spectral gap for  $I - L/\lambda_1(L)$  is at most  $\mathcal{O}(1/\sqrt{n})$ . Still it is possible to approach the matrices of this graph numerically thanks to the recent results presented in [39], recalled at the beginning of this chapter.

Let us start with investigating few examples for each graph matrix, see Fig. 6.2 and 6.3. As we can see, if the first node is marked then for the normalized Laplacian and the adjacency matrix, the success probability stays roughly at  $\Theta(1)$ , and the time grows steadily. For the Laplacian matrix the success probability decreases as  $n$  increases. Similarly, expected time  $T/p(T)$  increases far more rapidly compared to the normalized Laplacian and the adjacency matrix. For the last node, the success probability was stable for all graph matrices. For both the normalized Laplacian and the Laplacian the expected time grows similarly fast. However, for the adjacency matrix we observe far more robust behaviour compared to any case considered so far.

The above observations are confirmed by the statistics of exponent  $\alpha$  defined as  $T/p(T) = \Theta(n^\alpha)$ , see Fig. 6.4 and 6.5. We can see that for both scenarios of the marked nodes, the statistics for the normalized Laplacian reflect our predictions. In the case of the first node being marked, the Laplacian had a complexity mostly  $\Omega(n)$ , which is worse even compared to the classical procedure. We would like to emphasize that this may be due to incorrectly chosen transition rate  $\gamma$  and measurement time  $T$ , as the educated

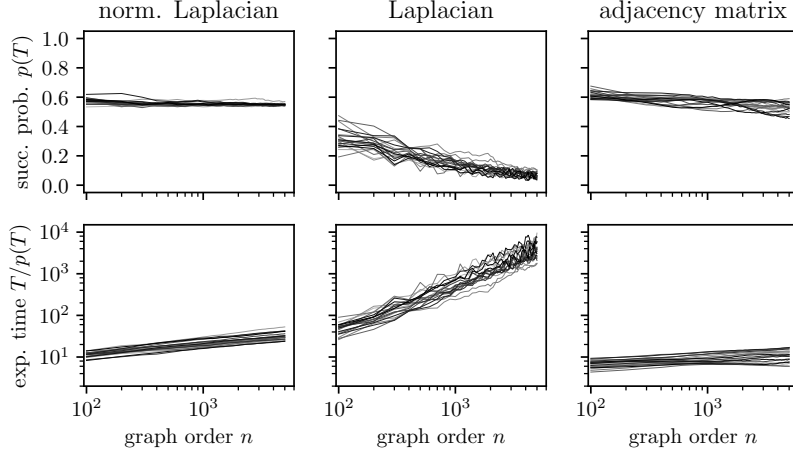


Figure 6.2: Analysis of search efficiency of  $\mathcal{G}^{\text{BA}}(3)$  where the first node is marked. For each graph matrix we sampled 20 trajectories of graphs with orders 100, 200,  $\dots$ , 5000. We chose a measurement time  $T = \frac{1}{|\langle w | \lambda_1 \rangle|} \frac{\sqrt{S_2}}{S_1}$  and transition rate equal to  $S_1$ . The first row presents the trajectory of success probability calculated at  $T$  for each trajectory of graphs. The second row presents the trajectory of  $T/p(T)$ .

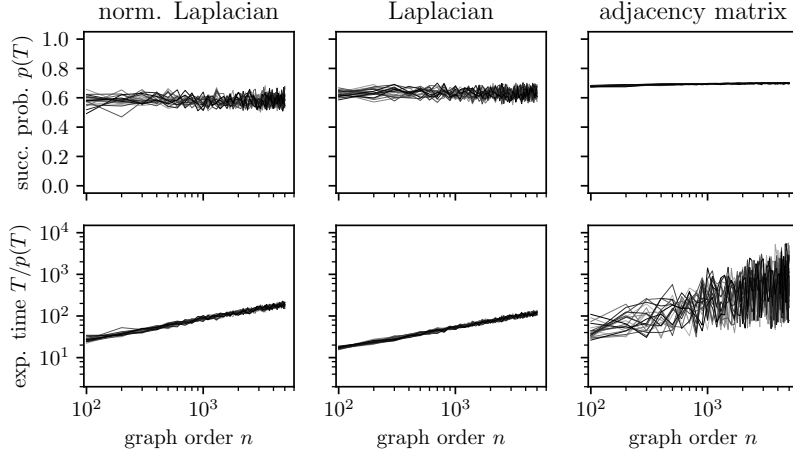


Figure 6.3: Analysis similar to the one presented in Fig. 6.2, except that the last node is marked.

guess presented in [39] may not be proper for the considered graph matrix. Finally, for the adjacency matrix we observe that the required time is far better even compared to the normalized Laplacian, which is in opposition to what was observed for Chung-Lu graphs.

Finally for the last node being marked, the Laplacian matrix has the same efficiency as the normalized Laplacian, namely roughly  $\Theta(\sqrt{n})$ . However, for the adjacency matrix the efficiency was between optimal for quantum search  $\Theta(\sqrt{n})$  and classically optimal  $\Theta(n)$ . Hence while we observed a speed-up compared to the classical search, clearly the normalized Laplacian seems to be better in this scenario. It is worth to note that as we observed in Fig. 6.3 the trajectory of optimal measurement time is very robust, which is also reflected in Fig. 6.5 in the regression quality measure.

Finally, let us see the counter-intuitive behavior of the Laplacian matrix. For both the normalized Laplacian and the adjacency matrix, finding the node with a higher degree was simpler compared to finding the node with small degree. Based on our educated guess for the normalized Laplacian, we may expect a similar property for the classical search. However, for the Laplacian matrix it is contrary – while small degree nodes can be found in  $\Theta(\sqrt{n})$  time, it seems to be difficult to find higher-order nodes. There may be two explanations of this phenomena. Firstly, our choice of transition rate and optimal measurement time is not good for the first node. Secondly, since the initial state of the Laplacian matrix is a uniform superposition of basic states, such state may promote typical-degree cases, which in case of Barabási-Albert are finite-degree nodes.

### 6.3 Optimal measurement time

In order to make the CTQW-based search applicable one has to a priori determine the optimal transition rate and the measurement time. However, as we have shown in the previous section, the measurement time does not only depend on the sampled graph, but also on the marked node. Note that the issue mentioned in the previous paragraphs is typical for heterogeneous graphs [40], and was also observed previously for very simple graphs [28]. For vertex-transitive graphs, the choice of the transition rate and the measurement time does not depend on the marked node, hence the analysis of the graphs is usually sufficient to design the algorithm. However, in other cases it is less evident.

In this section, we will show that the knowledge about the optimal measurement time may not be required, at least in the scenarios considered above. Suppose that the graph-depending search procedure  $\mathcal{A}_{G,w}(t)$  satisfies that for

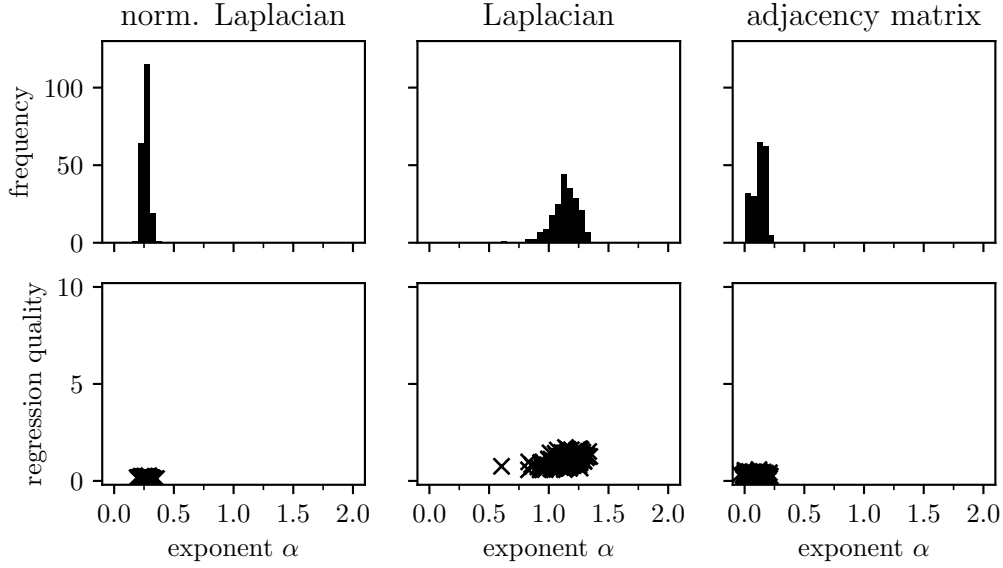


Figure 6.4: Analysis of exponent  $\alpha$  defined as  $T/p(T) = \Theta(n^\alpha)$  for  $\mathcal{G}^{\text{BA}}(3)$  model. The quantum evolution is defined as in Fig. 6.2, and for each graph matrix we sampled 200 trajectories. The first row describes the statistics of exponents  $\alpha$  calculated from linear regression fit  $\log(T/p(T)) = \alpha \log n + \beta$ . The second row presents a regression quality calculated based on the formula  $\|\log(T) - \alpha \log n - \beta\|_2$ .

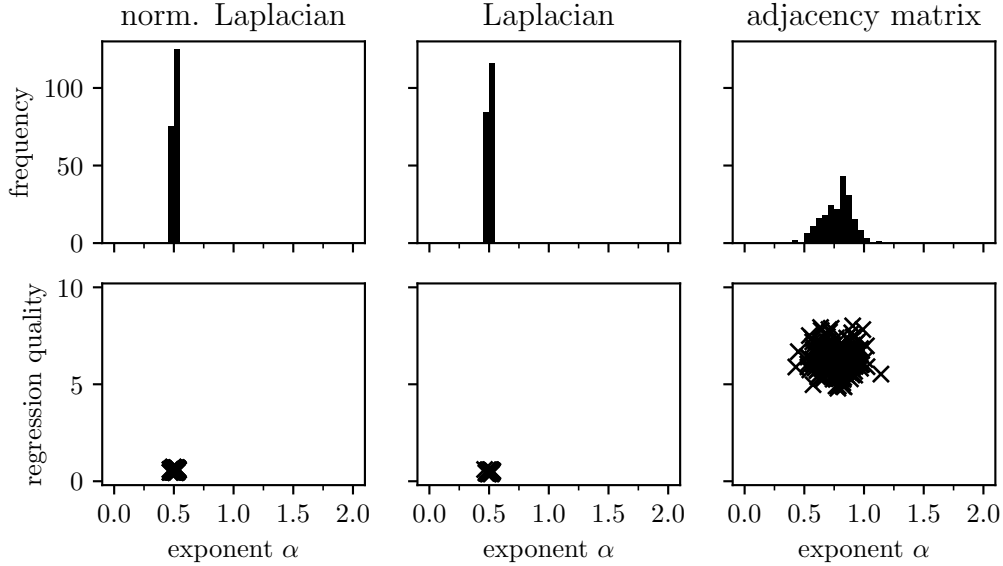


Figure 6.5: Analysis similar to the one presented in Fig. 6.4, except that the last node is marked.

$t \geq T_{\text{crit}}(\mathcal{A}_{G,w})$  procedure  $\mathcal{A}_{G,w}(t)$  finds the marked node with a probability 1. Also assume that  $\mathcal{A}_{G,w}(t)$  runs for time  $t$ . We will elaborate on the validity of this assumption for quantum search algorithms at the end of this section.

If such procedure is encountered one can simply run the procedure for  $\max_w T_{\text{crit}}(\mathcal{A}_{G,w})$  to find the arbitrary marked node with probability 1. However, if  $T_{\text{crit}}$  attains very different values (even in complexity when increasing the number of nodes), such approach should be considered as a waste of resources. For example based on Fig. 6.1, unifying the measurement time to the most demanding node would destroy the quadratic speed-up for almost all nodes in the case of the normalized Laplacian. For the adjacency matrix for sufficiently large  $b$  the time efficiency could be even worse compared to the classical search for the same nodes.

Suppose we know that any node of the graph  $G$  can be found by  $\mathcal{A}_{G,w}(t)$  for  $t \in [Cn^{\beta_0}, Cn^{\beta_0+\beta_1}]$ , and that in particular node  $w$  can be found after time  $Cn^\alpha$ . Let  $K \in \mathbb{Z}_{>0}$ . Then we can run  $\mathcal{A}(t)$  for  $t = Cn^{\beta_0}, Cn^{\beta_0+\frac{1}{K}\beta_1}, \dots, Cn^{\beta_0+\beta_1}$ . Based on our assumptions on procedure  $\mathcal{A}$ , the marked node will be found by  $\mathcal{A}(Cn^{\beta_0+\frac{k}{K}\beta_1})$  where  $\beta_0 + \frac{k_w-1}{K}\beta_1 < \alpha \leq \beta_0 + \frac{k_w}{K}\beta_1$ . The whole procedure takes

$$\Theta\left(\sum_{k=0}^{k_w} Cn^{\beta_0+\frac{k}{K}\beta_1}\right) = \Theta(n^{\beta_0+\frac{k_w}{K}\beta_1}). \quad (6.10)$$

Instead of the optimal complexity  $\Theta(n^\alpha)$  we obtained a complexity  $\Theta(n^{k_w})$ , hence the time complexity is increased by the factor  $n^{\beta_1/K}$  at the worst.

We can make  $n^{\beta_1/K}$  arbitrarily slow by increasing  $K$ . For large, yet fixed  $K$ , the complexity depends only on the time required for the longest run of  $\mathcal{A}$ , *i.e.*  $k = k_w$ . However, for  $n$ -dependent  $K$ , the overall time required for calculating  $k < k_w$  may have impact on the final time complexity.

Let us consider  $K = K' \log n$  for  $K' > 0$  being a real constant. The time complexity of the whole procedure equals

$$\sum_{k=0}^{k_w} Cn^{\beta_0+\frac{k}{K}\beta_1} = Cn^{\beta_0} \sum_{k=0}^{k_w} (n^{\beta_1/K})^k = Cn^{\beta_0} \frac{n^{\frac{k_w}{K}\beta_1} - 1}{n^{\beta_1/K} - 1}. \quad (6.11)$$

Note  $n^{1/K} = \exp(1/K')$ . Hence

$$\begin{aligned} Cn^{\beta_0} \frac{n^{\frac{k_w}{K}\beta_1} - 1}{n^{\beta_1/K} - 1} &= Cn^{\beta_0} \frac{n^{\frac{k_w}{K}\beta_1} - 1}{\exp(\beta_1/K') - 1} \\ &\sim \frac{C}{\exp(\beta_1/K') - 1} n^{\beta_0+\frac{k_w}{K}\beta_1} =: f(k_w). \end{aligned} \quad (6.12)$$



By this we have

$$\frac{f(k_w + 1)}{f(k_w)} = n^{\beta_1/K} = \exp(\beta_1/K') \quad (6.13)$$

and  $f(k_w + 1) = \Theta(f(k_w))$ . Furthermore, since  $f(k_w - 1) \leq Cn^\alpha \leq f(k_w)$ , we have that  $n^\alpha = \Theta(f(k_w))$ , hence our procedure works optimally.

As we can see, the knowledge about the optimal measurement time is not required given certain assumptions on the searching procedure  $\mathcal{A}$ . Let us now consider the validity of the assumptions taken. First, we assumed that the node can be found in the interval  $[Cn^{\beta_0}, Cn^{\beta_0+\beta_1}]$ . Without loss of generality we can assume  $\beta_0 = 0$ , as its value has no impact on the proof. For similar reason, the value of  $\beta_1$  is not required, although it is important to assure that it is constant so that searching will be polynomial. At least for the normalized Laplacian with a constant spectral gap it is guaranteed, as the probability of measuring the the marked node  $w$  at initial time  $t$  equals  $\frac{\deg w}{2|E|} \geq \frac{1}{2n^2}$ . Hence, if preparation of the initial state can be done polynomially fast, then search will take polynomial time as well.

The assumption that the success probability achieves one exactly may not be significant. The success probability can be arbitrarily close to one by repeating the internal procedure  $\mathcal{A}$ . In such scenario, the probability of measuring incorrect nodes decreases exponentially. Since for the graphs with a constant spectral gap there is a common lower bound  $\frac{1-\lambda_2}{1+\lambda_2} + o(1)$  on success probability, one can expect that at least for such graphs the assumption is not meaningful.

Finally, we made an assumption that for  $t \geq T$  the success probability is constantly one. This assumption is not valid for two reasons: first, the evolution is quasi-periodic which means that in large time regime the success probability can equal zero multiple times despite the fact that the time is greater than the optimal measurement time. This can be solved by measuring at different measurement time  $C_{\mathcal{U}}n^{\beta_0+\frac{k}{K}\beta_1}$  where  $C_{\mathcal{U}}$  follows the uniform distribution on interval  $[C - \exp(\beta_1/K')/2, C + \exp(\beta_1/K')/2]$ . Finally, for large time regimes, the eigenvalues of small magnitude may have crucial impact on the evolution, acting as a noise on the evolution defined by the oracle and the principal eigenvector. This issue can be solved by choosing a sufficiently small  $K'$  and increasing the number of repeating  $\mathcal{A}$  for each  $k$ .

We would like to stress out that the above consideration requires further investigations. The first step towards verifying these conjectures would be numerical confirmation of the proposed method. However, this is beyond the scope of the thesis.

## 6.4 Conclusions

In this section we analyzed the efficiency of CTQW-based spatial search on heterogeneous and complex graphs. We provided both analytical and numerical evidence that the optimal measurement time depends strongly on the marked vertex and the matrix graph. The first one is not surprising, as similar situation is observed for the random walk search.

In the case of graph matrix, the normalized Laplacian provided the most stable, always quadratic speed-up over the random walk search for the considered random graphs. Both the adjacency matrix and the Laplacian usually offered the speed-up compared to the classical search, although usually the normalized Laplacian turned out to require even less computational resources. Moreover, for the Laplacian matrix over Barabási-Albert graph it seems that searching for a high-degree nodes takes more time compared to small-degree nodes. We claim that this counter-intuitive result deserves additional attention, in order to fully address the impact of the choice of matrix graph on the efficiency of CTQW-based search.

Finally, we tackled the problem of choosing the optimal measurement time in case it is not known even in complexity. This is particularly relevant for heterogeneous graphs. We proposed a simple approach which we believe can solve the problem in cases considered in this chapter.

# Chapter 7

## Final remarks

In this dissertation we have investigated a hypothesis claiming that there exist simple, continuous-time quantum walk models which maintain interesting and crucial properties of quantum walks for nontrivial graphs.

In Chapter 3 we proposed and analyzed the time-independent nonmoralizing quantum stochastic walk. The model was an interpolation between two continuous-time models. It was a mixture of the original Childs-Goldstone Continuous-Time Quantum Walk [18] and the non-unitary model introduced by Whitefield et al. [41]. The interpolated model was shown to be at least superdiffusive (and likely ballistic) in the intermediate cases of interpolation. Moreover, based on our investigation presented in Chapter 4, this model still preserves the directed graph structure well. This property is true also for the well-known local interaction quantum stochastic walks.

There is still room for improvement for the presented results. First, the proposed model was propagating fast, but at the cost of small amplitude transfer going in the opposite direction than the graph structure. While based on the result presented in Sec. 4.4, its significance seems to be negligible, it is still an open question whether this transition can be removed completely. In our opinion, it is not possible with the mapping from measurement output to vertex set being fixed as proposed in [23]. In other words, the same measurement output would have to be interpreted as different vertices based on time or other context.

Furthermore, it is an open question how to implement the nonmoralizing quantum stochastic walk. Clearly, it should be possible to first transform the GKSL evolution into standard Schrödinger equation, and eventually into the gate model. Still, an effective procedure should be described and analyzed in order to confirm that the simulation on a quantum computer is possible. Alternatively, one could consider a physical process which directly implements the general quantum stochastic walk.

Finally, one could consider the algorithmic application of the introduced model. In particular, heuristic optimization algorithms like simulated annealing or Tabu Search are examples of algorithms which strongly rely on the concept of directed graphs. Indeed, these algorithms, defined as random walks over the objective spaces, share the property that passing to solution with smaller objective value (in the case of minimization procedure) is more likely than passing to solution with higher objective value. In this context, primary task would be to effectively encode the optimization problem into the introduced quantum walk.

In Chapters 5 and 6 we considered the efficiency of the first continuous-time quantum spatial search on non-trivial graphs. In Chapter 5 we analyzed Erdős-Rényi graphs, which was the first step to more advanced graphs. We presented that Laplacian seems to be a valid choice for almost-regular graphs, yielding full quadratic speed-up even close to the connectivity threshold. It is worth to note that for both adjacency matrix and Laplacian matrix it was in fact almost surely possible to find *all* nodes for still small value of the parameter  $p$ . In Chapter 6 we showed that the normalized Laplacian is a far better choice for heterogeneous graphs in most of the cases. Provided that the spectral gap of the graph is constant, the normalized Laplacian provided a full quadratic speed-up over the random walk search. Furthermore, we suggested the procedure which enable attaining the optimal time complexity for finding the vertex even if the optimal measurement time is not known.

It is still not evident what is the possible speed-up for other graphs for CTQW search. In order to better understand the limitations and capabilities of this simple model, it may be interesting to consider other random graph models. This would simplify introducing more general theorems which hopefully would mostly depend on simpler graph-theoretic properties. Note that currently the most general results presented in [39] depend on the *spectral* properties of the graph matrix, which is far harder to describe for general graph collections.

In this dissertation we have confirmed that fast quantum propagation is possible with preserving the structure of directed graphs. Furthermore, the quantum search defined on heterogeneous graphs like Barabási-Albert or Chung-Lu graphs is still quadratically faster with a careful choice of the graph matrix. Based on this, we claim that indeed simple quantum walk models maintain important properties of quantum walks for nontrivial graph structures.

# Bibliography

- [1] P. W. Shor, “Algorithms for quantum computation: Discrete logarithms and factoring,” in *Proceedings 35th annual symposium on foundations of computer science*, pp. 124–134, Ieee, 1994.
- [2] D. Deutsch and R. Jozsa, “Rapid solution of problems by quantum computation,” *Proceedings of the Royal Society of London. Series A: Mathematical and Physical Sciences*, vol. 439, no. 1907, pp. 553–558, 1992.
- [3] L. K. Grover, “A fast quantum mechanical algorithm for database search,” in *Proceedings of the twenty-eighth annual ACM symposium on Theory of computing*, pp. 212–219, ACM, 1996.
- [4] D. R. Simon, “On the power of quantum computation,” *SIAM Journal on computing*, vol. 26, no. 5, pp. 1474–1483, 1997.
- [5] S. Aaronson and A. Ambainis, “Forrelation: A problem that optimally separates quantum from classical computing,” *SIAM Journal on Computing*, vol. 47, no. 3, pp. 982–1038, 2018.
- [6] A. Ambainis, K. Balodis, J. Iraids, M. Kokainis, K. Prūsis, and J. Vihrovs, “Quantum speedups for exponential-time dynamic programming algorithms,” in *Proceedings of the Thirtieth Annual ACM-SIAM Symposium on Discrete Algorithms*, pp. 1783–1793, SIAM, 2019.
- [7] T. Kadowaki and H. Nishimori, “Quantum annealing in the transverse Ising model,” *Physical Review E*, vol. 58, no. 5, p. 5355, 1998.
- [8] A. Finnila, M. Gomez, C. Sebenik, C. Stenson, and J. Doll, “Quantum annealing: A new method for minimizing multidimensional functions,” *Chemical Physics Letters*, vol. 219, no. 5–6, pp. 343–348, 1994.
- [9] A. Peruzzo, J. McClean, P. Shadbolt, M.-H. Yung, X.-Q. Zhou, P. J. Love, A. Aspuru-Guzik, and J. L. O’Brien, “A variational eigenvalue solver on a photonic quantum processor,” *Nature communications*, vol. 5, p. 4213, 2014.

- [10] E. Farhi, J. Goldstone, and S. Gutmann, “A quantum approximate optimization algorithm,” *arXiv:1411.4028*, 2014.
- [11] A. Glos, A. Krawiec, and Z. Zimborás, “Space-efficient binary optimization for variational computing,” 2020.
- [12] Z. Tabi, K. H. El-Safty, Z. Kallus, P. Hąga, T. Kozsik, A. Glos, and Z. Zimborás, “Quantum optimization for the graph coloring problem with space-efficient embedding,” in *2020 IEEE International Conference on Quantum Computing and Engineering (QCE)*, pp. 56–62, IEEE, 2020.
- [13] G. D. Paparo and M. Martin-Delgado, “Google in a quantum network,” *Scientific Reports*, vol. 2, p. 444, 2012.
- [14] E. Sánchez-Burillo, J. Duch, J. Gómez-Gardenes, and D. Zueco, “Quantum navigation and ranking in complex networks,” *Scientific Reports*, vol. 2, p. 605, 2012.
- [15] A. Montanaro, “Quantum algorithms: an overview,” *npj Quantum Information*, vol. 2, p. 15023, 2016.
- [16] A. M. Childs, E. Farhi, and S. Gutmann, “An example of the difference between quantum and classical random walks,” *Quantum Information Processing*, vol. 1, no. 1–2, pp. 35–43, 2002.
- [17] D. Aharonov, A. Ambainis, J. Kempe, and U. Vazirani, “Quantum walks on graphs,” in *Proceedings of the thirty-third annual ACM symposium on Theory of computing*, pp. 50–59, 2001.
- [18] A. M. Childs and J. Goldstone, “Spatial search by quantum walk,” *Physical Review A*, vol. 70, no. 2, p. 022314, 2004.
- [19] R. Portugal, *Quantum walks and search algorithms*. Springer, 2013.
- [20] N. Konno, “Limit theorem for continuous-time quantum walk on the line,” *Physical Review E*, vol. 72, no. 2, p. 026113, 2005.
- [21] M. Szegedy, “Quantum speed-up of Markov chain based algorithms,” in *45th Annual IEEE symposium on foundations of computer science*, pp. 32–41, IEEE, 2004.
- [22] R. Portugal, R. A. Santos, T. D. Fernandes, and D. N. Gonçalves, “The staggered quantum walk model,” *Quantum Information Processing*, vol. 15, no. 1, pp. 85–101, 2016.

- [23] A. Montanaro, “Quantum walks on directed graphs,” *Quantum Information & Computation*, vol. 7, no. 1, pp. 93–102, 2007.
- [24] H. Bringuier, “Central limit theorem and large deviation principle for continuous time open quantum walks,” in *Annales Henri Poincaré*, vol. 18, pp. 3167–3192, Springer, 2017.
- [25] S. Attal, N. Guillotin-Plantard, and C. Sabot, “Central limit theorems for open quantum random walks and quantum measurement records,” in *Annales Henri Poincaré*, vol. 16, pp. 15–43, 2015.
- [26] P. Sadowski and Ł. Paweł, “Central limit theorem for reducible and irreducible open quantum walks,” *Quantum Information Processing*, vol. 15, no. 7, pp. 2725–2743, 2016.
- [27] A. Ambainis, A. Gilyén, S. Jeffery, and M. Kokainis, “Quadratic speedup for finding marked vertices by quantum walks,” in *Proceedings of the 52nd Annual ACM SIGACT Symposium on Theory of Computing*, pp. 412–424, 2020.
- [28] P. Philipp, L. Tarrataca, and S. Boettcher, “Continuous-time quantum search on balanced trees,” *Physical Review A*, vol. 93, no. 3, p. 032305, 2016.
- [29] D. A. Meyer and T. G. Wong, “Connectivity is a poor indicator of fast quantum search,” *Physical Review Letters*, vol. 114, no. 11, p. 110503, 2015.
- [30] L. Novo, S. Chakraborty, M. Mohseni, H. Neven, and Y. Omar, “Systematic dimensionality reduction for quantum walks: Optimal spatial search and transport on non-regular graphs,” *Scientific Reports*, vol. 5, p. 13304, 2015.
- [31] A. Glos and T. Januszek, “Impact of global and local interaction on quantum spatial search on Chimera graph,” *International Journal of Quantum Information*, vol. 17, no. 05, p. 1950040, 2019.
- [32] T. G. Wong, L. Tarrataca, and N. Nahimov, “Laplacian versus adjacency matrix in quantum walk search,” *Quantum Information Processing*, vol. 15, no. 10, pp. 4029–4048, 2016.
- [33] S. Chakraborty, L. Novo, A. Ambainis, and Y. Omar, “Spatial search by quantum walk is optimal for almost all graphs,” *Physical Review Letters*, vol. 116, no. 10, p. 100501, 2016.

- [34] S. Chakraborty, L. Novo, S. Di Giorgio, and Y. Omar, “Optimal quantum spatial search on random temporal networks,” *Physical Review Letters*, vol. 119, no. 22, p. 220503, 2017.
- [35] M. Cattaneo, M. A. Rossi, M. G. Paris, and S. Maniscalco, “Quantum spatial search on graphs subject to dynamical noise,” *Physical Review A*, vol. 98, no. 5, p. 052347, 2018.
- [36] A. Glos, A. Krawiec, R. Kukulski, and Z. Puchała, “Vertices cannot be hidden from quantum spatial search for almost all random graphs,” *Quantum Information Processing*, vol. 17, no. 4, p. 81, 2018.
- [37] R. Kukulski and A. Glos, “Comment to ‘Spatial search by quantum walk is optimal for almost all graphs’,” *arXiv:2009.13309*, 2020.
- [38] S. Chakraborty, L. Novo, and J. Roland, “Finding a marked node on any graph via continuous-time quantum walks,” *Physical Review A*, vol. 102, no. 2, p. 022227, 2020.
- [39] S. Chakraborty, L. Novo, and J. Roland, “Optimality of spatial search via continuous-time quantum walks,” *Physical Review A*, vol. 102, no. 3, p. 032214, 2020.
- [40] T. Osada, B. Coutinho, Y. Omar, K. Sanaka, W. J. Munro, and K. Nemoto, “Continuous-time quantum-walk spatial search on the bollobás scale-free network,” *Physical Review A*, vol. 101, no. 2, p. 022310, 2020.
- [41] J. D. Whitfield, C. A. Rodríguez-Rosario, and A. Aspuru-Guzik, “Quantum stochastic walks: A generalization of classical random walks and quantum walks,” *Physical Review A*, vol. 81, no. 2, p. 022323, 2010.
- [42] R. Albert and A.-L. Barabási, “Statistical mechanics of complex networks,” *Reviews of modern physics*, vol. 74, no. 1, p. 47, 2002.
- [43] K. Domino, A. Glos, M. Ostaszewski, P. Sadowski, and Ł. Paweła, “Properties of Quantum Stochastic Walks from the asymptotic scaling exponent,” *Quantum Information and Computation*, vol. 18, no. 3&4, pp. 0181–0199, 2018.
- [44] K. Domino, A. Glos, and M. Ostaszewski, “Superdiffusive quantum stochastic walk definable on arbitrary directed graph,” *Quantum Information & Computation*, vol. 17, no. 11–12, pp. 973–986, 2017.



- [45] A. Glos, J. A. Miszczak, and M. Ostaszewski, “Limiting properties of stochastic quantum walks on directed graphs,” *Journal of Physics A: Mathematical and Theoretical*, vol. 51, no. 3, p. 035304, 2017.
- [46] A. Glos and T. G. Wong, “Optimal quantum-walk search on Kronecker graphs with dominant or fixed regular initiators,” *Physical Review A*, vol. 98, no. 6, p. 062334, 2018.
- [47] A. Glos, B. Coutinho, and Y. Omar, “Continuous-time quantum spatial search on complex and heterogeneous graphs.” under preparation.
- [48] P. Erdős and A. Rényi, “On random graphs, I,” *Publicationes Mathematicae (Debrecen)*, vol. 6, pp. 290–297, 1959.
- [49] F. Chung and L. Lu, “Connected components in random graphs with given expected degree sequences,” *Annals of combinatorics*, vol. 6, no. 2, pp. 125–145, 2002.
- [50] F. Chung and M. Radcliffe, “On the spectra of general random graphs,” *The Electronic Journal of Combinatorics*, vol. 18, no. 1, p. 215, 2011.
- [51] R. Durrett, *Random Graph Dynamics*. Cambridge Series in Statistical and Probabilistic Mathematics, Cambridge University Press, 2006.
- [52] A. Flaxman, A. Frieze, and T. Fenner, “High degree vertices and eigenvalues in the preferential attachment graph,” *Internet Mathematics*, vol. 2, no. 1, pp. 1–19, 2005.
- [53] S. Bromberger, J. Fairbanks, and other contributors, “JuliaGraphs/-LightGraphs.jl: an optimized graphs package for the Julia programming language,” 2017.
- [54] V. Gorini, A. Kossakowski, and E. C. G. Sudarshan, “Completely positive dynamical semigroups of  $N$ -level systems,” *Journal of Mathematical Physics*, vol. 17, no. 5, pp. 821–825, 1976.
- [55] J. A. Miszczak, “Singular value decomposition and matrix reorderings in quantum information theory,” *International Journal of Modern Physics C*, vol. 22, no. 09, pp. 897–918, 2011.
- [56] A. Glos and J. A. Miszczak, “The role of quantum correlations in Cop and Robber game,” *Quantum Studies: Mathematics and Foundations*, vol. 6, no. 1, pp. 15–26, 2019.

- [57] Z. Zimborás, M. Faccin, Z. Kadar, J. D. Whitfield, B. P. Lanyon, and J. Biamonte, “Quantum transport enhancement by time-reversal symmetry breaking,” *Scientific Reports*, vol. 3, p. 2361, 2013.
- [58] J. D. Noh and H. Rieger, “Random walks on complex networks,” *Physical Review Letters*, vol. 92, no. 11, p. 118701, 2004.
- [59] T. G. Wong, *Nonlinear Quantum Search*. PhD thesis, University of California, San Diego, 2014.
- [60] F. Magniez, M. Santha, and M. Szegedy, “Quantum algorithms for the triangle problem,” *SIAM Journal on Computing*, vol. 37, no. 2, pp. 413–424, 2007.
- [61] J. Bezanson, S. Karpinski, V. B. Shah, and A. Edelman, “Julia: A fast dynamic language for technical computing,” *arXiv:1209.5145*, 2012.
- [62] “Julia implementations of some routines contained in EXPOKIT,” 2018. <https://github.com/acroy/Expokit.jl> (Accessed on 18/12/2017).
- [63] A. Glos, J. A. Miszczak, and M. Ostaszewski, “QSWalk.jl: Julia package for quantum stochastic walks analysis,” *Computer Physics Communications*, vol. 235, pp. 414–421, 2019.
- [64] P. Bocchieri and A. Loinger, “Quantum recurrence theorem,” *Physical Review*, vol. 107, no. 2, p. 337, 1957.
- [65] R. G. Cowell, P. Dawid, S. L. Lauritzen, and D. J. Spiegelhalter, *Probabilistic networks and expert systems: Exact computational methods for Bayesian networks*. Springer Science & Business Media, 2006.
- [66] B. Taketani, L. Govia, P. Schuhmacher, and F. Wilhelm, “On the physical realizability of quantum stochastic walks,” *Bulletin of the American Physical Society*, vol. 61, 2016.
- [67] H. Spohn, “An algebraic condition for the approach to equilibrium of an open  $N$ -level system,” *Letters in Mathematical Physics*, vol. 2, no. 1, pp. 33–38, 1977.
- [68] S. Schirmer and X. Wang, “Stabilizing open quantum systems by Markovian reservoir engineering,” *Physical Review A*, vol. 81, no. 6, p. 062306, 2010.

- [69] C. Liu and R. Balu, “Steady states of continuous-time open quantum walks,” *Quantum Information Processing*, vol. 16, no. 7, p. 173, 2017.
- [70] R. M. Gray *et al.*, “Toeplitz and circulant matrices: A review,” *Foundations and Trends® in Communications and Information Theory*, vol. 2, no. 3, pp. 155–239, 2006.
- [71] M. Boyer, G. Brassard, P. Høyer, and A. Tapp, “Tight bounds on quantum searching,” *Fortschritte der Physik: Progress of Physics*, vol. 46, no. 4–5, pp. 493–505, 1998.
- [72] V. H. Vu, “Spectral norm of random matrices,” *Combinatorica*, vol. 27, no. 6, pp. 721–736, 2007.
- [73] Z. Füredi and J. Komlós, “The eigenvalues of random symmetric matrices,” *Combinatorica*, vol. 1, no. 3, pp. 233–241, 1981.
- [74] P. Mitra, “Entrywise bounds for eigenvectors of random graphs,” *The Electronic Journal of Combinatorics*, pp. R131–R131, 2009.
- [75] T. Kolokolnikov, B. Osting, and J. Von Brecht, “Algebraic connectivity of Erdős-Rényi graphs near the connectivity threshold,” *Manuscript in preparation*, 2014.
- [76] W. Bryc, A. Dembo, T. Jiang, *et al.*, “Spectral measure of large random Hankel, Markov and Toeplitz matrices,” *The Annals of Probability*, vol. 34, no. 1, pp. 1–38, 2006.
- [77] B. Bollobás, “Random graphs. 2001,” *Cambridge Stud. Adv. Math*, 2001.
- [78] M. Fiedler, “Algebraic connectivity of graphs,” *Czechoslovak Mathematical Journal*, vol. 23, no. 2, pp. 298–305, 1973.
- [79] W. N. Anderson Jr and T. D. Morley, “Eigenvalues of the Laplacian of a graph,” *Linear and Multilinear Algebra*, vol. 18, no. 2, pp. 141–145, 1985.
- [80] S. Noschese, L. Pasquini, and L. Reichel, “Tridiagonal toeplitz matrices: properties and novel applications,” *Numerical Linear Algebra with Applications*, vol. 20, no. 2, pp. 302–326, 2013.
- [81] A. Jeffrey, D. Zwillinger, I. Gradshteyn, and I. Ryzhik, eds., *Table of Integrals, Series, and Products (sixth Edition)*. Academic Press, sixth edition ed., 2000. ISBN: 0-12-294757-6.

- [82] U. Feige and E. Ofek, “Spectral techniques applied to sparse random graphs,” *Random Structures & Algorithms*, vol. 27, no. 2, pp. 251–275, 2005.
- [83] A. Sinclair, *Algorithms for Random Generation and Counting: A Markov Chain Approach*. Birkhäuser Boston, 1993. doi:10.1007/978-1-4612-0323-0.

# Appendix A

## Proofs for Quantum Stochastic Walks

### A.1 Probability distributions of GQSW on finite and infinite paths

#### A.1.1 Probability distribution for finite path

*Proof of Theorem 3.3.* Let  $L$  and  $H$  be an operators defined according to the theorem. Using Eq. (2.26) we have

$$M_{\omega}^t = \exp \left[ t\omega \left( L \otimes L - \frac{1}{2}L^2 \otimes \mathbf{I} - \frac{1}{2}\mathbf{I} \otimes L^2 \right) - it(1 - \omega)(H \otimes \mathbf{I} - \mathbf{I} \otimes H) \right]. \quad (\text{A.1})$$

Now we note that in the case of the walk on a path, we have  $L = H$  and  $[L \otimes L, L^m \otimes \mathbf{I}] = 0$ . Hence, the eigenvectors of  $M_{\omega}^t$  are the same as the eigenvectors of  $L \otimes L$ . It is straightforward to check that

$$M_{\omega}^t = \sum_{i,j} \exp \left( -\omega \frac{t}{2} (\lambda_i - \lambda_j)^2 \right) \exp(-it(1 - \omega)(\lambda_i - \lambda_j)) |\lambda_i, \lambda_j\rangle \langle \lambda_i, \lambda_j|, \quad (\text{A.2})$$

where  $\lambda_i$  and  $|\lambda_i\rangle$  denote the eigenvalues and eigenvectors of  $L$  and  $H$ . As  $L$  is a tridiagonal Toeplitz matrix, its eigenvalues are given by [80]

$$\lambda_j = 2 \cos \left( \frac{j\pi}{n+1} \right), \quad (\text{A.3})$$

where  $1 \leq j \leq n$ . Furthermore the elements of the eigenvectors are

$$\langle j | \lambda_i \rangle = \sqrt{\frac{2}{n+1}} \sin \left( \frac{ij\pi}{n+1} \right) = \langle i | \lambda_j \rangle. \quad (\text{A.4})$$

From this we get that the elements of  $M_\omega^t$  in the computational basis are

$$\begin{aligned}
\langle \gamma, \delta | M_\omega^t | \kappa, \beta \rangle &= \sum_{i,j=1}^n \langle i | \lambda_\kappa \rangle \langle j | \lambda_\beta \rangle \langle i | \lambda_\gamma \rangle \langle j | \lambda_\delta \rangle \times \\
&\quad \times \exp\left(-\omega \frac{t}{2} (\lambda_i - \lambda_j)^2\right) \exp(it(1-\omega)(\lambda_i - \lambda_j)) \\
&= \left(\frac{2}{n+1}\right)^2 \sum_{i,j=1}^n \sin\left(\frac{\kappa i \pi}{n+1}\right) \sin\left(\frac{\beta j \pi}{n+1}\right) \sin\left(\frac{\gamma i \pi}{n+1}\right) \times \\
&\quad \times \sin\left(\frac{\delta j \pi}{n+1}\right) \exp\left(-\omega \frac{t}{2} (\lambda_i - \lambda_j)^2\right) \exp(-it(1-\omega)(\lambda_i - \lambda_j)).
\end{aligned} \tag{A.5}$$

Putting  $\kappa = \beta = k$  and  $\gamma = \delta = l$  we recover the desired result.  $\square$

### A.1.2 Probability distribution for infinite path

*Proof of Theorem 3.4.* In the case of a walk on a path  $[-n, \dots, n]$ , the diagonal part of  $\varrho(t)$  with initial state  $\varrho(0) = |0\rangle\langle 0|$  satisfies

$$\begin{aligned}
\langle k | \varrho(t) | k \rangle &= \left(\frac{2}{2n+2}\right)^2 \sum_{i,j=1}^{2n+1} \sin\left(\frac{(k+n+1)i\pi}{2n+2}\right) \sin\left(\frac{(k+n+1)j\pi}{2n+2}\right) \times \\
&\quad \times \sin\left(\frac{(n+1)i\pi}{2n+2}\right) \sin\left(\frac{(n+1)j\pi}{2n+2}\right) \times \\
&\quad \times \exp\left[-\frac{t}{2}\omega(\lambda_i - \lambda_j)^2\right] \exp[-it(1-\omega)(\lambda_i - \lambda_j)] \\
&= \frac{1}{(n+1)^2} \sum_{i,j=1}^{2n+1} \sin\left(\frac{ki\pi}{2n+2} + \frac{i\pi}{2}\right) \sin\left(\frac{kj\pi}{2n+2} + \frac{j\pi}{2}\right) \sin\left(\frac{i\pi}{2}\right) \times \\
&\quad \times \sin\left(\frac{j\pi}{2}\right) \exp\left[-\frac{t}{2}\omega(\lambda_i - \lambda_j)^2\right] \exp[-it(1-\omega)(\lambda_i - \lambda_j)].
\end{aligned} \tag{A.6}$$

Note, that for even  $i$  or even  $j$ , the elements under the sum are equal to zero. We get

$$\begin{aligned}
\langle k | \varrho(t) | k \rangle &= \frac{1}{(n+1)^2} \sum_{i,j=1,3,\dots,2n+1} \cos\left(\frac{ki\pi}{2(n+1)}\right) \cos\left(\frac{kj\pi}{2(n+1)}\right) \times \\
&\quad \times \exp\left[-2\omega t \left(\sin\frac{\pi i}{2(n+1)} - \sin\frac{\pi j}{2(n+1)}\right)^2\right] \times \\
&\quad \times \exp\left[-2i(1-\omega)t \left(\sin\frac{\pi i}{2(n+1)} - \sin\frac{\pi j}{2(n+1)}\right)\right].
\end{aligned} \tag{A.7}$$

The formula above is  $1/4$  of the Riemann sum of the function

$$f(x) = \cos\left(\frac{k\pi x}{2}\right) \cos\left(\frac{k\pi y}{2}\right) \exp\left[-2\omega t \left(\sin\frac{\pi x}{2} - \sin\frac{\pi y}{2}\right)^2\right] \times \\ \times \exp\left[-2i(1-\omega)t \left(\sin\frac{\pi x}{2} - \sin\frac{\pi y}{2}\right)\right] \quad (\text{A.8})$$

over the square  $[0, 2] \times [0, 2]$  when we divide the region into equal squares. Hence, taking the limit  $n \rightarrow \infty$  we get

$$\langle k | \varrho(t) | k \rangle = \frac{1}{4} \int_0^2 \int_0^2 \cos\left(\frac{k\pi x}{2}\right) \cos\left(\frac{k\pi y}{2}\right) \times \\ \times \exp\left[-2\omega t \left(\sin\frac{\pi x}{2} - \sin\frac{\pi y}{2}\right)^2\right] \times \\ \times \exp\left[-2i(1-\omega)t \left(\sin\frac{\pi x}{2} - \sin\frac{\pi y}{2}\right)\right] dx dy. \quad (\text{A.9})$$

After substituting  $u = \frac{x\pi}{2}$  and  $v = \frac{y\pi}{2}$  we have

$$\langle k | \varrho(t) | k \rangle = \frac{1}{\pi^2} \int_0^\pi \int_0^\pi \cos(ku) \cos(kv) \exp\left[-2\omega t (\cos u - \cos v)^2\right] \times \\ \times \exp\left[-2i(1-\omega)t (\cos u - \cos v)\right] du dv. \quad (\text{A.10})$$

By symmetry with respect to  $x = 0$  and  $y = 0$  we obtain the result.  $\square$

## A.2 Scaling exponent of interpolated standard GQSW on infinite path graph

### A.2.1 Case $\omega = 1$

**Lemma A.1** ([81]). *For arbitrary  $\alpha \in \mathbb{R}$ ,  $n, m \in \mathbb{N}$  such that  $m \leq n$  we have*

$$\sum_{k=0}^n (-1)^k (k - \alpha)^m \binom{n}{k} = \begin{cases} 0, & m < n, \\ (-1)^n n!, & m = n. \end{cases} \quad (\text{A.11})$$

**Lemma A.2** ([81]). *For arbitrary  $n, p \in \mathbb{N}$  such that  $p \leq n$  we have*

$$\sum_{k=0}^{n-p} \binom{n}{k} \binom{n}{p+k} = \binom{2n}{n-p}. \quad (\text{A.12})$$

**Lemma A.3.** *For arbitrary  $k, l \in \mathbb{N}$  we have*

$$\begin{aligned} \int_{-\pi}^{\pi} \cos(kx) [\cos(x)]^l dx \\ = \begin{cases} \frac{2\pi}{2^{l-k}} \binom{l-k}{\frac{l-k}{2}} \prod_{i=0}^{k-1} \frac{l-i}{l+k-2i}, & l \geq k \text{ and } (l = k \pmod{2}), \\ 0, & \text{otherwise.} \end{cases} \end{aligned} \quad (\text{A.13})$$

*Proof.* Using the formula [81]

$$\int [\cos(x)]^l \cos(kx) dx = \frac{1}{l+k} \left[ (\cos(x))^l \sin(kx) + l \int [\cos(x)]^{l-1} \cos((k-1)x) dx \right] \quad (\text{A.14})$$

we obtain

$$\int_{-\pi}^{\pi} [\cos(x)]^l \cos(kx) dx = \frac{l}{l+k} \int_{-\pi}^{\pi} [\cos(x)]^{l-1} \cos((k-1)x) dx. \quad (\text{A.15})$$

Moreover for arbitrary  $l \in \mathbb{N}$  we have [81]

$$\int [\cos(x)]^{2l} dx = \frac{1}{4^l} \binom{2l}{l} x + \frac{2}{4^l} \sum_{k=0}^{l-1} \binom{2l}{k} \frac{\sin((2l-2k)x)}{2l-2k}, \quad (\text{A.16})$$

which provides us the formula

$$\int_{-\pi}^{\pi} [\cos(x)]^{2l} dx = \frac{2\pi}{4^l} \binom{2l}{l}. \quad (\text{A.17})$$

Suppose  $l < k$ . Then using Eq. (A.15) we have

$$\int_{-\pi}^{\pi} [\cos(x)]^l \cos(kx) dx = \prod_{i=0}^{l-1} \frac{l-i}{l+k-2i} \int_{-\pi}^{\pi} \cos((k-l)x) dx = 0. \quad (\text{A.18})$$

If  $l \geq k$ , then we obtain

$$\int_{-\pi}^{\pi} [\cos(x)]^l \cos(kx) dx = \prod_{i=0}^{k-1} \frac{l-i}{l+k-2i} \int_{-\pi}^{\pi} \cos^{l-k}(x) dx. \quad (\text{A.19})$$

If  $l-k$  is odd, then the integral equals 0. Otherwise using Eq. (A.17) we have

$$\int_{-\pi}^{\pi} \cos(kx) \cos^l(x) dx = \frac{2\pi}{2^{l-k}} \binom{l-k}{\frac{l-k}{2}} \prod_{i=0}^{k-1} \frac{l-i}{l+k-2i}. \quad (\text{A.20})$$

□



**Proposition A.4.** *For an interpolated standard GQSW on an infinite path with an initial state  $\varrho(0) = |0\rangle\langle 0|$  and  $\omega = 1$ , the diagonal part of  $\varrho(t)$  is given by*

$$\langle k | \varrho(t) | k \rangle = \sum_{n=|k|}^{\infty} \frac{(-1)^{n+k}}{2^n} \binom{2n}{n} \binom{2n}{n+k} \frac{t^n}{n!}. \quad (\text{A.21})$$

*Proof.* Since the elements  $\varrho_{kk}(t) := \langle k | \varrho(t) | k \rangle$  are symmetric with respect to  $k = 0$ , we assume  $k \geq 0$ . By Theorem 3.4 we have

$$\varrho_{kk}(t) = \frac{1}{4\pi^2} \int_{-\pi}^{\pi} \int_{-\pi}^{\pi} \cos(kx) \cos(ky) \exp[-2t(\cos(x) - \cos(y))^2] dx dy. \quad (\text{A.22})$$

Suppose we have the Taylor series representation  $\varrho_{kk}(t) = \sum_{n=0}^{\infty} \frac{A_{n,k}}{n!} t^n$ . Then  $A_{n,k}$  is of the form

$$\begin{aligned} A_{n,k} &= \frac{(-1)^n 2^n}{4\pi^2} \int_{-\pi}^{\pi} \int_{-\pi}^{\pi} \cos(kx) \cos(ky) (\cos(x) - \cos(y))^{2n} dx dy \\ &= \frac{(-1)^n 2^n}{4\pi^2} \sum_{l=0}^{2n} \binom{2n}{l} (-1)^l \int_{-\pi}^{\pi} \cos(kx) [\cos(x)]^l dx \times \\ &\quad \times \int_{-\pi}^{\pi} \cos(ky) [\cos(y)]^{2n-l} dy. \end{aligned} \quad (\text{A.23})$$

Let us define for simplicity

$$A_{n,k,l} := \binom{2n}{l} (-1)^l \int_{-\pi}^{\pi} \cos(kx) [\cos(x)]^l dx \int_{-\pi}^{\pi} \cos(ky) [\cos(y)]^{2n-l} dy. \quad (\text{A.24})$$

By Lemma A.3 we have that  $A_{n,k,l}$  is non-zero when  $k - l$  is even and takes the form

$$A_{n,k,l} = \frac{(-1)^l 4\pi^2}{2^{2n-2k}} \binom{2n}{l} \binom{l-k}{\frac{l-k}{2}} \binom{2n-l-k}{n-\frac{l+k}{2}} \prod_{i=0}^{k-1} \frac{l-i}{l+k-2i} \frac{2n-l-i}{2n-l+k-2i}. \quad (\text{A.25})$$

Furthermore from condition  $2n \geq 2n-l \geq k$  for  $A_{n,k,l} \neq 0$ , for  $n < k$  we have  $A_{n,k} = 0$ .

Again it is straightforward to find

$$A_{n,k,k} = \frac{(-1)^k 4\pi^2}{4^n} \binom{2n}{n} \binom{n}{k} \quad (\text{A.26})$$

and

$$\frac{A_{n,k,l+2}}{A_{n,k,l}} = \frac{(n - \frac{l-k}{2})(n - \frac{l-k}{2})}{(\frac{l+k}{2} + 1)(\frac{l-k}{2} + 1)}. \quad (\text{A.27})$$

Note that we increment  $l$  by two instead of one because of the assumption that  $l - k$  is even. One can verify, that the  $A_{n,k,l}$  is of the form

$$A_{n,k,l} = \frac{(-1)^k 4\pi^2}{4^n} \binom{2n}{n} \binom{n}{\frac{l+k}{2}} \binom{n}{\frac{l-k}{2}}. \quad (\text{A.28})$$

Finally we have

$$\begin{aligned} A_{n,k} &= \frac{(-1)^n 2^n}{4 \cdot \pi^2} \sum_{l \in \{k, k+2, \dots, 2n-k\}} A_{n,k,l} \\ &= \frac{(-1)^{n+k}}{2^n} \binom{2n}{n} \sum_{l \in \{k, k+2, \dots, 2n-k\}} \binom{n}{\frac{l+k}{2}} \binom{n}{\frac{l-k}{2}} \\ &= \frac{(-1)^{n+k}}{2^n} \binom{2n}{n} \sum_{l=0}^{n-k} \binom{n}{l+k} \binom{n}{l} \\ &= \frac{(-1)^{n+k}}{2^n} \binom{2n}{n} \binom{2n}{n+k}, \end{aligned} \quad (\text{A.29})$$

where in the third line we change the indices range and in the last line we use Lemma A.2.  $\square$

**Proposition A.5.** *For an interpolated standard GQSW on an infinite path with an initial state  $\varrho(0) = |0\rangle\langle 0|$ ,  $\omega = 1$ , the  $m$ -th central moment  $\mu_m(t)$  is polynomial in  $t$  for  $m$  even, and zero otherwise. Moreover for even  $m$  we have*

$$\lim_{t \rightarrow \infty} \frac{\mu_m(t)}{t^{\frac{m}{2}}} = \frac{m!}{(\frac{m}{2})! 2^{\frac{m}{2}}} \binom{m}{\frac{m}{2}}. \quad (\text{A.30})$$

*Proof.* Note that odd moments equals 0 by symmetry of the probability distribution. Suppose  $m$  is even and  $m > 0$ . Then by Proposition A.4 we have

$$\begin{aligned} \mu_m(t) &= \sum_{k=-\infty}^{\infty} k^m \sum_{n=|k|}^{\infty} \frac{(-1)^{n+k}}{2^n} \binom{2n}{n} \binom{2n}{n+k} \frac{t^n}{n!} \\ &= \sum_{n=0}^{\infty} \frac{(-1)^n}{2^n} \binom{2n}{n} \frac{t^n}{n!} \sum_{k=-n}^n k^m (-1)^k \binom{2n}{n+k} \\ &= \sum_{n=0}^{\infty} \frac{1}{2^n} \binom{2n}{n} \frac{t^n}{n!} \sum_{k=0}^{2n} (k-n)^m (-1)^k \binom{2n}{k}. \end{aligned} \quad (\text{A.31})$$

By Lemma A.1 formula above can be simplified

$$\mu_m(t) = \sum_{n=1}^{\frac{m}{2}} \frac{1}{2^n} \binom{2n}{n} \frac{t^n}{n!} \sum_{k=0}^{2n} (k-n)^m (-1)^k \binom{2n}{k}, \quad (\text{A.32})$$

hence the  $m$ -th central moment is a polynomial of degree  $\frac{m}{2}$  with respect to  $t$ . Moreover, the coefficient next to  $t^{\frac{m}{2}}$  is

$$a_{\frac{m}{2}} = \frac{m!}{\left(\frac{m}{2}\right)! 2^{\frac{m}{2}}} \left(\frac{m}{2}\right). \quad (\text{A.33})$$

□

### A.2.2 Case $\omega < 1$

**Proposition A.6.** *For an interpolated standard GQSW on an infinite path with an initial state  $\varrho(0) = |0\rangle\langle 0|$  and  $\omega \in (0, 1)$ , the diagonal part of  $\varrho(t)$  is given by*

$$\langle k | \varrho(t) | k \rangle = \sum_{n=|k|}^{\infty} B_{n,k} \frac{t^n}{n!}, \quad (\text{A.34})$$

where

$$B_{n,k} = \frac{(-1)^{n+k}}{2^n} \sum_{l=0}^{\min(\lfloor \frac{n}{2} \rfloor, n-|k|)} \binom{n}{2l} 4^l \omega^{n-2l} (1-\omega)^{2l} (-1)^l \binom{2n-2l}{n-l} \binom{2n-2l}{n-l+k}. \quad (\text{A.35})$$

*Proof.* If we denote  $\varrho_{kk}(t) := \langle k | \varrho(t) | k \rangle = \sum_{n=0}^{\infty} \frac{B_{n,k}}{n!} t^n$ , then one can find that  $B_{n,k}$  is of the form

$$B_{n,k} = \sum_{l=0}^n \binom{n}{l} \frac{1}{4\pi^2} \int_{-\pi}^{\pi} \int_{-\pi}^{\pi} \cos(kx) \cos(ky) (-\omega)^{n-l} 2^{n-l} \times \\ \times (\cos(x) - \cos(y))^{2n-l} 2^l i^l (1-\omega)^l dx dy. \quad (\text{A.36})$$

Since  $\varrho_{kk}(t) \in \mathbb{R}$ , we can exclude the imaginary terms and we can simplify the formula

$$B_{n,k} = \sum_{l=0}^{\lfloor \frac{n}{2} \rfloor} \binom{n}{2l} 2^{2n-l} \omega^{n-2l} (1-\omega)^{2l} \times \\ \times \frac{(-1)^{n-l}}{2^{n-l} 4\pi^2} \int_{-\pi}^{\pi} \int_{-\pi}^{\pi} \cos(kx) \cos(ky) (\cos(x) - \cos(y))^{2n-2l} dx dy \\ = \sum_{l=0}^{\lfloor \frac{n}{2} \rfloor} \binom{n}{2l} 2^{2n-l} \omega^{n-2l} (1-\omega)^{2l} A_{n-l,k}. \quad (\text{A.37})$$

From the proof of Proposition A.4 we know, that  $A_{n,k}$  takes the form

$$A_{n,k} = \begin{cases} 0, & |k| > n, \\ \frac{(-1)^{n+k}}{8^n} \binom{2n}{n} \binom{2n}{n+k}, & |k| \leq n. \end{cases} \quad (\text{A.38})$$

In our case we have the condition  $|k| \leq n - \frac{l}{2} \leq n$ . Hence we conclude, that  $B_{n,k}$  is of the form

$$B_{n,k} = \frac{(-1)^{n+k}}{2^n} \sum_{l=0}^{\min(\lfloor \frac{n}{2} \rfloor, n-|k|)} \binom{n}{2l} 4^l \omega^{n-2l} (1-\omega)^{2l} (-1)^l \binom{2n-2l}{n-l} \binom{2n-2l}{n-l+k}. \quad (\text{A.39})$$

□

**Proposition A.7.** *For a interpolated standard GQSW on an infinite path with an initial state  $\varrho(0) = |0\rangle\langle 0|$ ,  $\omega \in (0, 1)$ , the  $m$ -th central moment  $\mu_m(t)$  is polynomial in  $t$  for  $m$  even, and zero otherwise. Moreover for even  $m$  we have*

$$\lim_{t \rightarrow \infty} \frac{\mu_m(t)}{t^m} = \left(\frac{m}{2}\right) (1-\omega)^m. \quad (\text{A.40})$$

*Proof.* Thanks to the Proposition A.6, for even  $m$  we have

$$\begin{aligned} \mu_m(t) &= \sum_{k=-\infty}^{\infty} k^m \sum_{n=0}^{\infty} B_{n,k} \frac{t^n}{n!} \\ &= \sum_{n=0}^{\infty} \frac{t^n}{n!} \sum_{k=-n}^n k^m B_{n,k} \\ &= \sum_{n=0}^{\infty} \frac{(-1)^n t^n}{2^n n!} \sum_{k=-n}^n k^m (-1)^k \times \\ &\quad \times \sum_{l=0}^{\min(\lfloor \frac{n}{2} \rfloor, n-|k|)} \binom{n}{2l} 4^l \omega^{n-2l} (1-\omega)^{2l} (-1)^l \binom{2n-2l}{n-l} \binom{2n-2l}{n-l+k} \\ &= \sum_{n=0}^{\infty} \sum_{k=-n}^n \sum_{l=0}^{\min(\lfloor \frac{n}{2} \rfloor, n-|k|)} C_{n,l,t} \omega^{n-2l} (1-\omega)^{2l} (-1)^k k^m \binom{2n-2l}{n-l+k}, \\ &= \sum_{n=0}^{\infty} \sum_{l=0}^{\lfloor \frac{n}{2} \rfloor} C_{n,l,t} \omega^{n-2l} (1-\omega)^{2l} \sum_{k=-(n-l)}^{n-l} (-1)^k k^m \binom{2n-2l}{n-l+k}, \\ &= \sum_{n=0}^{\infty} \sum_{l=0}^{\lfloor \frac{n}{2} \rfloor} C_{n,l,t} \omega^{n-2l} (1-\omega)^{2l} (-1)^{n-l} \sum_{k=0}^{2n-2l} (-1)^k (k - (n-l))^m \binom{2n-2l}{k}, \end{aligned} \quad (\text{A.41})$$

where

$$C_{n,l,t} = \frac{(-1)^n t^n}{2^n n!} 4^l (-1)^l \binom{n}{2l} \binom{2n-2l}{n-l}. \quad (\text{A.42})$$

Let us denote

$$\alpha_{2n-2l,m} = \sum_{k=0}^{2n-2l} (-1)^k (k - (n-l))^m \binom{2n-2l}{k}. \quad (\text{A.43})$$

From Lemma A.1  $\alpha_{2n-2l,m}$  is nonzero if  $m \geq 2n-2l \iff l \geq n - \frac{m}{2}$ . Hence Eq. (A.41) can be simplified

$$\mu_m(t) = \sum_{n=0}^{\infty} \sum_{l=n-\frac{m}{2}}^{\lfloor \frac{n}{2} \rfloor} C_{n,l,t} (-1)^{n-l} \omega^{n-2l} (1-\omega)^{2l} \alpha_{2n-2l,m} \quad (\text{A.44})$$

The condition  $n - \frac{m}{2} \leq l \leq \lfloor \frac{n}{2} \rfloor$  implies that for  $n > m$  we have necessarily zero elements in Taylor sequence. Hence, we have

$$\begin{aligned} \mu_m(t) &= \sum_{n=0}^m \sum_{l=n-\frac{m}{2}}^{\lfloor \frac{n}{2} \rfloor} C_{n,l,t} (-1)^{n-l} \omega^{n-2l} (1-\omega)^{2l} \alpha_{2n-2l,m} \\ &= \sum_{n=0}^m \sum_{l=n-\frac{m}{2}}^{\lfloor \frac{n}{2} \rfloor} \frac{(-1)^n t^n}{2^n n!} 4^l (-1)^n \binom{n}{2l} \binom{2n-2l}{n-l} \omega^{n-2l} (1-\omega)^{2l} \alpha_{2n-2l,m} \\ &= \sum_{n=0}^m \beta_{n,\omega} t^n. \end{aligned} \quad (\text{A.45})$$

Let us calculate the leading term,  $\beta_{m,\omega}$ . Then we have  $l \in \{\frac{m}{2}\}$ ,  $n = m$  with even  $m$ .

$$\begin{aligned} \beta_{m,\omega} &= \sum_{l=m-\frac{m}{2}}^{\lfloor \frac{m}{2} \rfloor} \frac{(-1)^m}{2^m m!} 4^l (-1)^m \binom{m}{2l} \binom{2m-2l}{m-l} \omega^{m-2l} (1-\omega)^{2l} \alpha_{2m-2l,m} \\ &= \frac{1}{2^m m!} 2^m \binom{m}{m} \binom{m}{\frac{m}{2}} (1-\omega)^m \alpha_{m,m} \\ &= \frac{1}{m!} \binom{m}{\frac{m}{2}} (1-\omega)^m (-1)^m m! = \binom{m}{\frac{m}{2}} (1-\omega)^m, \end{aligned} \quad (\text{A.46})$$

where we used the fact, that  $\alpha_{m,m} = (-1)^m m!$  by Lemma A.1.  $\square$



# Appendix B

## Proofs for quantum search

### B.1 Proofs for Erdős-Rényi graphs

#### B.1.1 Convergence of the principal eigenvector of adjacency matrix

**Proposition** ([36]). Let  $|\lambda_1\rangle$  be a principal eigenvector of adjacency matrix of random Erdős-Rényi graph with parameter  $p$ . For the probability  $p = \omega(\log^3(n)/(n \log^2 \log n))$  and some constant  $c > 0$  we have

$$\| |\lambda_1\rangle - |s\rangle \|_\infty \leq c \frac{1}{\sqrt{n}} \frac{\ln^{3/2}(n)}{\sqrt{np} \ln(np)} \quad (\text{B.1})$$

with probability  $1 - o(1)$ .

*Proof.* Note  $\deg(v)$  follows a binomial distribution. Using Lindenberg's CLT and the fact that the convergence is uniform one can show that

$$\begin{aligned} P\left(|\deg(v) - np| \leq 2\sqrt{\ln(n)np(1-p)}\right) &\approx P\left(|\mathcal{X}| \leq 2\sqrt{\ln(n)}\right) \\ &\geq 1 - \frac{1}{\sqrt{2\pi \ln(n)n^2}}, \end{aligned} \quad (\text{B.2})$$

where  $\mathcal{X}$  is a random variable with standard normal distribution. Let  $A = \lambda_1 |\lambda_1\rangle\langle\lambda_1| + \sum_{i \geq 2} \lambda_i |\lambda_i\rangle\langle\lambda_i|$  and  $|s\rangle = \alpha |\lambda_1\rangle + \beta |\lambda_1^\perp\rangle$ . Assume that  $|\lambda_1\rangle, |\lambda_1^\perp\rangle, |\lambda_i\rangle$  are normed vectors and  $|\lambda_1^\perp\rangle = \sum_{i \geq 2} \gamma_i |\lambda_i\rangle$ . By the Perron-Frobenius Theorem we can choose a vector  $|\lambda_1\rangle$  such that  $\langle v | \lambda_1 \rangle \geq 0$  for all  $v$  and hence obtain  $\langle s | \lambda_1 \rangle = \alpha > 0$ . Thus

$$\begin{aligned} (A - E(A)) |\lambda_1\rangle &= \left( \lambda_1 |\lambda_1\rangle\langle\lambda_1| + \sum_{i \geq 2} \lambda_i |\lambda_i\rangle\langle\lambda_i| - np |s\rangle\langle s| \right) |\lambda_1\rangle \\ &= (\lambda_1 - np\alpha^2) |\lambda_1\rangle - np\alpha\beta |\lambda_1^\perp\rangle. \end{aligned} \quad (\text{B.3})$$

With probability  $1 - o(1)$ , using Theorem 5.5 we have

$$(\lambda_1 - np\alpha^2)^2 + (np)^2\alpha^2\beta^2 = \| (A - E(A)) |\lambda_1\rangle \|^2 \leq 8np \ln(n), \quad (\text{B.4})$$

and by  $\beta^2 = 1 - \alpha^2$

$$\alpha^2 np(np - 2\lambda_1) + \lambda_1^2 \leq 8np \ln(n). \quad (\text{B.5})$$

Eventually, we receive

$$1 \geq \alpha \geq \alpha^2 \geq \frac{\lambda_1^2 - 8np \ln(n)}{2\lambda_1 np - (np)^2} \geq 1 - \frac{4}{2 + \sqrt{\frac{np}{8 \ln(\sqrt{2}n)}}} \geq 1 - \frac{16}{\sqrt{\frac{np}{\ln(n)}}}, \quad (\text{B.6})$$

where the fourth inequality comes from Theorem 5.4. We know that  $|\deg(v) - np| \leq 2\sqrt{n \ln(n)p(1-p)}$  with probability greater than  $1 - \frac{1}{n^2}$ . Thus, with probability  $1 - \frac{1}{n}$ , the above is true for all  $v \in V$  simultaneously. Now, since  $\deg(v) = \langle v | A | \mathbf{1} \rangle$ , we have

$$\frac{np - 2\sqrt{n \ln(n)p(1-p)}}{\lambda_1} \leq \frac{1}{\lambda_1} \langle v | A | \mathbf{1} \rangle \leq \frac{np + 2\sqrt{n \ln(n)p(1-p)}}{\lambda_1}. \quad (\text{B.7})$$

The lower bound can be estimated as

$$\frac{np - 2\sqrt{n \ln(n)p(1-p)}}{\lambda_1} \geq \frac{1 - 2\sqrt{\ln(n)\frac{1-p}{np}}}{1 + \sqrt{8\frac{\ln(\sqrt{2}n)}{np}}} \geq \frac{1 - 2\sqrt{\frac{\ln(n)}{np}}}{1 + 4\sqrt{\frac{\ln(n)}{np}}} =: d. \quad (\text{B.8})$$

Where we use bound on  $\lambda_1$  from Theorem 5.4. Similarly the upper bound

$$\frac{np + 2\sqrt{n \ln(n)p(1-p)}}{\lambda_1} \leq \frac{1 + 2\sqrt{\frac{\ln(n)}{np}}}{1 - 4\sqrt{\frac{\ln(n)}{np}}} =: u. \quad (\text{B.9})$$

Consequently

$$\frac{d}{\sqrt{n}} \leq \frac{1}{\lambda_1} \langle v | A | s \rangle \leq \frac{u}{\sqrt{n}} \quad (\text{B.10})$$

for all  $v \in V$ . Let  $l = c \frac{\ln(n)}{\ln(\sqrt{\frac{np}{\ln(n)}}/4)}$ , where  $c = c(n, p) \in [1, 2)$  is chosen to satisfy  $l = \left\lceil \frac{\ln(n)}{\ln(\sqrt{\frac{np}{\ln(n)}}/4)} \right\rceil$ . Hence

$$\frac{d^l}{\sqrt{n}} \leq \langle v | \left( \frac{A}{\lambda} \right)^l | s \rangle \leq \frac{u^l}{\sqrt{n}} \quad (\text{B.11})$$



for all  $v \in V$ . On the other hand

$$\begin{aligned} \left(\frac{1}{\lambda_1} A\right)^l (\alpha |\lambda_1\rangle + \beta |\lambda_1^\perp\rangle) &= \left(|\lambda_1\rangle\langle\lambda_1| + \sum_{i \geq 2} \left(\frac{\lambda_i}{\lambda_1}\right)^l |\lambda_i\rangle\langle\lambda_i|\right) \times \\ &\quad \times (\alpha |\lambda_1\rangle + \beta |\lambda_1^\perp\rangle) \\ &= \alpha |\lambda_1\rangle + \beta \sum_{i \geq 2} \left(\frac{\lambda_i}{\lambda_1}\right)^l \gamma_i |\lambda_i\rangle. \end{aligned} \quad (\text{B.12})$$

Using Theorems 5.4 and 5.5 we are able to estimate  $\frac{\lambda_i}{\lambda_1}$  by

$$\frac{\lambda_i}{\lambda_1} \leq \frac{\sqrt{8np \ln(\sqrt{2}n)}}{np - \sqrt{8np \ln(\sqrt{2}n)}} = \frac{1}{\sqrt{\frac{np}{8 \ln(\sqrt{2}n)}} - 1} \leq \frac{4}{\sqrt{\frac{np}{\ln(n)}}}. \quad (\text{B.13})$$

Thus

$$\begin{aligned} \left\| \beta \sum_{i \geq 2} \left(\frac{\lambda_i}{\lambda_1}\right)^l \gamma_i |\lambda_i\rangle \right\|_\infty &\leq |\beta| \left\| \sum_{i \geq 2} \left(\frac{\lambda_i}{\lambda_1}\right)^l \gamma_i |\lambda_i\rangle \right\|_2 \\ &\leq |\beta| \sqrt{\sum_{i \geq 2} \gamma_i^2 \left(\frac{4}{\sqrt{\frac{np}{\ln(n)}}}\right)^{2l}} \\ &= \frac{|\beta|}{\left(\frac{\sqrt{\frac{np}{\ln(n)}}}{4}\right)^l} = \frac{|\beta|}{n^c} \\ &\leq \frac{4}{\left(\frac{np}{\ln(n)}\right)^{1/4} n}, \end{aligned} \quad (\text{B.14})$$

where the last inequality comes from Eq. (B.6) and  $\|\cdot\|_2$  denotes the Euclidean norm. By Eq. (B.10) and (B.12) we get

$$\frac{d^l}{\sqrt{n}} \leq \alpha \langle v | \lambda_1 \rangle + \langle v | \left( \beta \sum_{i \geq 2} \left(\frac{\lambda_i}{\lambda_1}\right)^l \gamma_i |\lambda_i\rangle \right) \leq \frac{u^l}{\sqrt{n}}, \quad (\text{B.15})$$

for all  $v \in V$  and using Eq. (B.6) and (B.14) we eventually obtain

$$\frac{\frac{d^l}{\sqrt{n}} - \frac{4}{\left(\frac{np}{\ln(n)}\right)^{1/4} n}}{1} \leq \langle v | \lambda_1 \rangle \leq \frac{\frac{u^l}{\sqrt{n}} + \frac{4}{\left(\frac{np}{\ln(n)}\right)^{1/4} n}}{1 - \frac{16}{\sqrt{\frac{np}{\ln(n)}}}} \quad (\text{B.16})$$

for all  $v \in V$ . In order to finish the proof it is necessary to show that

$$(1 - d^l) + \frac{4}{\left(\frac{np}{\ln(n)}\right)^{1/4} \sqrt{n}} = \mathcal{O}\left(\frac{\log^{3/2}(n)}{\sqrt{np} \ln(np)}\right) \quad (\text{B.17})$$

and

$$(u^l - 1) + \frac{4}{\left(\frac{np}{\ln(n)}\right)^{1/4} \sqrt{n}} = \mathcal{O}\left(\frac{\log^{3/2}(n)}{\sqrt{np} \ln(np)}\right). \quad (\text{B.18})$$

We need to estimate how quickly  $d^l$  converges to 1. Using the fact that  $d \rightarrow 1$ , it is enough to observe that

$$(1 - d)l = \mathcal{O}\left(\frac{\ln^{3/2}(n)}{\sqrt{np} \log\left(\sqrt{\frac{np}{\log(n)}}/4\right)}\right), \quad (\text{B.19})$$

and thus

$$1 - d^l \approx 1 - e^{(d-1)l} = \mathcal{O}\left(\frac{\ln^{3/2}(n)}{\sqrt{np} \ln(np)}\right). \quad (\text{B.20})$$

The second term of LHS of Eq. (B.17) converges to 0 more rapidly than the bound, so it completes the proof for the lower bound. The same fact for the upper bound can be shown analogously.  $\square$

### B.1.2 Convergence of the largest eigenvalue of Laplacian

**Theorem.** Let  $G$  be a random graph chosen according to  $\mathcal{G}_n^{\text{ER}}(p)$ . Let  $p_0 > 0$  be such that  $np \geq p_0 \log(n)$ . Let  $\delta_{\max} \sim cnp$  for some  $c > 0$  almost surely. Then almost surely  $\lambda_1(L(G)) \sim cnp$ .

*Proof.* Note, that since the eigenvector corresponding to 0 eigenvalue is the equal superposition, we have

$$\begin{aligned} \lambda_1 &= \max_{\{|\phi\rangle \perp |s\rangle : \langle \phi | \phi \rangle = 1\}} \langle \phi | L | \phi \rangle \\ &= \max_{\{|\phi\rangle \perp |s\rangle : \langle \phi | \phi \rangle = 1\}} (\langle \phi | D | \phi \rangle - \langle \phi | A | \phi \rangle). \end{aligned} \quad (\text{B.21})$$

Note that

$$\begin{aligned} \lambda_1 &\leq \max_{\{|\phi\rangle \perp |s\rangle : \langle \phi | \phi \rangle = 1\}} \langle \phi | D | \phi \rangle + \max_{\{|\phi\rangle \perp |s\rangle : \langle \phi | \phi \rangle = 1\}} |\langle \phi | A | \phi \rangle| \\ &\leq \delta_{\max} + C\sqrt{np} \end{aligned} \quad (\text{B.22})$$

by Theorem 2.5 from [82]. Furthermore, we have

$$\lambda_1 = \max_{|\phi\rangle} \langle \phi | L | \phi \rangle \geq \max_{i=1, \dots, n} \langle i | L | i \rangle = \delta_{\max}. \quad (\text{B.23})$$

Since  $\sqrt{np} = o(np)$  we have  $\lambda_1 \sim cnp$ .  $\square$

## B.2 Proofs for Chung-Lu graphs

In this section we assume  $\omega_i = n^{a+\frac{i}{n}b}$ .

### B.2.1 Complexity of $p$ -norm of $\omega$

**Theorem B.1.** *Let  $\alpha, \beta > 0$  be fixed numbers. Let  $f_{a,b}(n) = \sum_{i=1}^n n^{a+bi/n}$ . Then  $f(n) = \frac{n^{1+\alpha+\beta}}{\beta \log(n)}(1 + o(1))$ .*

*Proof.* Let us consider the inner sum first

$$\sum_{i=1}^n n^{\alpha+\beta \frac{i}{n}} = n^\alpha \sum_{i=1}^n \left(n^{\beta/n}\right)^i = n^\alpha n^{\frac{\beta}{n}} \frac{n^\beta - 1}{n^{\frac{\beta}{n}} - 1} \quad (\text{B.24})$$

Note that  $n^\alpha n^{\beta/n}(n^\beta - 1) = \Theta(n^{\alpha+\beta})$ , hence we only need to derive the complexity of the denominator:

$$\begin{aligned} \frac{1}{1 - n^{\beta/n}} &= \frac{1}{1 - \exp\left(\frac{\beta}{n} \log(n)\right)} = \frac{n}{\beta \log(n)} \frac{\frac{\beta}{n} \log(n)}{1 - \exp\left(\frac{\beta}{n} \log(n)\right)} \\ &= \frac{n}{\beta \log(n)}(1 + o(1)), \end{aligned} \quad (\text{B.25})$$

which ends the proof.  $\square$

Note that in particular  $\|\omega\|_1 = f_{a,b}(n) \sim \frac{n^{1+a+b}}{b \log(n)}$  and  $\|\omega\|_2 = \sqrt{f_{2a,2b}(n)} \sim \frac{n^{\frac{1}{2}+a+b}}{\sqrt{2b \log(n)}}$ . Since  $b$  is a constant, we can discard it with  $\Theta$  notation.

### B.2.2 Number of edges for Chung-Lu graphs

Let  $\mathcal{E}$  be a random variable denoting the number of edges of random Chung-Lu graph with the proposed  $\omega$ . Let  $p_{ij} = \frac{\omega_i \omega_j}{\|\omega\|_1}$ . Then

$$\begin{aligned} \mathbb{E}\mathcal{E} &= \sum_{i,j} p_{ij} = \sum_{i,j} \frac{\omega_i \omega_j}{\|\omega\|_1} = \|\omega\|_1, \\ \text{Var}[\mathcal{E}] &= \sum_{i,j} p_{ij}(1 - p_{ij}) = \mathbb{E}\mathcal{E} - \sum_{i,j} p_{ij}^2 \leq \mathbb{E}\mathcal{E}. \end{aligned} \quad (\text{B.26})$$

By the Chebyshev inequality

$$\mathbb{P}(|\mathcal{E} - \mathbb{E}\mathcal{E}| \geq \varepsilon \mathbb{E}\mathcal{E}) \leq \frac{\text{Var}[\mathcal{E}]}{\varepsilon^2 (\mathbb{E}\mathcal{E})^2} \leq \frac{\mathbb{E}\mathcal{E}}{\varepsilon^2 (\mathbb{E}\mathcal{E})^2} = \frac{1}{\varepsilon^2 \|\omega\|_1}. \quad (\text{B.27})$$

Let us take  $\varepsilon = 1/\log n$ . Then we have

$$\mathbb{P}(|\mathcal{E} - \mathbb{E}\mathcal{E}| \geq \mathbb{E}\mathcal{E}/\log n) \leq \frac{1}{\varepsilon^2 \|\omega\|_1} \sim \frac{\log^3(n)}{n^{1+a+b}} \leq \frac{1}{n^{1+a+b+\varepsilon}}. \quad (\text{B.28})$$

Hence the number of edges  $\mathcal{E}$  concentrates around  $\mathbb{E}\mathcal{E}$ . Note that the upper bound on the probability is  $1/n^{1+\varepsilon}$  for  $\varepsilon$ , which, thanks to Borel-Cantelli lemma, means that the almost all graphs in a sequence will have this property.

### B.2.3 Degree convergence

Let  $\mathcal{D}_i$  be a random variable denoting the degree of the  $i$ -th vertex of edges of random Chung-Lu graph with the proposed  $\omega$ . We do not assume  $i$  is fixed. Let  $p_{ij} = \frac{\omega_i \omega_j}{\|\omega\|_1}$ . Then

$$\begin{aligned} \mathbb{E}\mathcal{D}_i &= \omega_i, \\ \text{Var}[\mathcal{D}_i] &= \sum_j p_{ij}(1 - p_{ij}) = \omega_i - \sum_j \frac{\omega_i^2 \omega_j^2}{\|\omega\|_1^2} \leq \omega_i. \end{aligned} \quad (\text{B.29})$$

By the Chebyshev inequality

$$\mathbb{P}(|\mathcal{D}_i - \omega_i| \geq \varepsilon \omega_i) \leq \frac{\omega_i}{\varepsilon^2 \omega_i^2} = \frac{1}{\varepsilon^2 \omega_i}. \quad (\text{B.30})$$

Let us take  $\varepsilon = 1/\log n$ . Then we have

$$\mathbb{P}(|\mathcal{D}_i - \omega_i| \geq \omega_i/\log n) \leq \frac{\log^2 n}{n^{a+\frac{i}{n}b}}. \quad (\text{B.31})$$

Note that for any choice of  $i$  and  $a, b > 0$  the probability converges to 0, but the series of probabilities is not converging for any choice of  $i$ . Hence we can say at best there is infinite subsequence of graphs s.t. the degree is close to the expected degree.

Let us use the Hoeffding theorem this time we have

$$\begin{aligned} \mathbb{P}(|\mathcal{D}_i - \omega_i| \geq \varepsilon \omega_i) &\leq 2 \exp\left(-\frac{2\varepsilon^2 \omega_i^2}{n}\right) = 2 \exp\left(-2\varepsilon^2 n^{2a+2\frac{i}{n}b-1}\right) \\ &= \frac{2}{n^{\frac{2\varepsilon^2 n^{2a+2\frac{i}{n}b-1}}{\log n}}} \end{aligned} \quad (\text{B.32})$$

Note that the series of probabilities is convergent if  $\frac{2\varepsilon^2 n^{2a+2\frac{i}{n}b-1}}{\log n} \geq C > 1$  for some fixed  $C$ , which is can be relaxed by  $\varepsilon = 1/\log n$  to

$$\begin{aligned} n^{2a+2\frac{i}{n}b-1} &\geq \frac{C}{2} \log^3 n \\ 2a + 2\frac{i}{n}b - 1 &> 0 \\ a + \frac{i}{n}b &> \frac{1}{2} \end{aligned} \tag{B.33}$$

So if  $i$  is chosen in such a way that  $\omega_i > n^{\frac{1}{2}+\varepsilon}$ , then almost all degrees concentrate around their expectation. Thus, for almost all graphs,  $\mathcal{D}_i = \Theta(\omega_i)$ .

#### B.2.4 Convergence of $|\lambda_1\rangle$ for adjacency graphs

**The overlap** Let  $A = \sum_i \lambda_i |\lambda_i\rangle$ . Let  $|\omega\rangle = \sum_i \omega_i |i\rangle$ . Note that  $\mathbb{E}A = \frac{1}{\|\omega\|_1} |\omega\rangle\langle\omega|$ . By [50] we have a.a.s.

$$\|A - \mathbb{E}A\| \leq \sqrt{8\delta_{\max} \log n}. \tag{B.34}$$

Let  $\frac{1}{\|\omega\|_2} |\omega\rangle = \alpha |\lambda_1\rangle + \beta |\lambda_1^\perp\rangle$ . Note that

$$\begin{aligned} (A - \mathbb{E}A) |\lambda_1\rangle &= \lambda_1 |\lambda_1\rangle - \frac{\|\omega\|_2}{\|\omega\|_1} \alpha |\omega\rangle \\ &= \left( \lambda_1 - \frac{\|\omega\|_2^2}{\|\omega\|_1} \alpha^2 \right) |\lambda_1\rangle - \frac{\|\omega\|_2^2}{\|\omega\|_1} \alpha \beta |\lambda_1^\perp\rangle. \end{aligned} \tag{B.35}$$

By this we have  $\|(A - \mathbb{E}A) |\lambda_1\rangle\|_2^2 \geq \left( \lambda_1 - \frac{\|\omega\|_2^2}{\|\omega\|_1} \alpha^2 \right)^2$ . Since  $\|(A - \mathbb{E}A) |\lambda_1\rangle\| \leq \|(A - \mathbb{E}A)\| \|\lambda_1\rangle\| = \|A - \mathbb{E}A\|$ , we have

$$\begin{aligned} \left( \lambda_1 - \frac{\|\omega\|_2^2}{\|\omega\|_1} \alpha^2 \right)^2 &\leq 8\delta_{\max} \log n \\ \alpha^2 &\geq \frac{\|\omega\|_1}{\|\omega\|_2^2} \left( \lambda_1 - \sqrt{8\delta_{\max} \log n} \right) \\ &\geq \frac{\|\omega\|_1}{\|\omega\|_2^2} \left( \frac{\|\omega\|_2^2}{\|\omega\|_1} - 2\sqrt{8\delta_{\max} \log n} \right) \\ &\geq 1 - 2 \frac{\|\omega\|_1}{\|\omega\|_2^2} \sqrt{8\delta_{\max} \log n}. \end{aligned} \tag{B.36}$$

So as long as  $\frac{\|\omega\|_1}{\|\omega\|_2^2} \sqrt{\delta_{\max} \ln n} = o(1)$  we have that  $\alpha = 1 - o(1)$ .

This is satisfied for the proposed  $\omega$  for any  $a, b > 0$ .

**Convergence for almost all nodes** We follow the proof similar to the one presented in [37]. Let  $|\lambda_1\rangle = \sum_i \gamma_i |i\rangle$  and  $|\bar{\omega}\rangle = \sum_i \bar{\omega}_i |i\rangle$  where  $\bar{\omega}_i = \frac{\omega_i}{\|\omega\|_2}$ . We know that  $\alpha := \langle \lambda_1 | \bar{\omega} \rangle = 1 - o(1)$ . We will search for a indexes set  $I_n \subseteq \{1, \dots, n\}$  such that  $|I_n| = n(1 - o(1))$  and

$$\max_{i \in I_n} |\gamma_{i,n} - 1| = o(1). \quad (\text{B.37})$$

Let  $|\lambda_1\rangle = \alpha |\bar{\omega}\rangle + \beta |\bar{\omega}^\perp\rangle$ , with  $|\bar{\omega}^\perp\rangle = \sum_i \bar{\omega}_i^\perp |i\rangle$  being a normed vector. Let

$$I_\varepsilon(n)^c := \{i \in \{1, \dots, n\} : |\gamma_i/\bar{\omega}_i - \alpha| > \varepsilon\} \quad (\text{B.38})$$

be the collection of indices for which values in vectors are not sufficiently close. Since  $\gamma_i/\bar{\omega}_i - \alpha = \beta \bar{\omega}_i^\perp / \bar{\omega}_i$ , we have

$$1 \geq |\langle \bar{\omega}^\perp | \bar{\omega}^\perp \rangle|^2 = \sum_{i=0}^{n-1} |\bar{\omega}_i^\perp|^2 \geq \sum_{i \in I_\varepsilon(n)} |\bar{\omega}_i^\perp|^2 > \left( \frac{\varepsilon \min_i \bar{\omega}_i}{\beta} \right)^2 |I_\varepsilon(n)|, \quad (\text{B.39})$$

hence  $|I_\varepsilon(n)| < \left( \frac{\beta}{\varepsilon \min_i \bar{\omega}_i} \right)^2$ . We will expect  $|I_\varepsilon(n)| = o(n)$ , which gives us following condition on  $a, b$ :

$$\begin{aligned} |I_\varepsilon(n)| &< \left( \frac{\beta}{\varepsilon \min_i \bar{\omega}_i} \right)^2 \leq \frac{\frac{\|\omega\|_1}{\|\omega\|_2^2} \sqrt{8\delta_{\max} \log n}}{\varepsilon^2 \frac{n^{2a}}{\|\omega\|_2^2}} = \frac{\|\omega\|_1 \sqrt{8n^{a+b} \log n}}{\varepsilon^2 n^{2a}} \\ &\sim 2\sqrt{2} \frac{n^{1+a+b}}{b \log n} \frac{\sqrt{n^{a+b} \log n}}{\varepsilon^2 n^{2a}} = \frac{2\sqrt{2} n^{1-\frac{1}{2}a+\frac{3}{2}b}}{b\varepsilon^2 \sqrt{\log n}} \end{aligned} \quad (\text{B.40})$$

We require  $|I_\varepsilon(n)| = o(n)$ , which translates to

$$\begin{aligned} \frac{2\sqrt{2} n^{1-\frac{1}{2}a+\frac{3}{2}b}}{b\varepsilon^2 \sqrt{\log n}} &= o(n) \\ \frac{1}{\varepsilon^2} &= o\left(\frac{\sqrt{\log n}}{n^{\frac{1}{2}a-\frac{3}{2}b}}\right) \\ \varepsilon &= \omega\left(\frac{n^{\frac{1}{4}a-\frac{3}{4}b}}{\sqrt{\log n}}\right). \end{aligned} \quad (\text{B.41})$$

We also will require  $\varepsilon = o(1)$ . In order to satisfy both condition we will need  $\frac{1}{4}a - \frac{3}{4}b < 0$ , which is equivalent to  $a < 3b$ .

Let  $I_n := \{1, \dots, n\} \setminus I_{\varepsilon'}(n)$  with  $\varepsilon' = n^{\frac{1}{4}(a-3b)}$ . Then  $\varepsilon' = o(1)$  and  $I_n = n(1 - o(1))$ , and furthermore

$$\max_{i \in I_n} |\gamma_i/\bar{\omega}_i - 1| \leq \max_{i \in I_n} |\gamma_i/\bar{\omega}_i - \alpha| + |1 - \alpha| \leq \varepsilon' + |1 - \alpha| = o(1). \quad (\text{B.42})$$

## B.3 Classical search

Let  $P = AD^{-1}$  be a stochastic matrix of uniform walk on undirected graph. Let  $P_j^\infty$  be its unique stationary state. Let  $P_{ij}(t)$  be the probability of being at  $j$  at time  $t$  starting at node  $i$ . Finally let  $R_{ij} := \sum_{t=0}^{\infty} (P_{ij}(t) - P_j^\infty)$ . Then we have

$$\begin{aligned} R_{jj} - R_{ij} &= \sum_{t=0}^{\infty} (P_{jj}(t) - P_j^\infty - P_{ij}(t) + P_j^\infty) = \sum_{t=0}^{\infty} (P_{jj}(t) - P_{ij}(t)) \\ &= \sum_{t=0}^{\infty} (\langle j | P^t | j \rangle - \langle j | P^t | i \rangle) = \langle j | \sum_{t=0}^{\infty} (P^t(|j\rangle - |i\rangle)) \rangle. \end{aligned} \quad (\text{B.43})$$

Note we cannot move  $|j\rangle - |i\rangle$  outside the series, since  $\sum_{t=0}^{\infty} P^t$  is not converging. Let  $\langle T_{ij} \rangle$  be a mean first passage time from  $i$  to  $j$ . Then  $\langle T_{ij} \rangle = \frac{2|E|}{d_j} [R_{jj} - R_{ij}]$  for  $i \neq j$  [58] and  $\langle T_{jj} \rangle = 0$ . The mean first passage time starting at stationary state equals

$$\begin{aligned} \langle T_j \rangle &:= \sum_{i=1}^n \frac{d_i}{2|E|} \langle T_{ij} \rangle = \frac{1}{d_j} \sum_{\substack{i=1 \\ i \neq j}}^n d_i (R_{jj} - R_{ij}) \\ &= \frac{1}{d_j} \langle j | \sum_{t=0}^{\infty} P^t \left( (2|E| - d_j) |j\rangle - d_i \sum_{\substack{i=1 \\ i \neq j}}^n |i\rangle \right) \\ &= \frac{1}{d_j} \langle j | \sum_{t=0}^{\infty} (P^t(2|E| |j\rangle - |P^\infty\rangle)) \rangle = \frac{1}{d_j} \sum_{t=0}^{\infty} (2|E| \langle j | P^t | j \rangle - \langle j | P^\infty \rangle) \\ &= \frac{1}{d_j} \sum_{t=0}^{\infty} (2|E| \langle j | P^t | j \rangle - d_j) = \frac{2|E|}{d_j} \sum_{t=0}^{\infty} \left( \langle j | P^t | j \rangle - \frac{d_j}{2|E|} \right) \\ &= \frac{2|E|}{d_j} \sum_{t=0}^{\infty} \left( \langle j | P^t | j \rangle - \frac{d_j}{2|E|} \right). \end{aligned} \quad (\text{B.44})$$

Let  $|\mu_i\rangle$  be an eigenvector of normalized Laplacian with eigenvalue  $\mu_i > 0$ . Based on the formula for  $P_{jj}(t)$  before Eq. (2.1) from [83] we have

$$\sum_{i=1}^n \frac{d_i}{|E|} \langle T_{ij} \rangle = \frac{2|E|}{d_j} \sum_{t=0}^{\infty} \sum_{i \geq 2} \lambda_i^t \langle j | \mu_i \rangle^2 = \frac{2|E|}{d_j} \sum_{i \geq 2} \frac{1}{1 - \lambda_i} \langle j | \mu_i \rangle^2 = \frac{2|E|}{d_j} S_1. \quad (\text{B.45})$$

Let us upper bound it from the above and from below

$$\langle T_j \rangle = \frac{2|E|}{d_j} \sum_{i \geq 2} \frac{1}{1 - \lambda_i} \langle j | \mu_i \rangle^2 \leq \frac{2|E|}{d_j} \frac{1}{1 - \lambda_2} \sum_{i \geq 2} \langle j | \mu_i \rangle^2 \leq \frac{2|E|}{d_j} \frac{1}{\Delta}. \quad (\text{B.46})$$

Note that  $\varepsilon = \frac{d_j}{2|E|}$ , which confirms one bound. Similarly for the other side we have.

$$\begin{aligned}
\langle T_j \rangle &= \frac{2|E|}{d_j} \sum_{t=0}^{\infty} \sum_{i \geq 2} \lambda_i^t \langle j | \mu_i \rangle^2 = \frac{2|E|}{d_j} \sum_{i \geq 2} \frac{1}{1 - \lambda_i} (e_j^{(i)})^2 \\
&> \frac{|E|}{d_j} \sum_{i \geq 2} (e_j^{(i)})^2 = \frac{|E|}{d_j} (1 - (e_j^{(1)})^2) \\
&= \frac{|E|}{d_j} \left(1 - \frac{d_j}{2|E|}\right) = \frac{|E|}{d_j} - \frac{1}{2}.
\end{aligned} \tag{B.47}$$